Ion vs electron heating in astrophysical gyrokinetic turbulence

Yohei Kawazura, Michael Barnes & Alex Schekochihin

University of Oxford

Plasma Kinetics workshop — WPI 2018

Outline

- ✓ Background
- ✓ Ion vs heating ratio
- ✓ k-spectrum ($\beta_{\rm i} = 0.1$ vs 100)
- ✓ phase space-spectrum ($\beta_{\rm i} = 0.1$ vs 100)
- ✓ summary
  - ✓ Ultrahigh beta ($\beta_{\rm i} = 10000$) simulation

Turbulent heating in collisionless plasma

✓ Large scale free energy source (e.g., Keplerian shear) drives turbulence

✓ Turbulence dissipates at small scales

✓ Unequal distribution of heating between ions and electrons

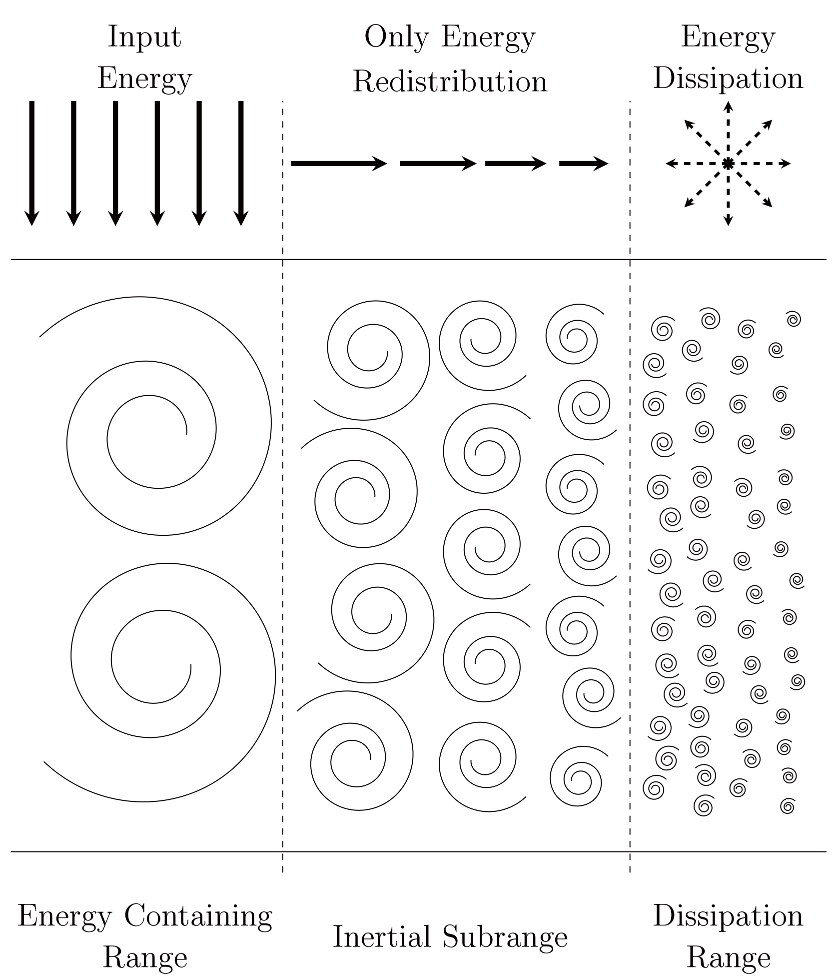

Puhales+, 2015

$$Q_{\rm i} \neq Q_{\rm e}$$

- What is $Q_{\rm i}/Q_{\rm e}$?
- How does it depend on parameters?

Turbulent heating in collisionless plasma

- ✓ Large scale free energy source (e.g., Keplerian shear) drives turbulence
- ✓ Turbulence dissipates at small scales
- ✓ Unequal distribution of heating between ions and electrons
- ✓ Does turbulence prefer equilibration between species?

$$T_{\rm i} > T_{\rm e} \quad \rightarrow \quad Q_{\rm i} < Q_{\rm e}$$

- ✓ Or pushes toward further disequilibration?

$$T_{\rm i} > T_{\rm e} \quad \rightarrow \quad Q_{\rm i} > Q_{\rm e}$$

Turbulent heating in collisionless plasma

- ✓ Large scale free energy source (e.g., Keplerian shear) drives turbulence
- ✓ Turbulence dissipates at small scales
- ✓ Unequal distribution of heating between ions and electrons

Turbulent heating in collisionless plasma

- ✓ Large scale free energy source (e.g., Keplerian shear) drives turbulence
- ✓ Turbulence dissipates at small scales
- ✓ Unequal distribution of heating between ions and electrons
- ✓ Crucial in blackhole accretion flows (Quataert, 1999)

Turbulent heating in collisionless plasma

- ✓ Large scale free energy source (e.g., Keplerian shear) drives turbulence
- ✓ Turbulence dissipates at small scales
- ✓ Unequal distribution of heating between ions and electrons
- ✓ Crucial in blackhole accretion flows (Quataert, 1999)
- ✓ MRI → Turbulence → Momentum transport

Turbulent heating in collisionless plasma

- ✓ Large scale free energy source (e.g., Keplerian shear) drives turbulence
- ✓ Turbulence dissipates at small scales
- ✓ Unequal distribution of heating between ions and electrons
- ✓ Crucial in blackhole accretion flows (Quataert, 1999)
- ✓ MRI → Turbulence → Momentum transport

Turbulence → Heating

Heating → Electrons, Ions

collisionless disk, e.g. RIAF

Turbulent heating in collisionless plasma

- ✓ Large scale free energy source (e.g., Keplerian shear) drives turbulence
- ✓ Turbulence dissipates at small scales
- ✓ Unequal distribution of heating between ions and electrons
- ✓ Crucial in blackhole accretion flows (Quataert, 1999)
- ✓ MRI → Turbulence → Momentum transport

Turbulence → Heating

Heating → Electrons → Radiation

Heating → Ions → Advection, outflow

collisionless disk, e.g. RIAF

Turbulent heating in collisionless plasma

- ✓ Large scale free energy source (e.g., Keplerian shear) drives turbulence
- ✓ Turbulence dissipates at small scales
- ✓ Unequal distribution of heating between ions and electrons
- ✓ Crucial in blackhole accretion flows (Quataert, 1999)
- ✓ MRI → Turbulence → Momentum transport

Turbulence → Heating

collisionless disk, e.g. RIAF

Heating → Electrons → Radiation

Heating → Ions → Advection, outflow

- ✓ To estimate T_{i}, heating ratio is important

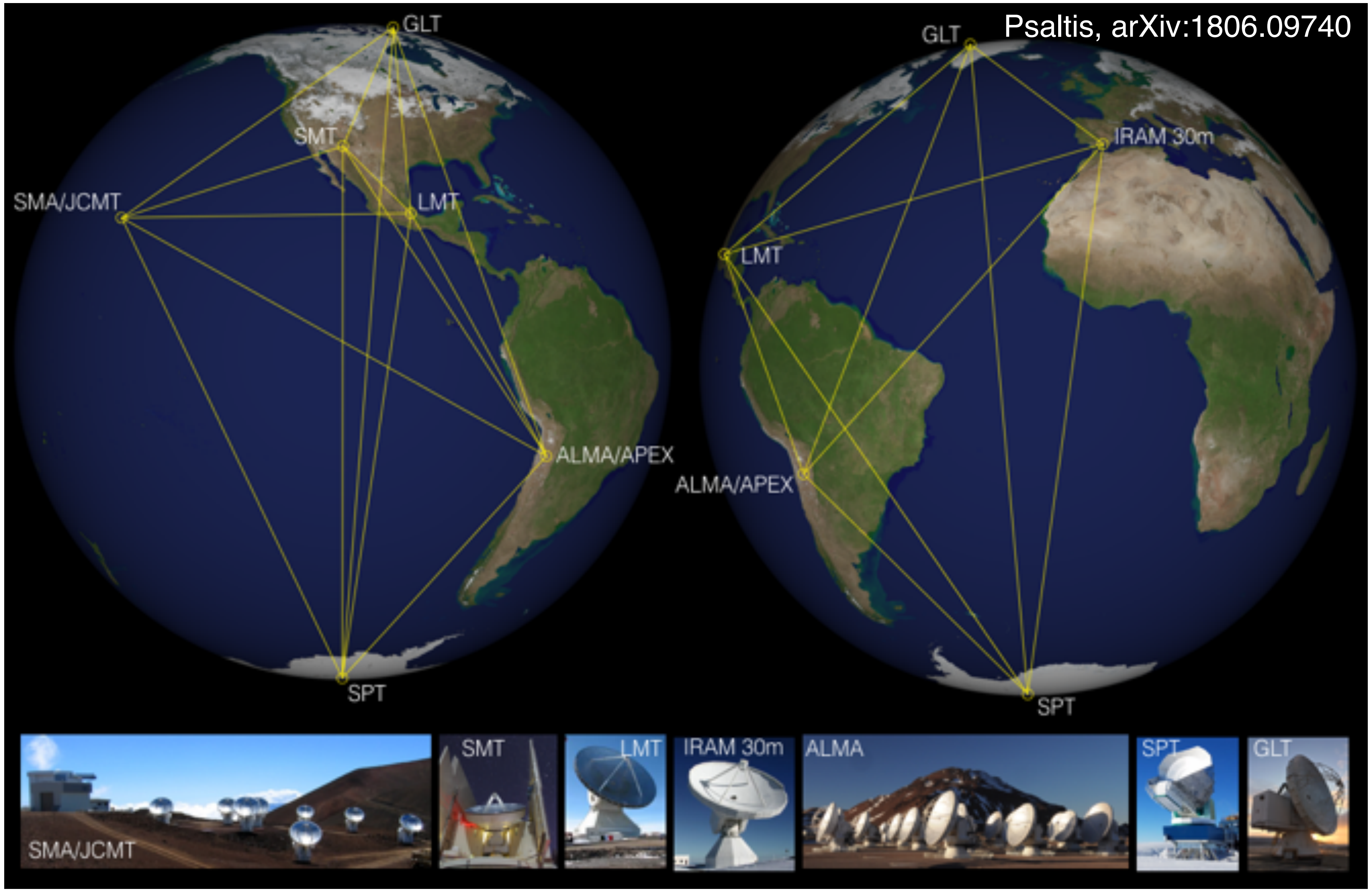

✓ Event Horizon Telescope → Photograph near Sgr A*

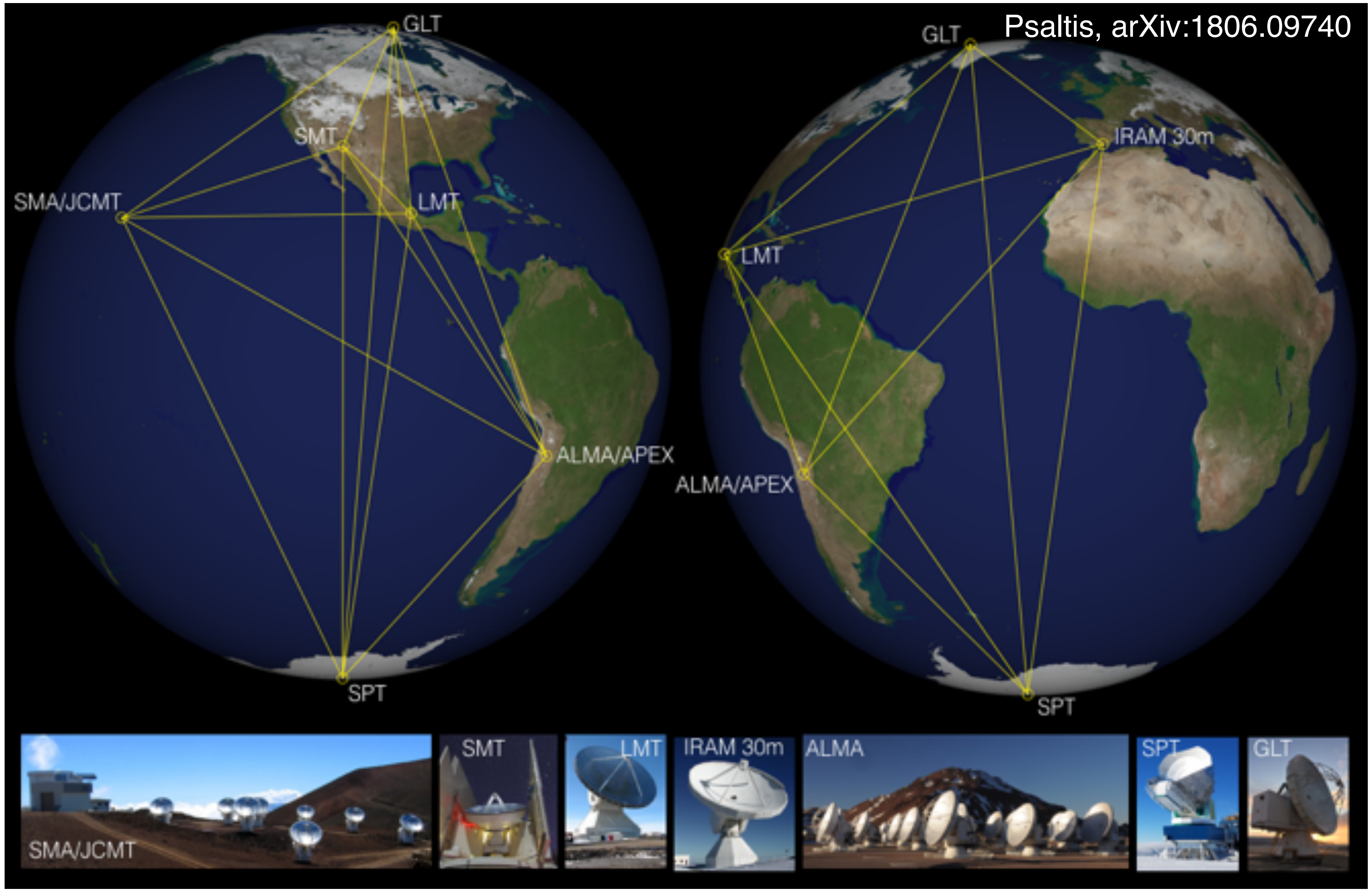

✓ Event Horizon Telescope → Photograph near Sgr A*

✓ Prediction via GR Radiative MHD simulation

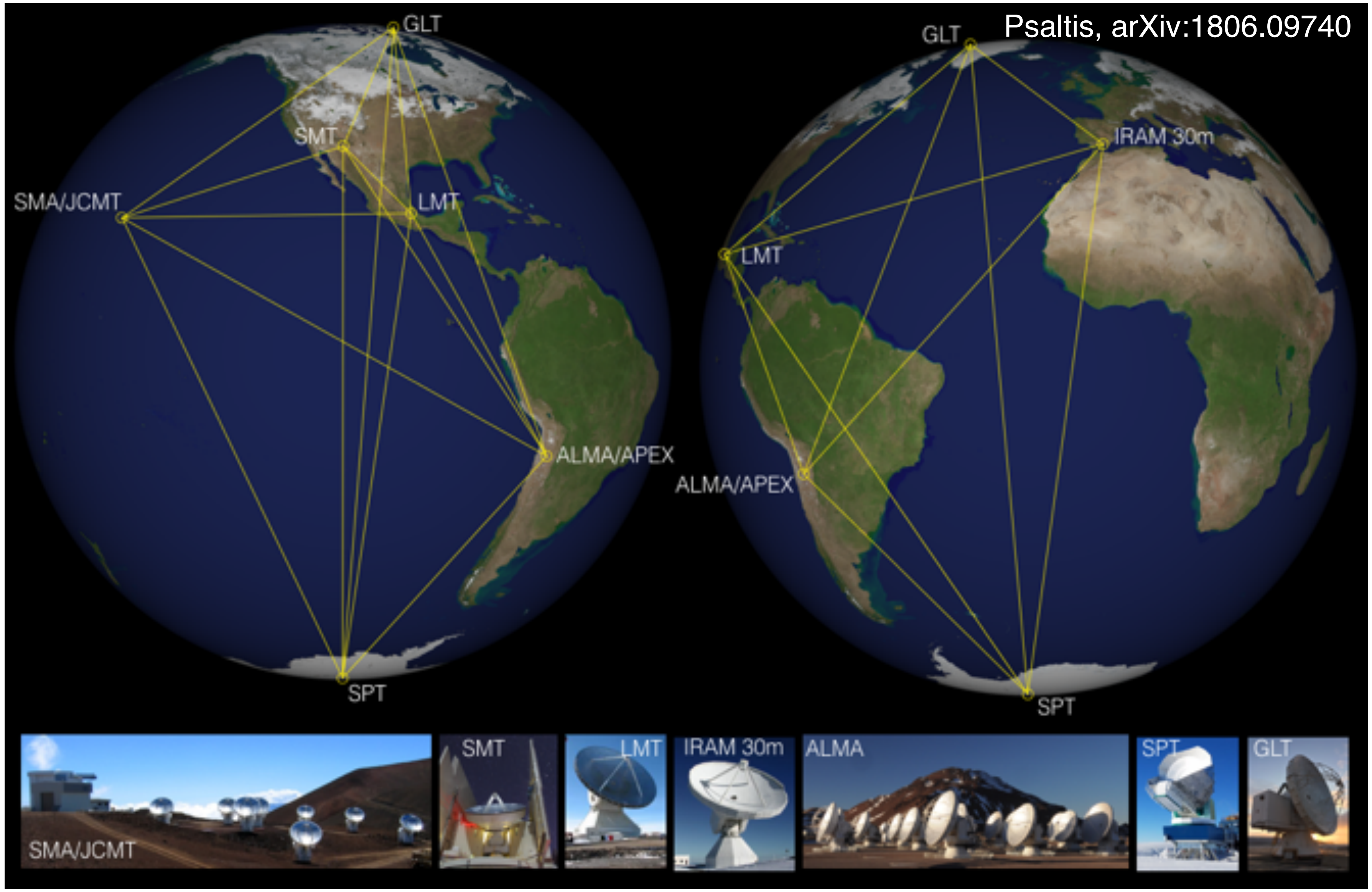

- ✓ Event Horizon Telescope → Photograph near Sgr A*
- ✓ Prediction via GR Radiative MHD simulation
- ✓ Different results depending on the heating prescription

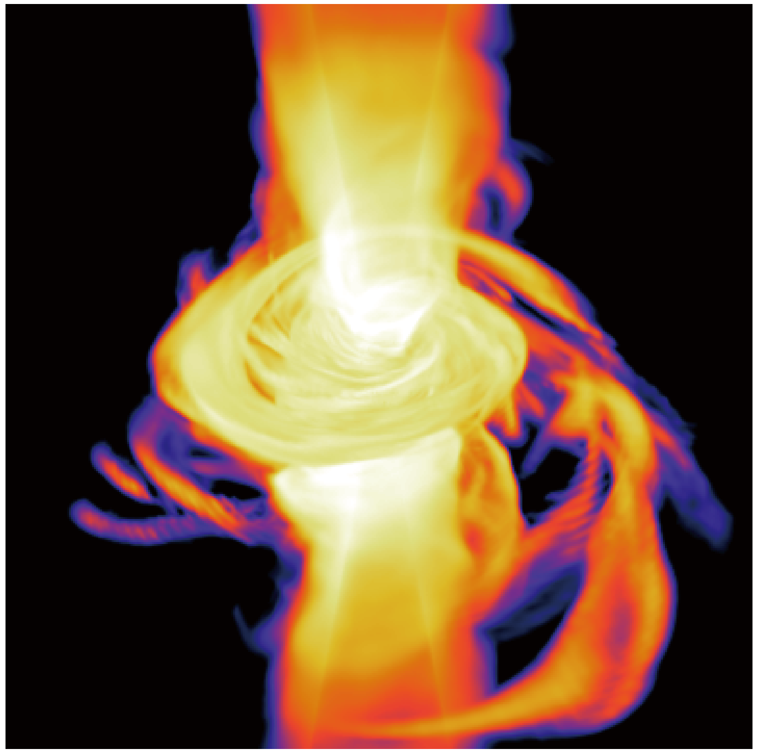

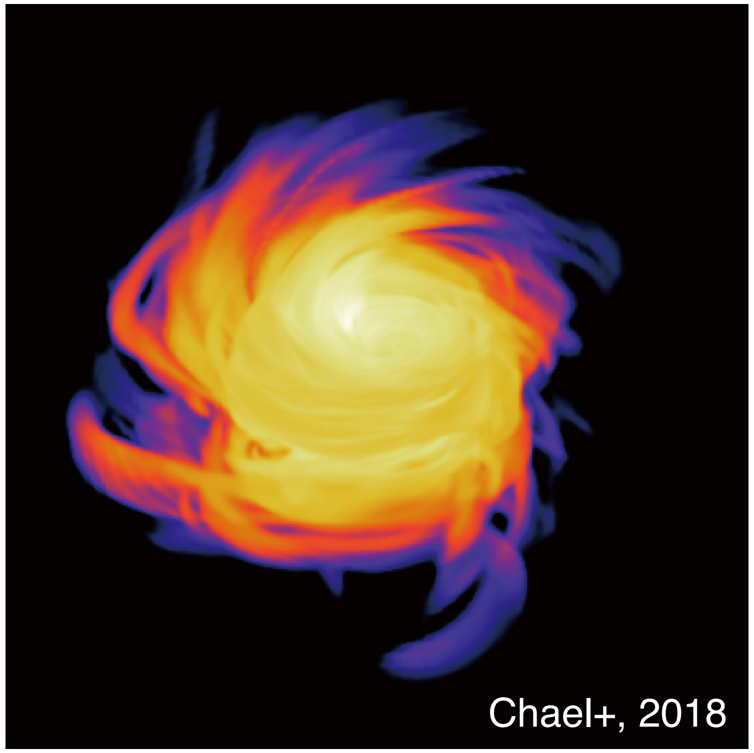
Chael+, 2018

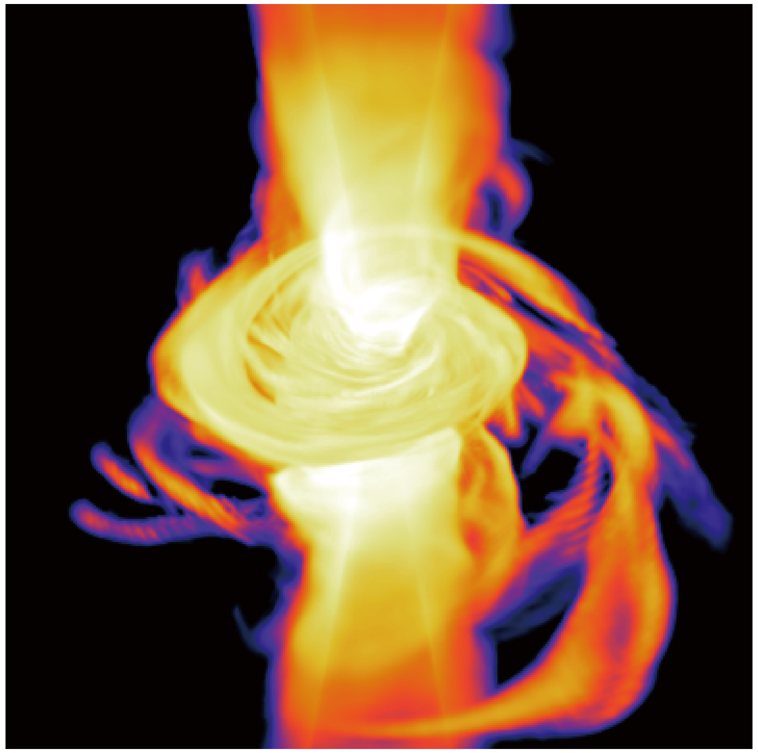

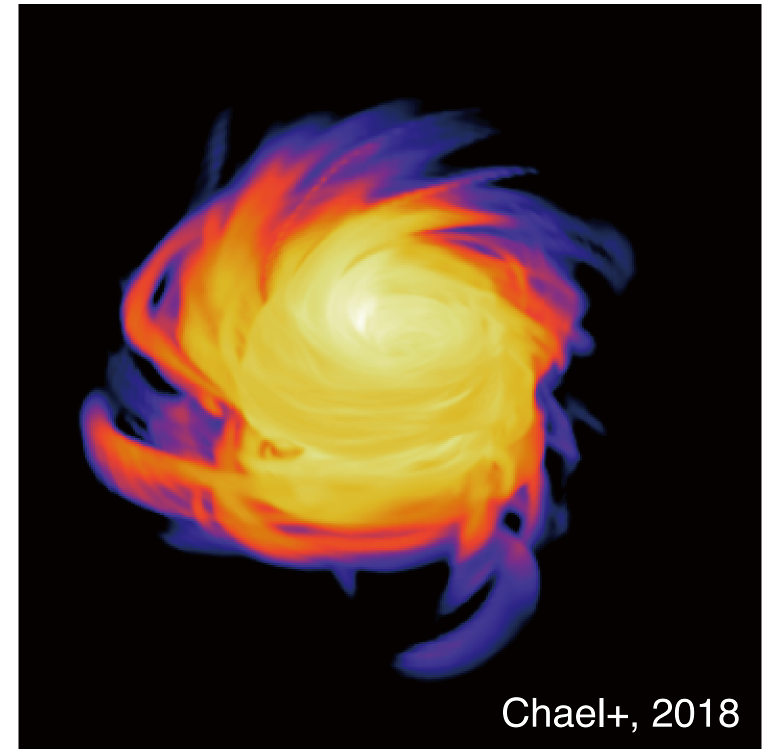

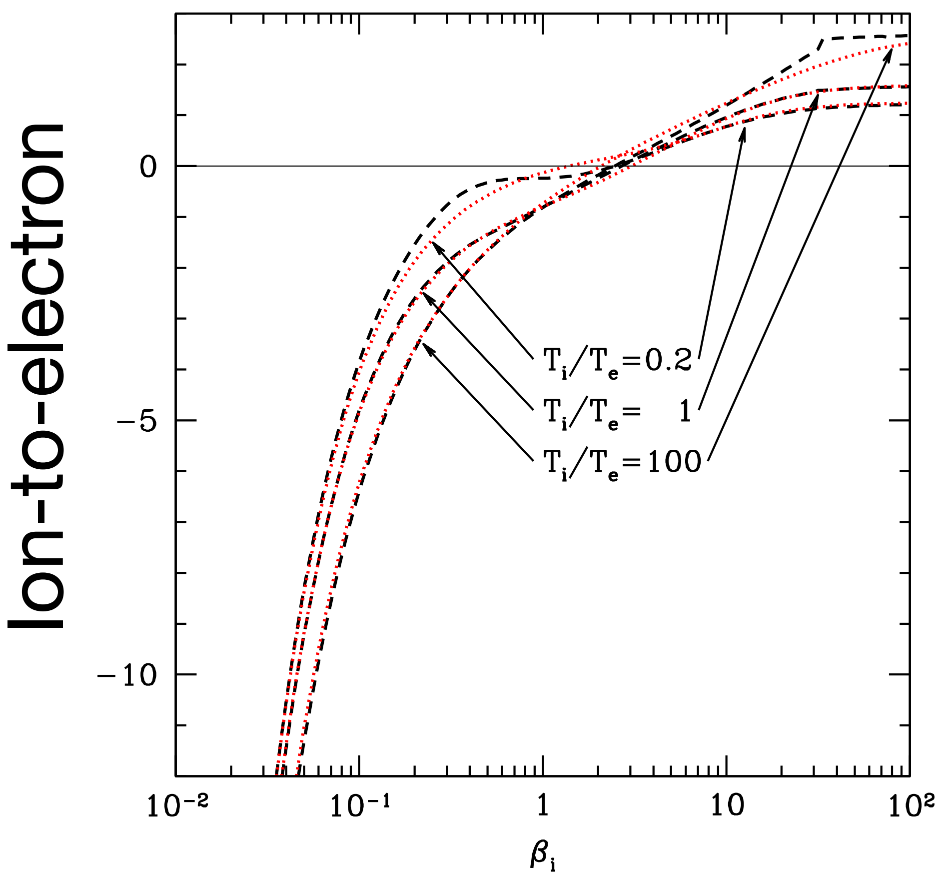

GK turbulence, theory (Howes 2010)

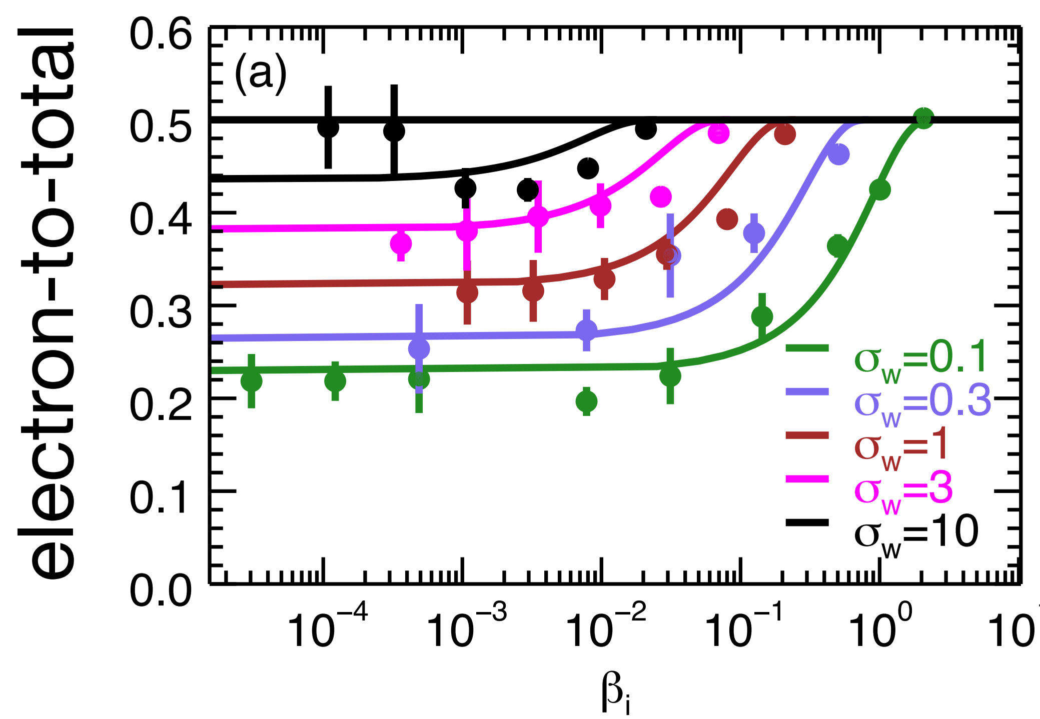

Reconnection, 2D PIC (Rowan+ 2017)

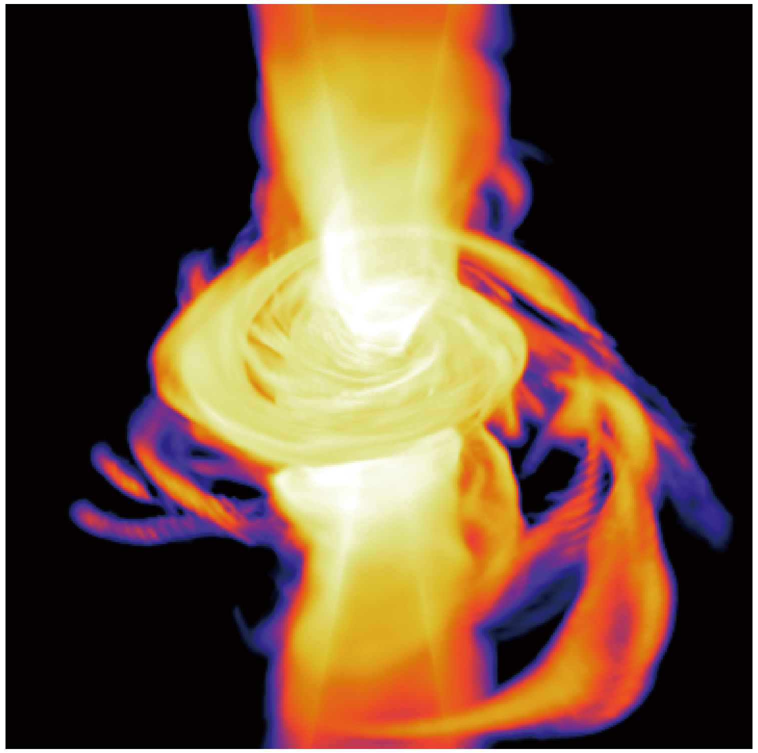

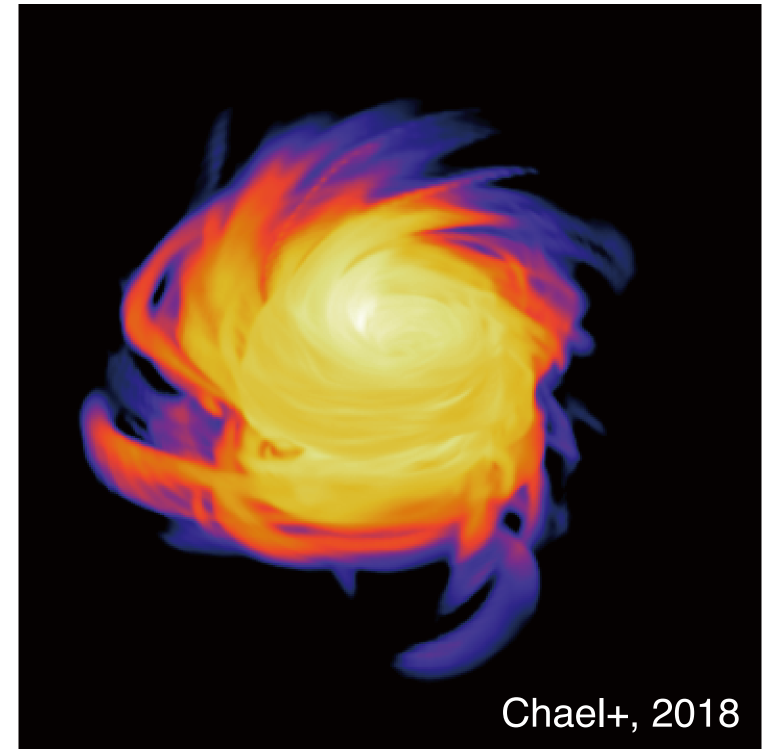

Revise this prescription via nonlinear simulation

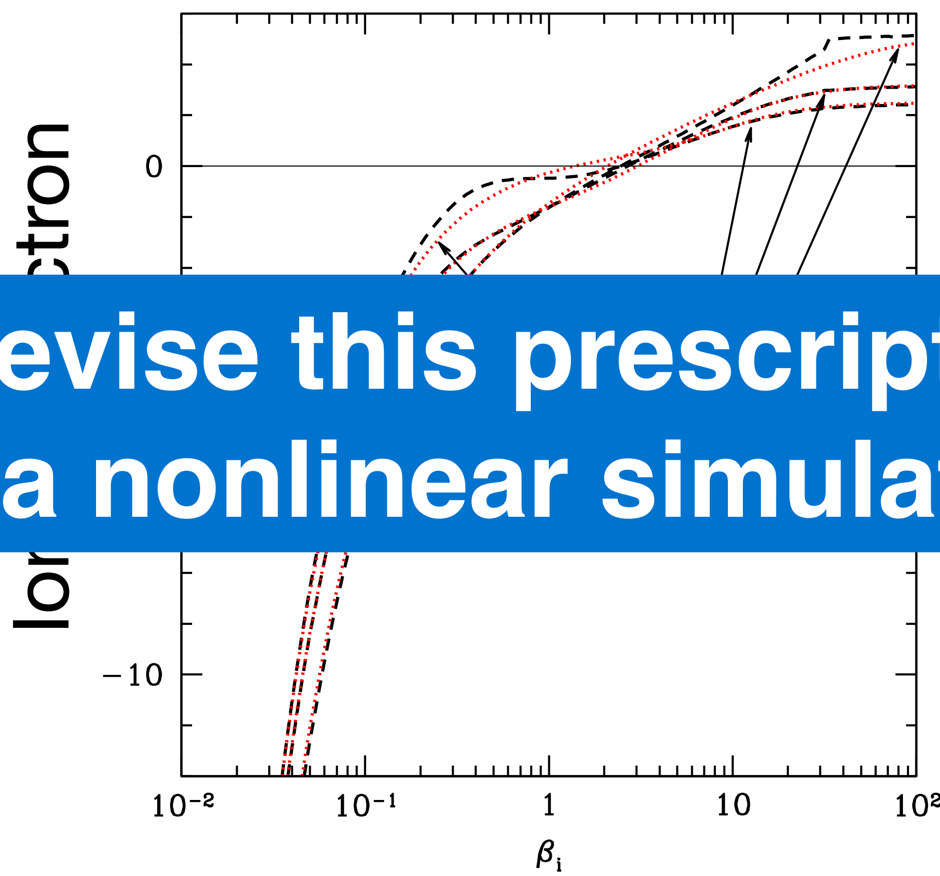

GK turbulence, theory (Howes 2010)

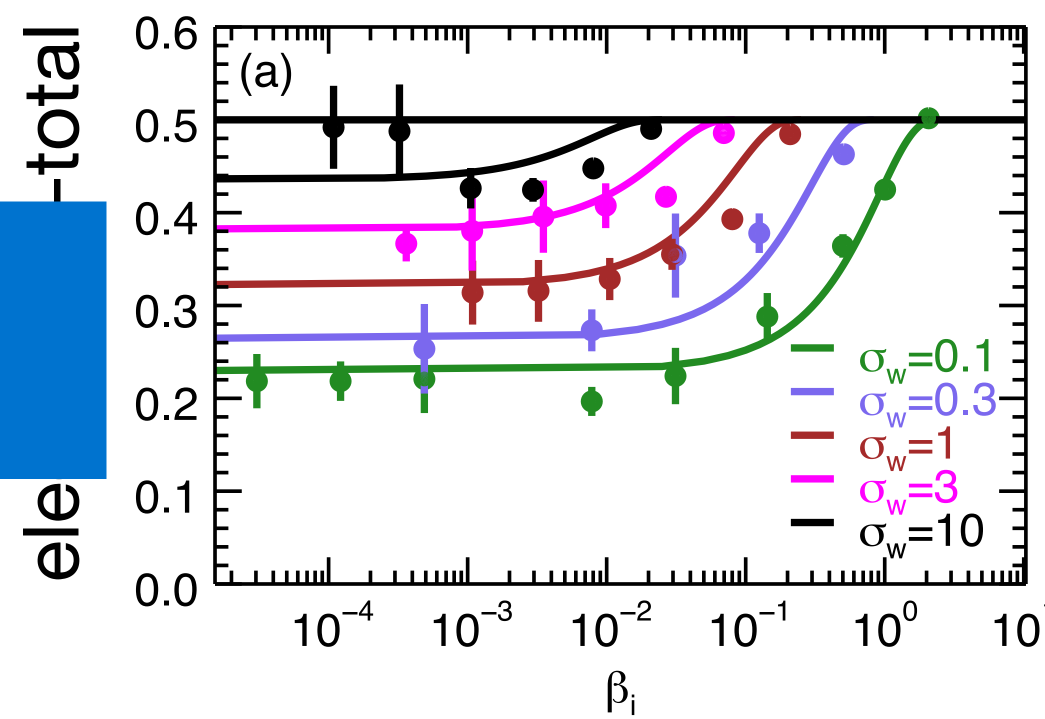

Reconnection, 2D PIC (Rowan+ 2017)

Dissipation scale turbulence in accretion disks

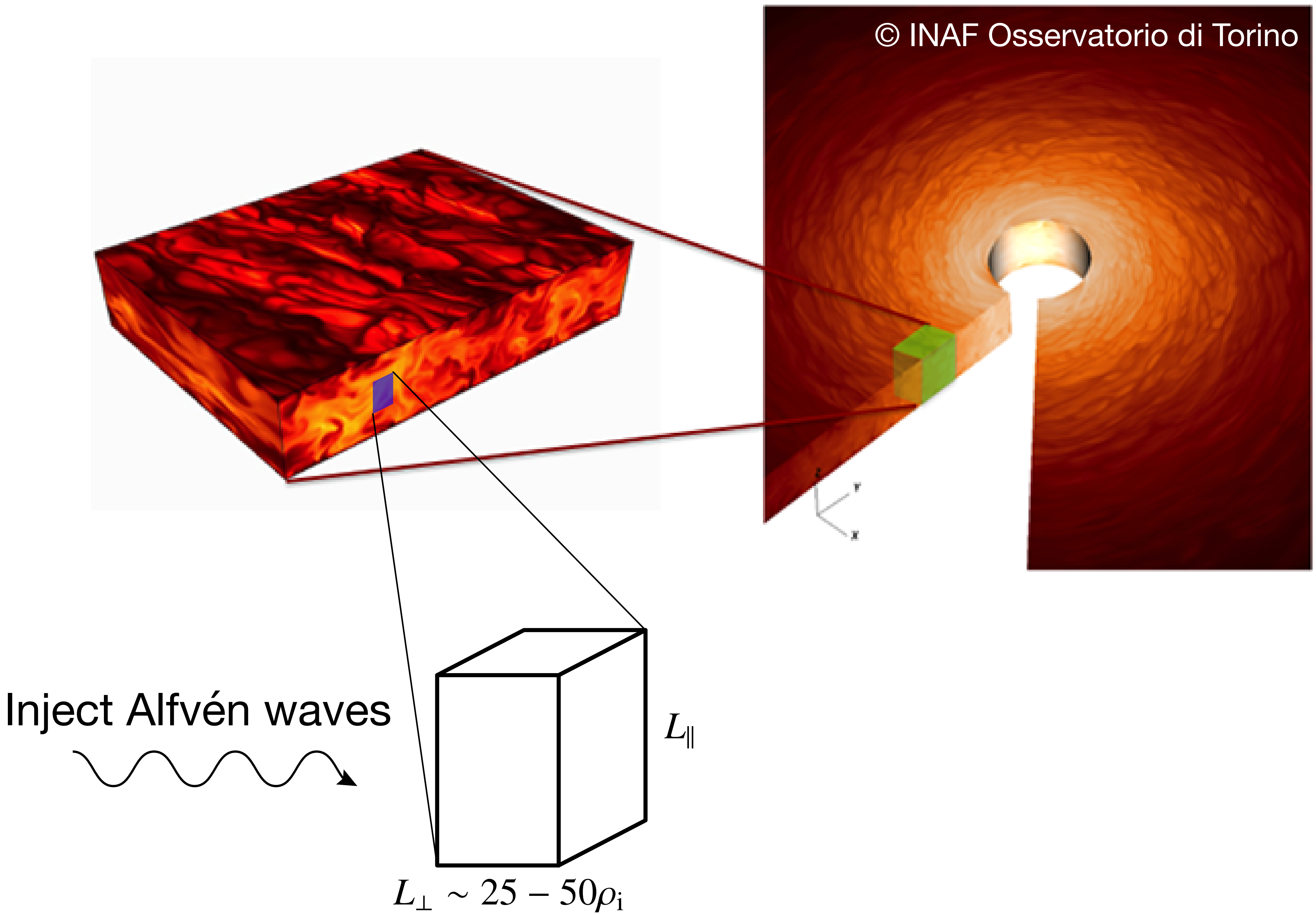

Anisotropy $k_{\perp} \gg k_{\|}$

Dissipation scale turbulence in accretion disks

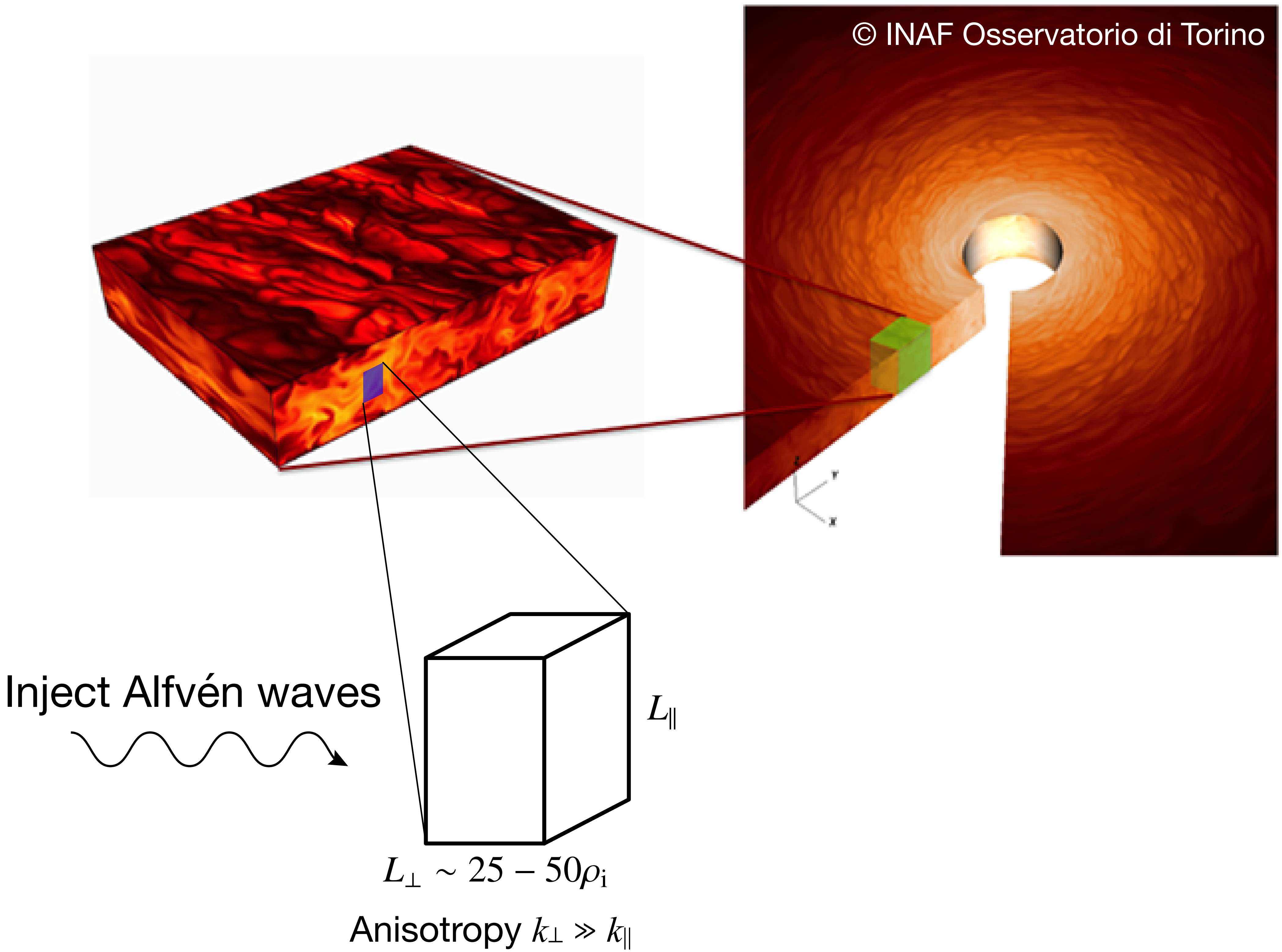

Dissipation scale turbulence in accretion disks

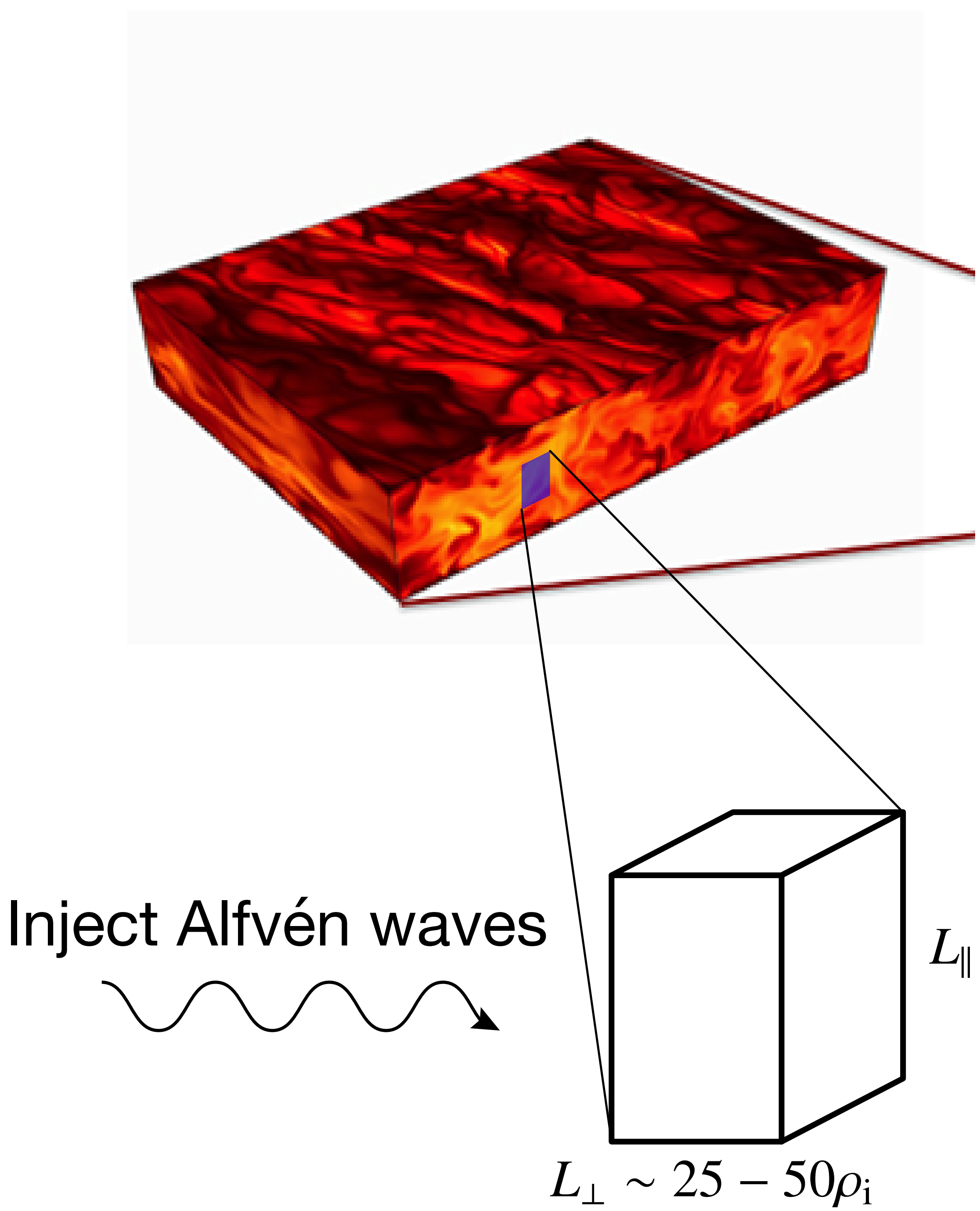

Anisotropy $k_\perp \gg k_\parallel$

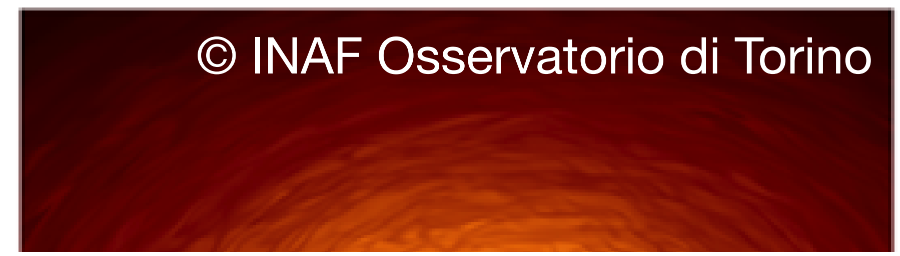

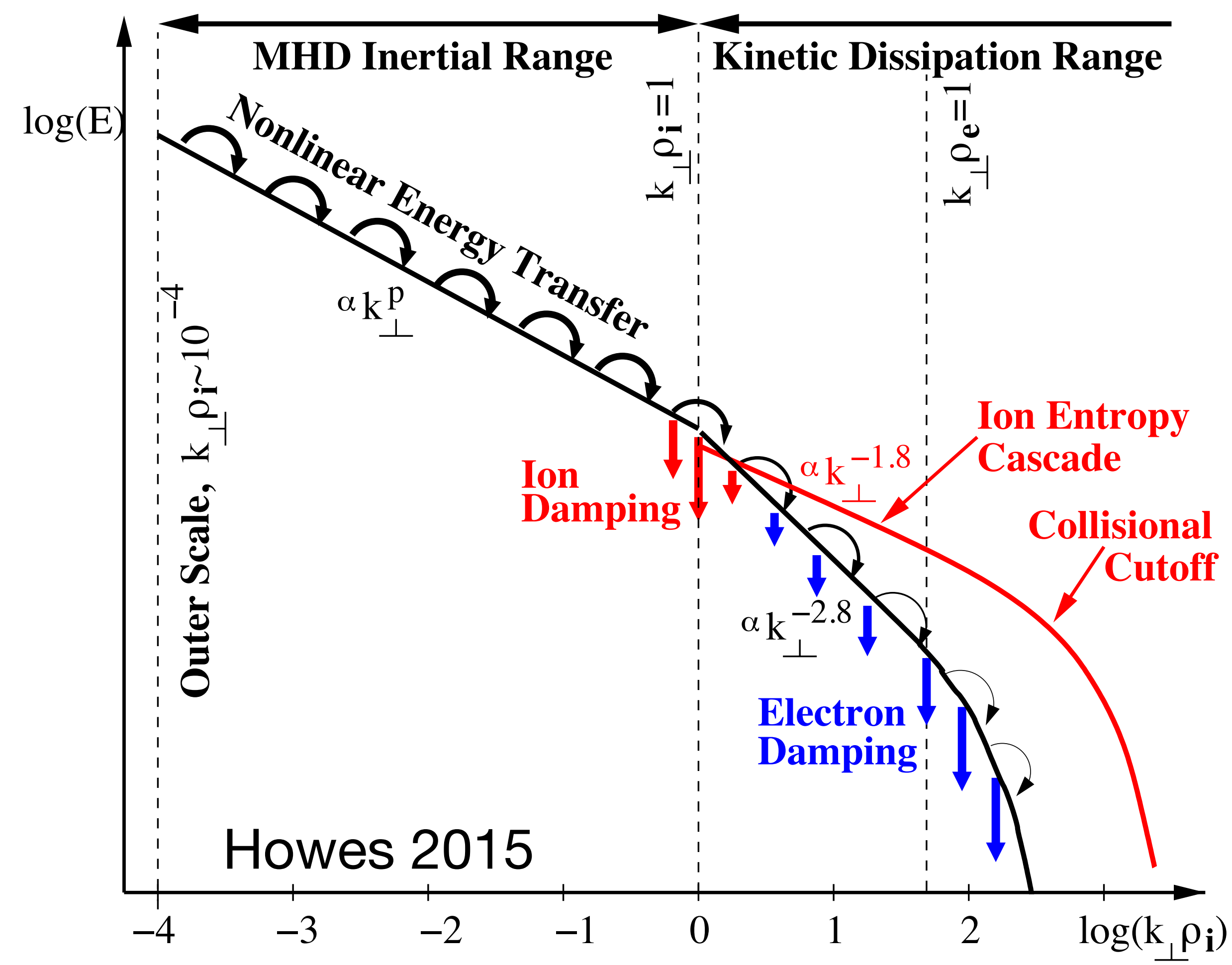

Dissipation scale turbulence in accretion disks

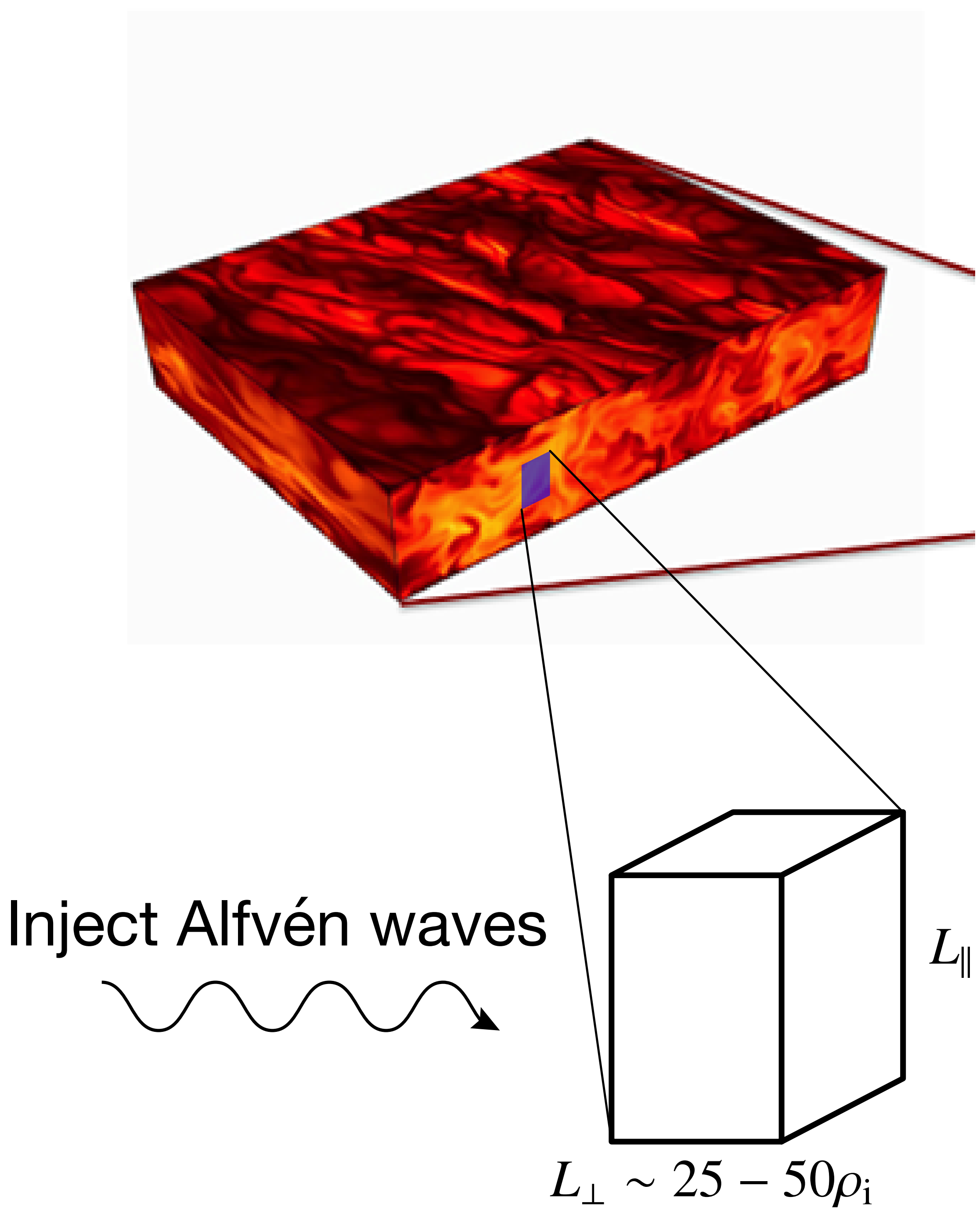

Anisotropy $k_{\perp} \gg k_{\parallel}$

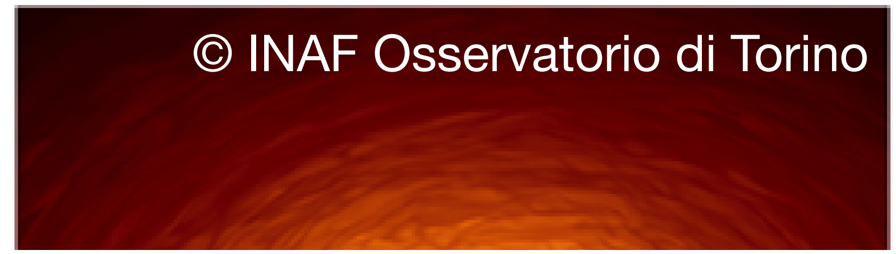

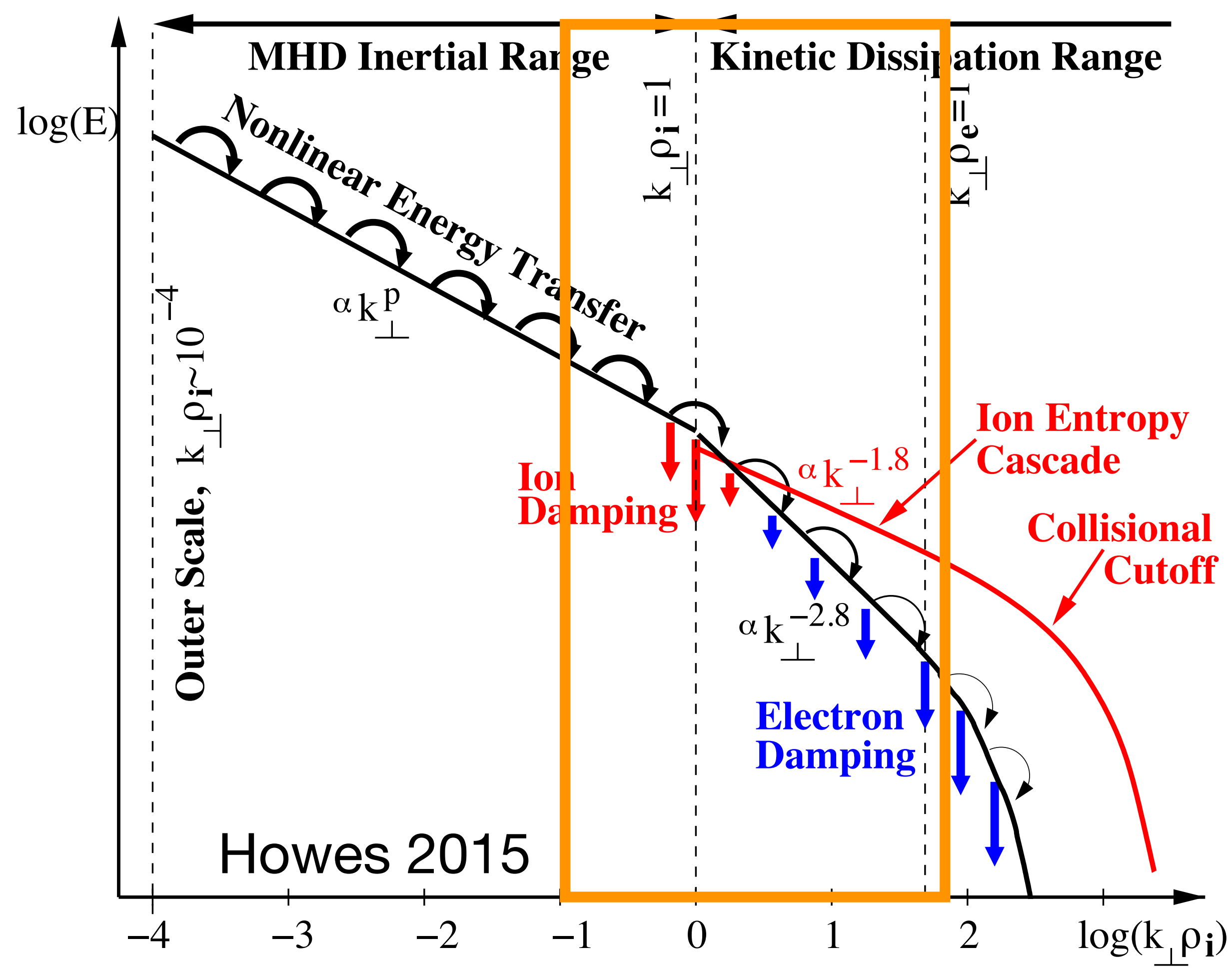

Full GK simulation (ion-electron scales)

$$\frac{\partial h_s}{\partial t} + v_\parallel \frac{\partial h_s}{\partial z} + \frac{c}{B_0}\{\langle\chi\rangle_{\mathbf{R}_s}, h_s\} = \frac{q_s}{T_s}\frac{\partial \langle\chi\rangle_{\mathbf{R}_s}}{\partial t}F_s + \langle C[h_s]\rangle_{\mathbf{R}_s}$$ & Maxwell's eqs

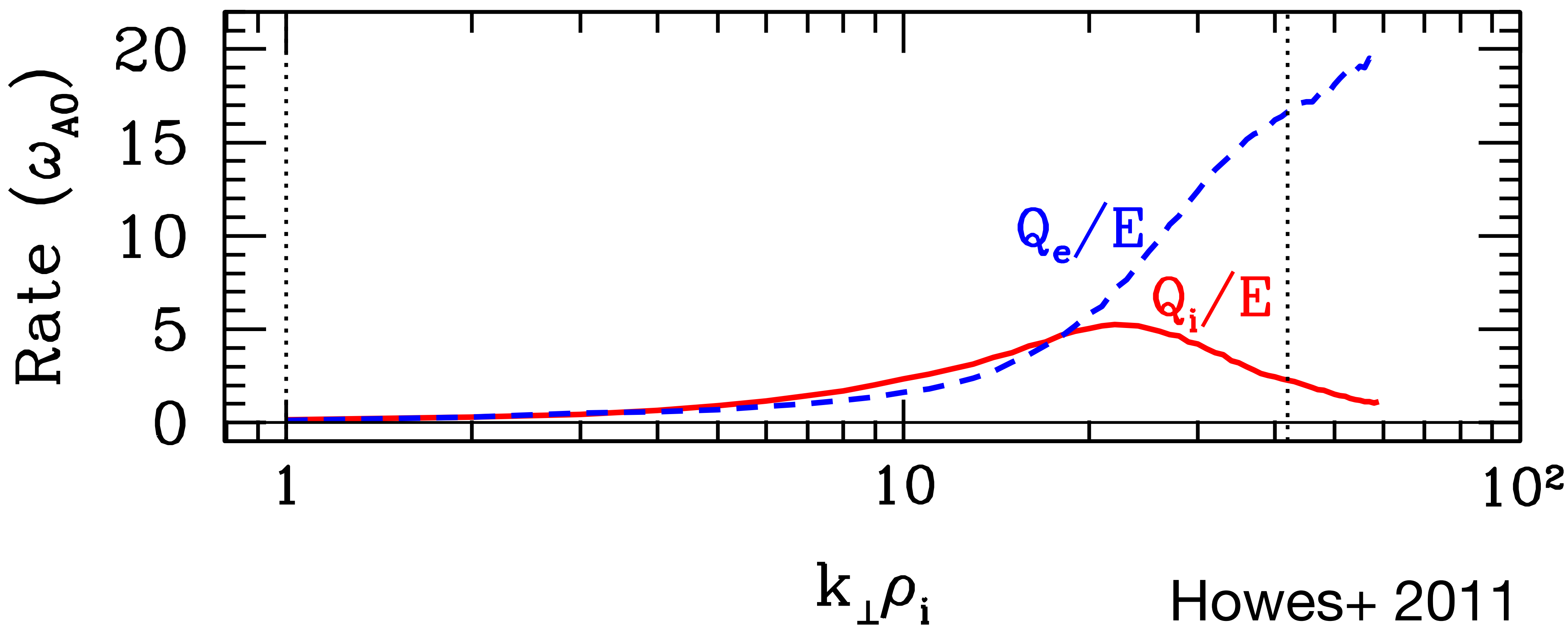

Howes+ 2011

✓ For $(\beta_i, T_i/T_e) = (1, 1)$

✓ $Q_e > Q_i$

✓ Q_i peaks at electron scale ← nonlinear phase mixing

(Tatsuno+ 2009)

Full GK simulation (MHD-ion-electron scales)

$$\frac{\partial h_s}{\partial t} + v_\parallel \frac{\partial h_s}{\partial z} + \frac{c}{B_0}\{\langle\chi\rangle_{\mathbf{R}_s}, h_s\} = \frac{q_s}{T_s}\frac{\partial \langle\chi\rangle_{\mathbf{R}_s}}{\partial t} F_s + \langle C[h_s]\rangle_{\mathbf{R}_s}$$ & Maxwell's eqs

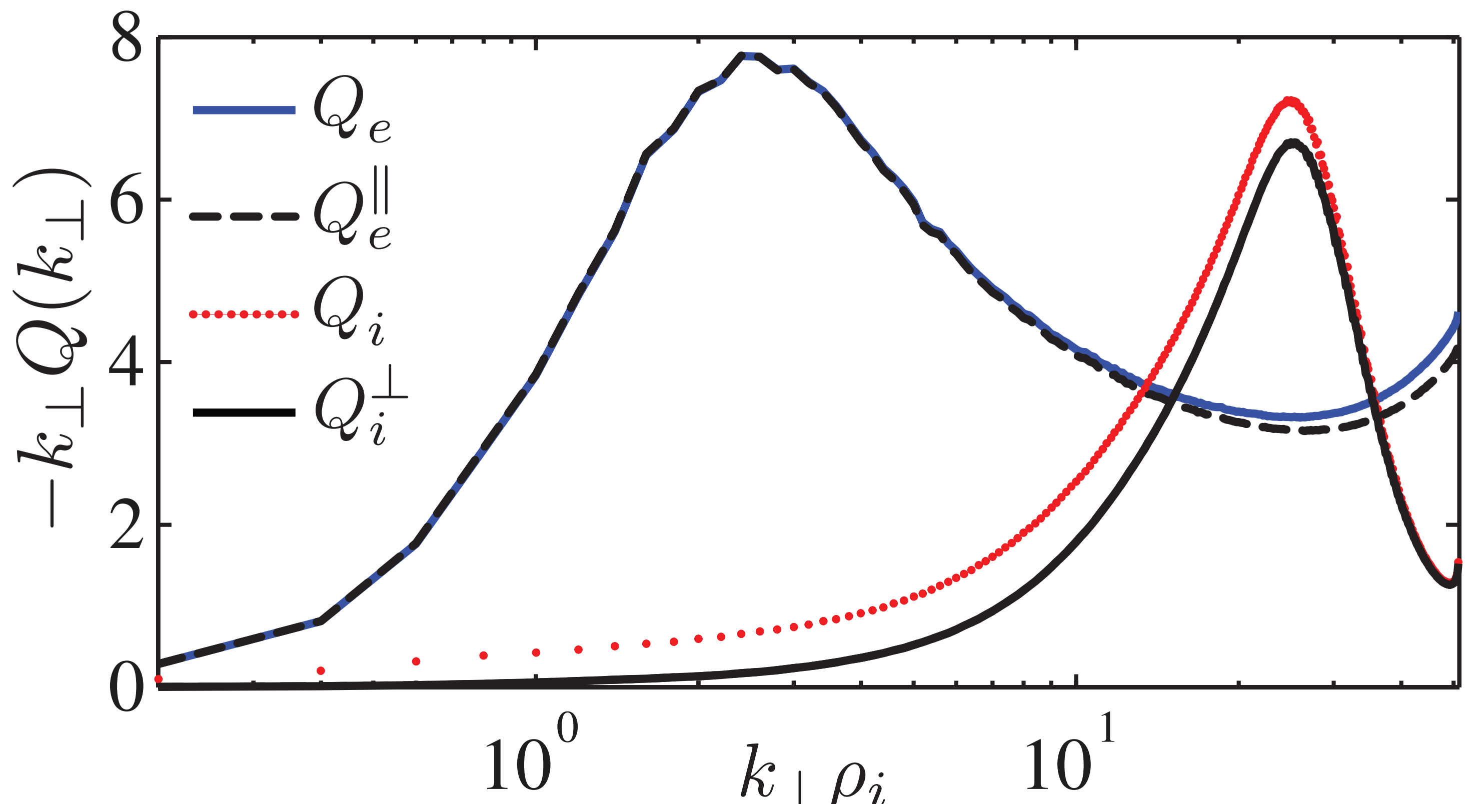

Told+ 2015, Navarro+ 2016

✓ For $(\beta_\mathrm{i}, T_\mathrm{i}/T_\mathrm{e}) = (1, 1)$

✓ $Q_\mathrm{e} / Q_\mathrm{total} \sim 70\%$

✓ Q_i via $v_\perp$ derivative ← nonlinear entropy cascade

✓ Q_e via $v_\parallel$ derivative ← linear Landau damping

Hybrid GK approach

- We need wide-ranged scan in the parameter space (β_i, T_i/T_e)
- Cannot afford full GK approach → Hybrid approach
- Heating partition is decided at $k_\perp \rho_i \sim 1$ (Schekochihin+ 2009)

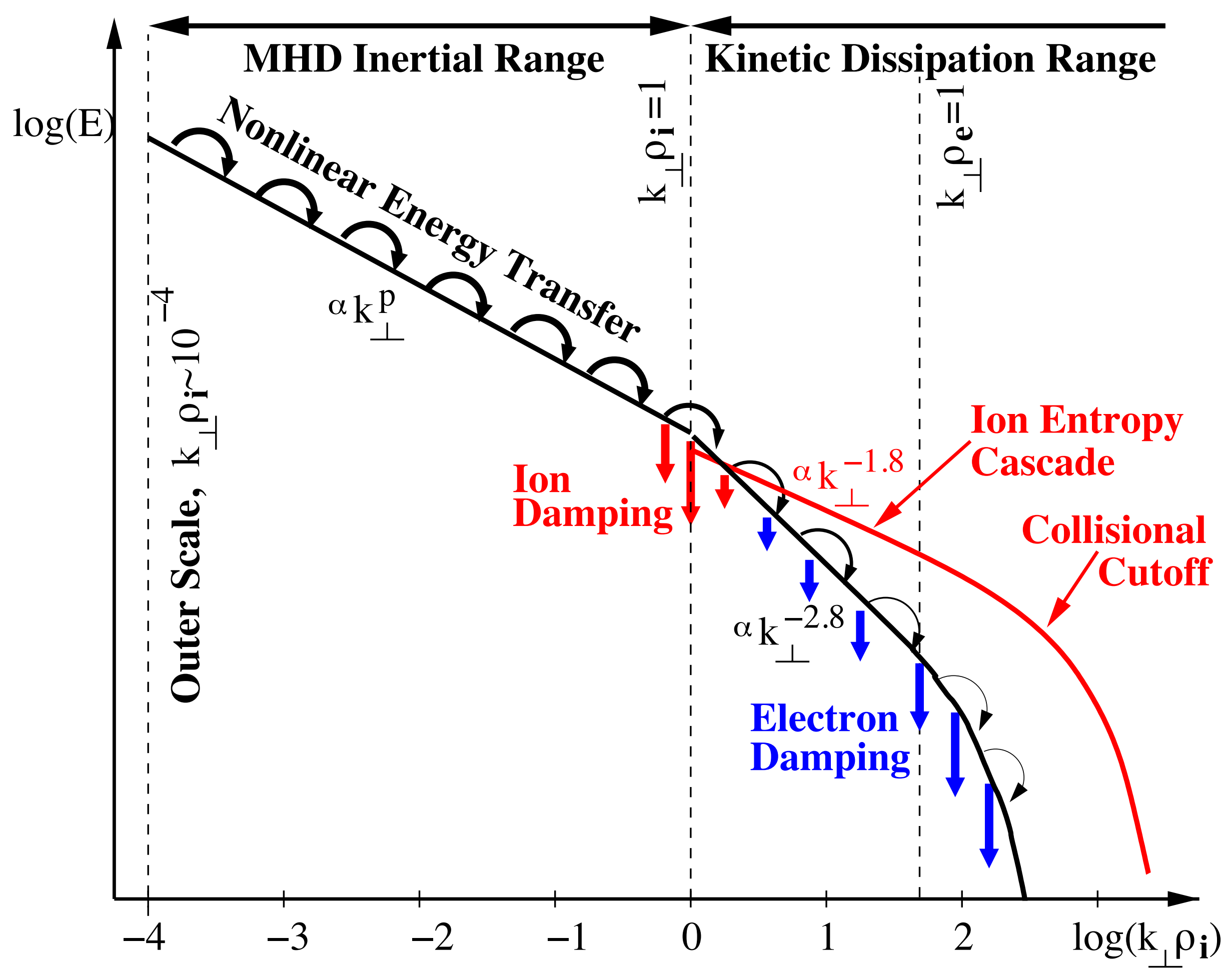

Hybrid GK approach

- ✓ We need wide-ranged scan in the parameter space (β_i, T_i/T_e)
- ✓ Cannot afford full GK approach → Hybrid approach
- ✓ Heating partition is decided at $k_\perp \rho_i \sim 1$ (Schekochihin+ 2009)

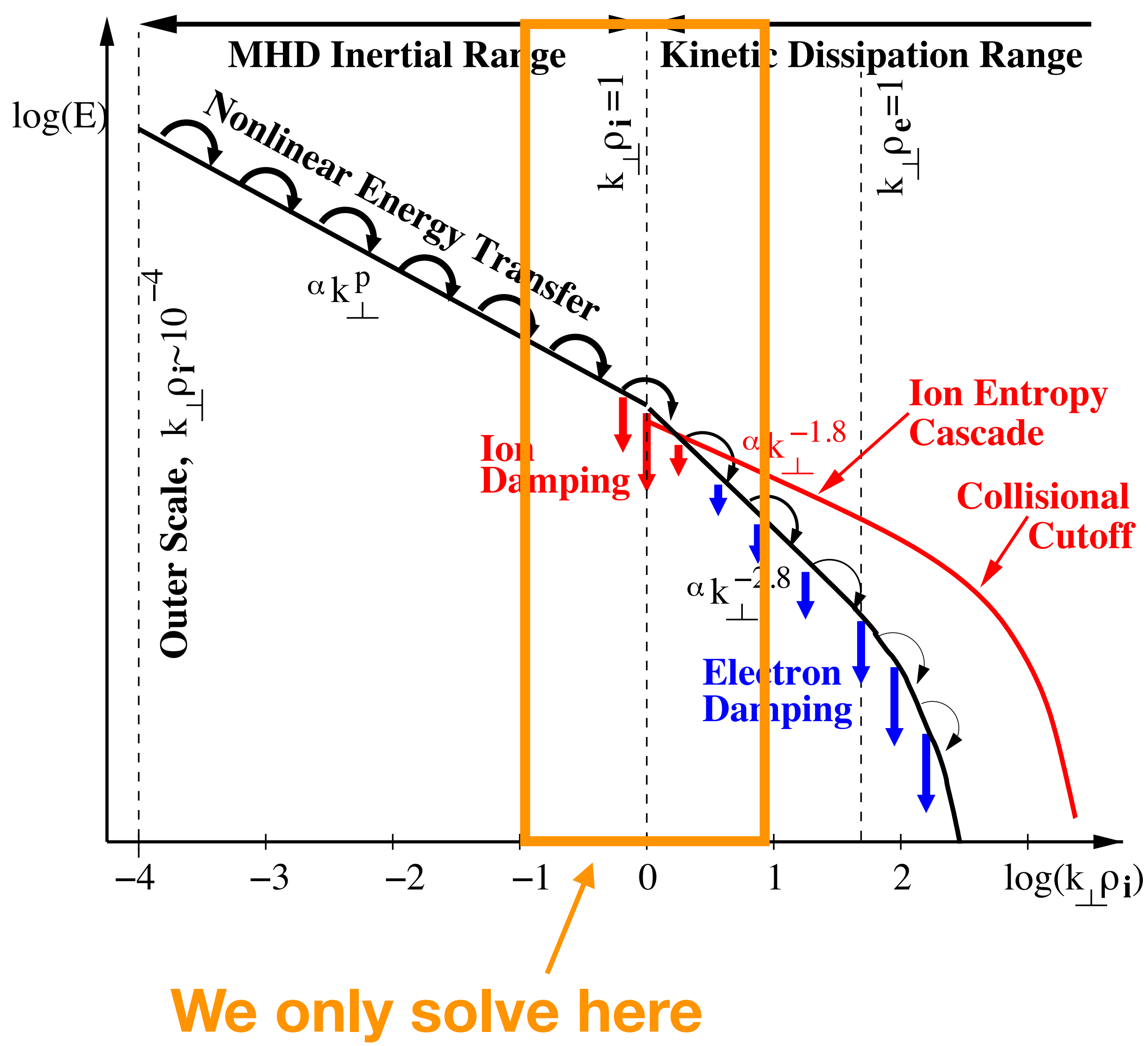

Hybrid GK approach

✓ Gyrokinetic ions + isothermal electron fluid model

[$(m_e/m_i)^{1/2} \ll 1$ limit of electron GK eq.]

$$\frac{\partial h_i}{\partial t} + v_\parallel \frac{\partial h_i}{\partial z} + \frac{c}{B_0}\{\langle\chi\rangle_{\mathbf{R}_i}, h_i\} = \frac{Ze}{T_i}\frac{\partial\langle\chi\rangle_{\mathbf{R}_i}}{\partial t}F_i + \langle C[h_i]\rangle_{\mathbf{R}_i}$$

$$\frac{\partial}{\partial t}\left(\frac{\delta n_e}{n_e} - \frac{\delta B_\parallel}{B_0}\right) + \frac{c}{B_0}\left\{\phi - \frac{T_e}{e}\frac{\delta n_e}{n_e}, \frac{\delta n_e}{n_e} - \frac{\delta B_\parallel}{B_0}\right\} + \frac{\partial u_{\parallel e}}{\partial z} = \frac{1}{B_0}\{A_\parallel, u_{\parallel e}\}$$

$$\frac{\partial A_\parallel}{\partial t} + \frac{c}{B_0}\left\{\phi - \frac{T_e}{e}\frac{\delta n_e}{n_e}, A_\parallel\right\} + c\frac{\partial\phi}{\partial z} - \frac{cT_e}{e}\frac{\partial}{\partial z}\left(\frac{\delta n_e}{n_e}\right) = 0$$

& Maxwell's eqs

✓ Use `AstroGK` code (Numata+ 2010) with isothermal electron fluid

(Kawazura & Barnes 2018)

Numerical set up

- ✓ Simulation box : $0.125 \leqq k_x\rho_\mathrm{i},\ k_y\rho_\mathrm{i} \leqq 5.25$ or $(0.25 \leqq k_x\rho_\mathrm{i},\ k_y\rho_\mathrm{i} \leqq 5.25)$
- ✓ Inject Alfvén wave at the box scale via oscillating Langevin antennas (TenBarge+ 2014) $\rightarrow$ P_ant
- ✓ Ion dissipation via collision + hypercollision $\rightarrow$ Q_i
- ✓ Electron dissipation via hyperviscosity + hyperresistivity $\rightarrow$ Q_e

$$\frac{\mathrm{d}W_\mathrm{tot}}{\mathrm{d}t} = P_\mathrm{ant} - Q_\mathrm{i} - Q_\mathrm{e}$$

- ✓ In a stationary state, $\langle \mathrm{d}W_\mathrm{tot}/\mathrm{d}t \rangle \simeq 0$

Result : heating ratio

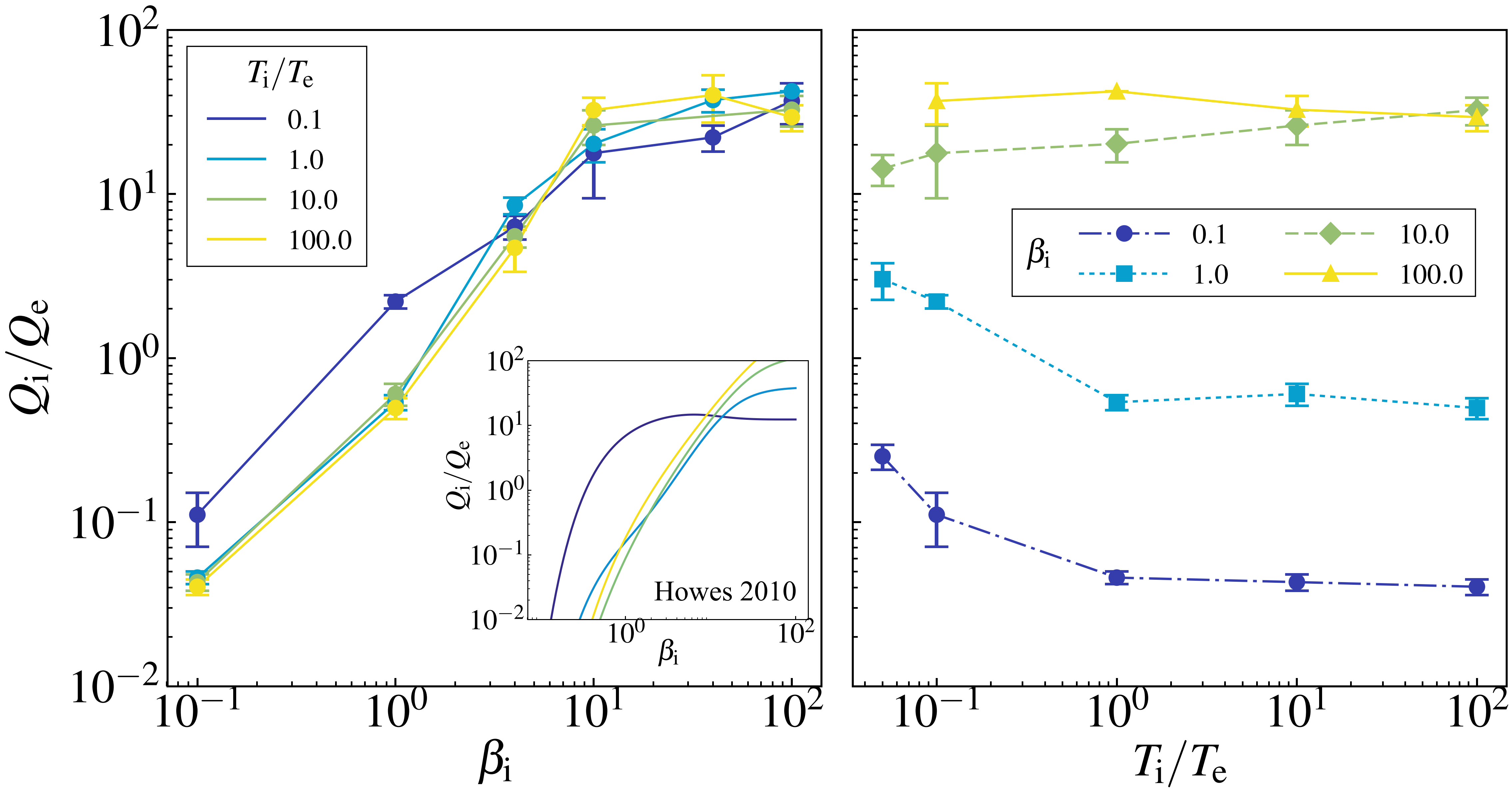

- ✓ $Q_i/Q_e \sim 0.6$ at $(\beta_i, T_i/T_e) = (1, 1)$ ← Consistent with full GK (Navarro+ 2016)
- ✓ Increasing function of β_i ← The same trend as Howes'
- ✓ Insensitive to T_i/T_e
- ✓ $Q_i/Q_e \rightarrow 0$ when $\beta_i \rightarrow 0$ (as predicted in Zocco & Schekochihin, 2011)

Result : heating ratio

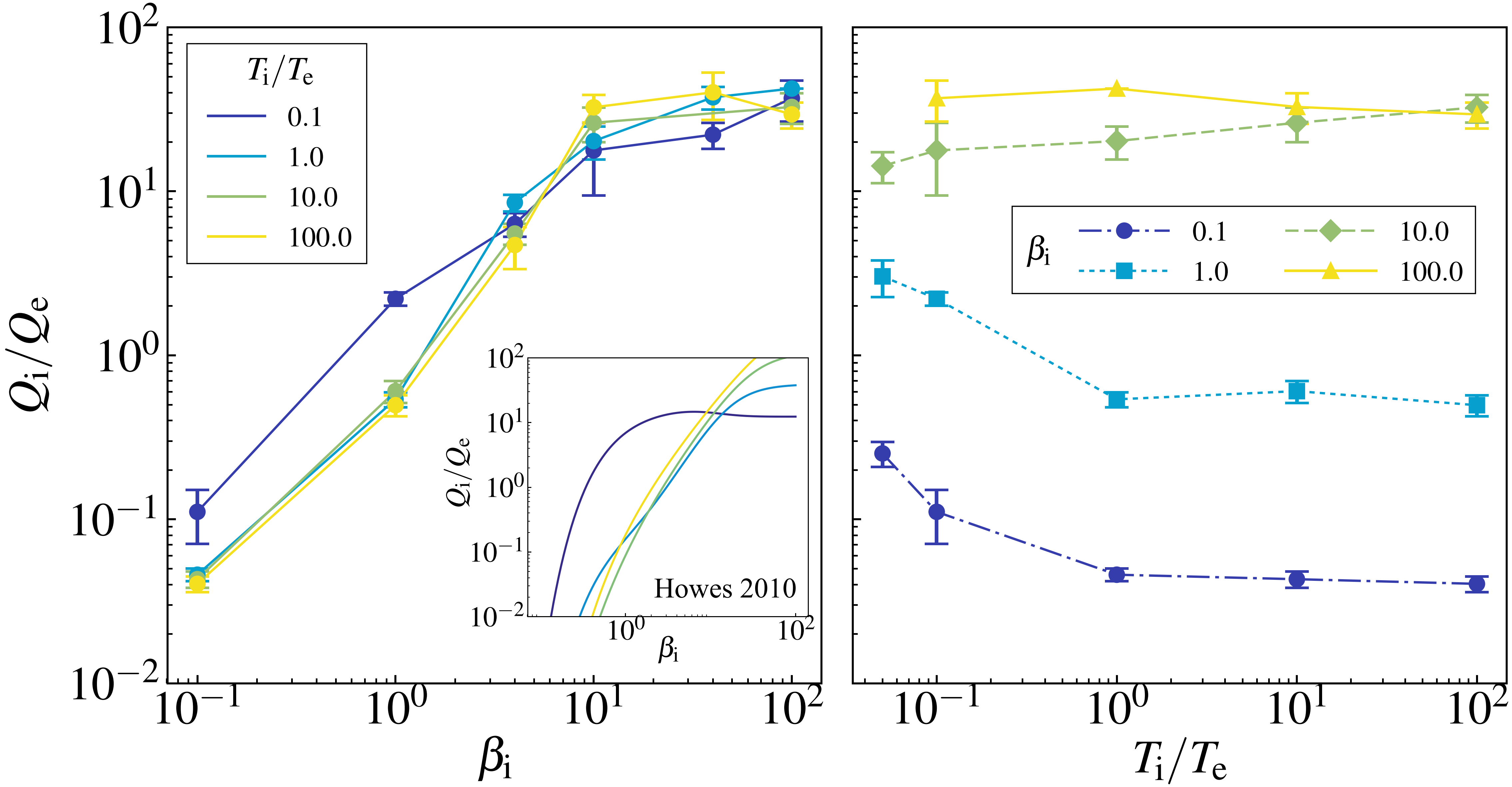

- ✓ Significantly different from Howes' at high β_i and low β_i
- ✓ At high β_i, Q_i/Q_e has ceiling ($\lesssim$ 30)
- ✓ At low β_i, Q_i/Q_e is several orders of magnitude larger than Howes'
- ✓ In Sgr A*, mid plane : $\beta_i \sim 10$, Jet region : $\beta_i \sim 0.1$

Result : heating ratio

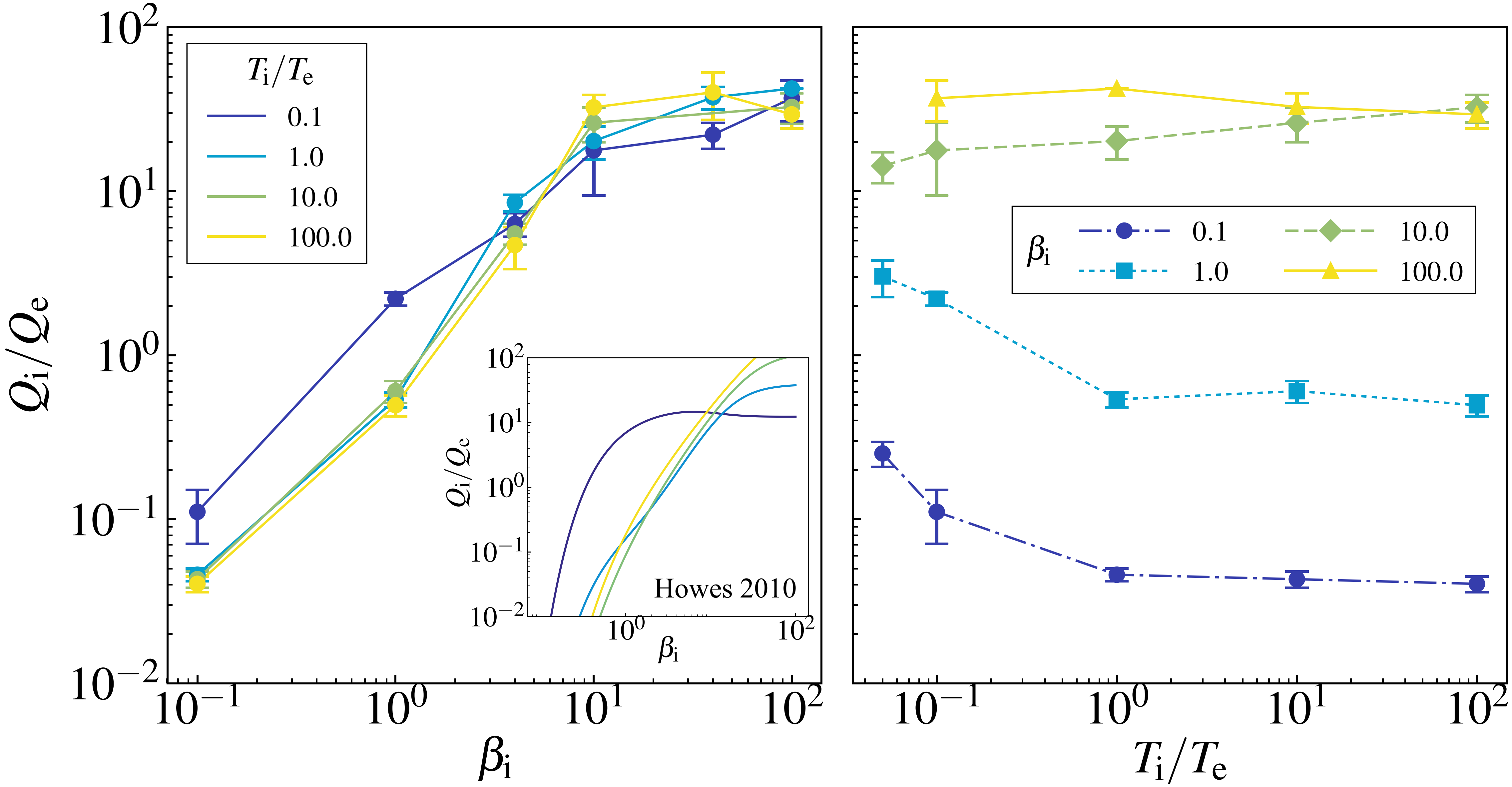

Why is there a ceiling at high β_i?

Why is it greater than Howes' at low β_i?

→ Future work

Result : heating ratio

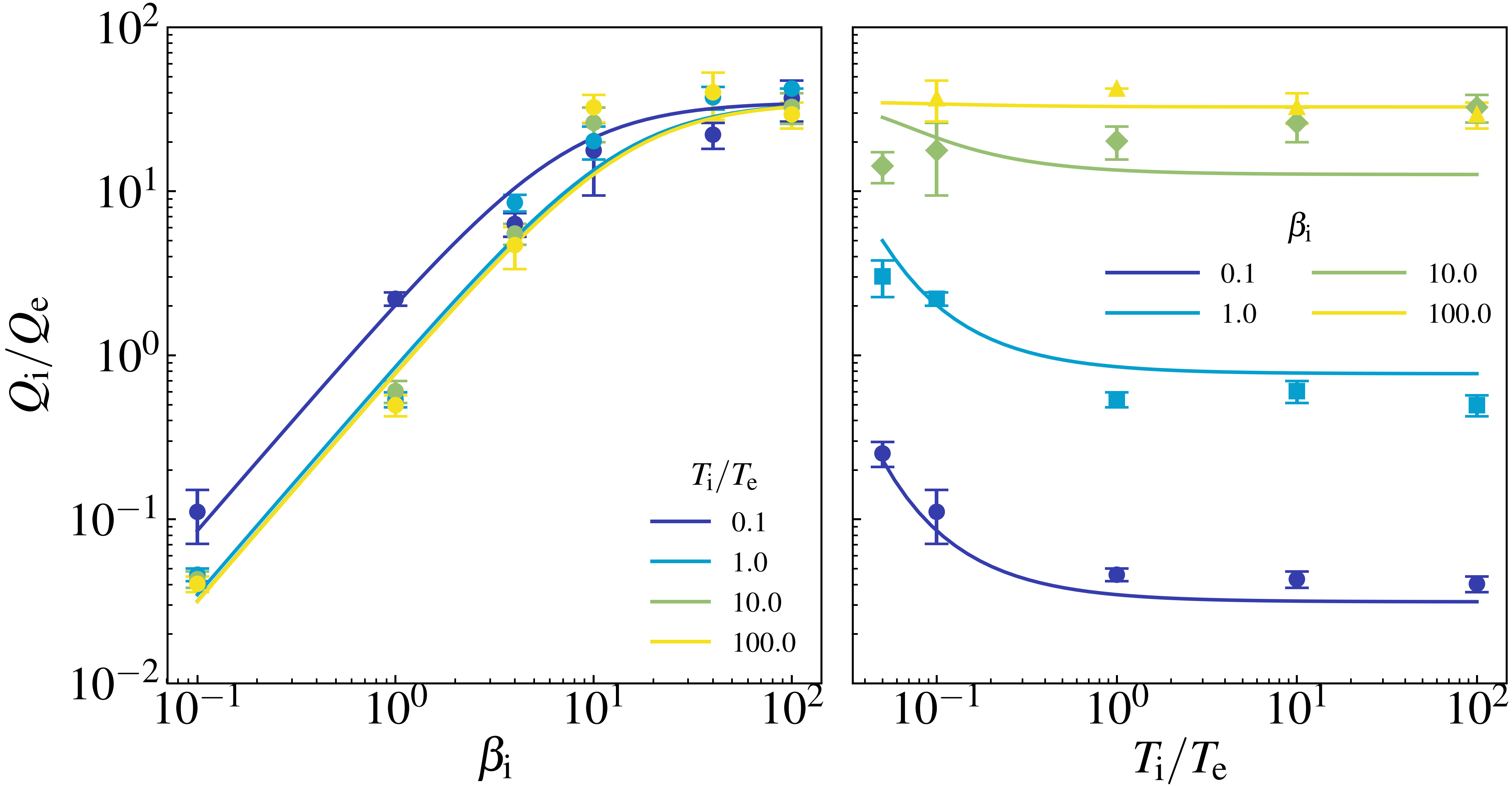

✓ New heating ratio prescription

$$\frac{Q_i}{Q_e}(\beta_i, T_i/T_e) = \frac{35.0}{1 + (\beta_i/15.0)^{-1.4}\exp(-0.1T_e/T_i)}$$

Result : k-spectrum

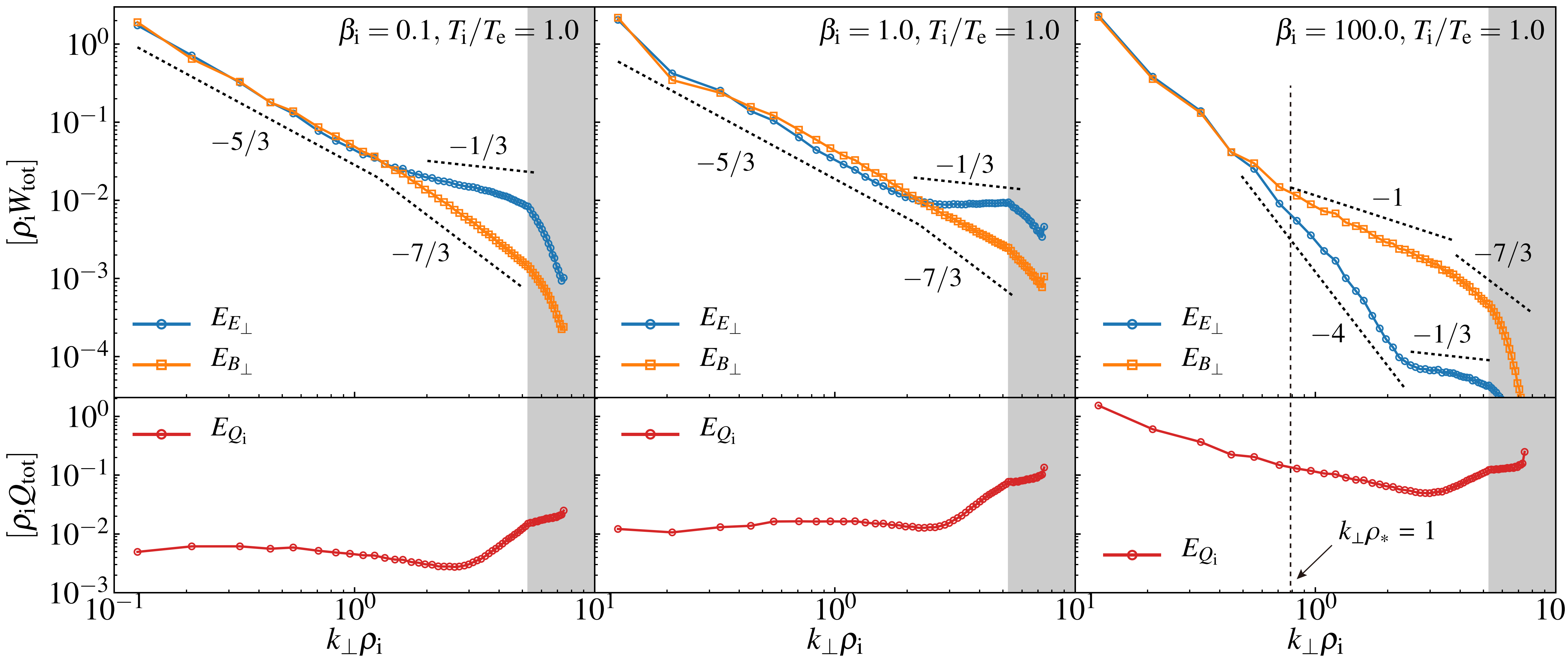

Result : k-spectrum (low-mid β_i)

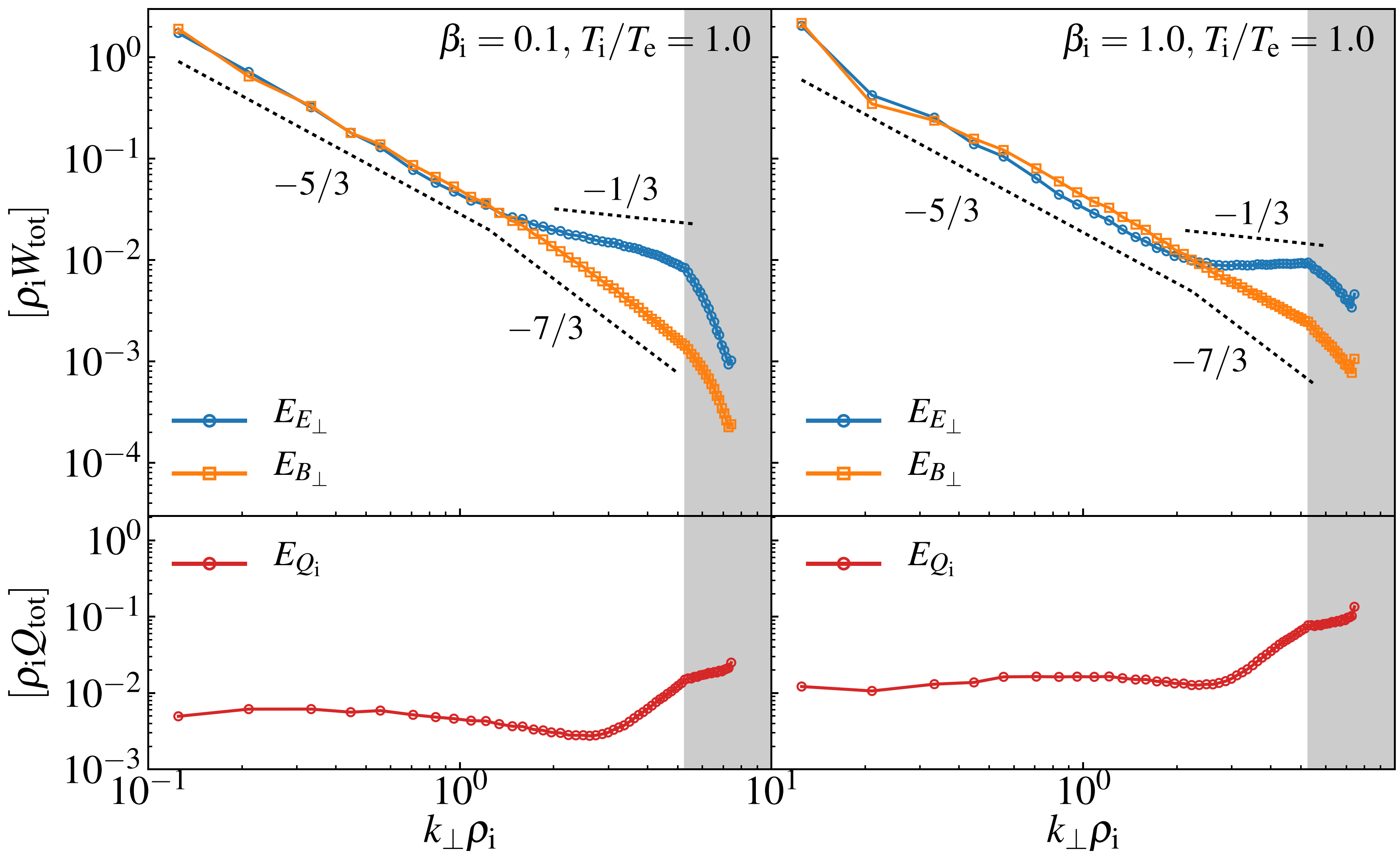

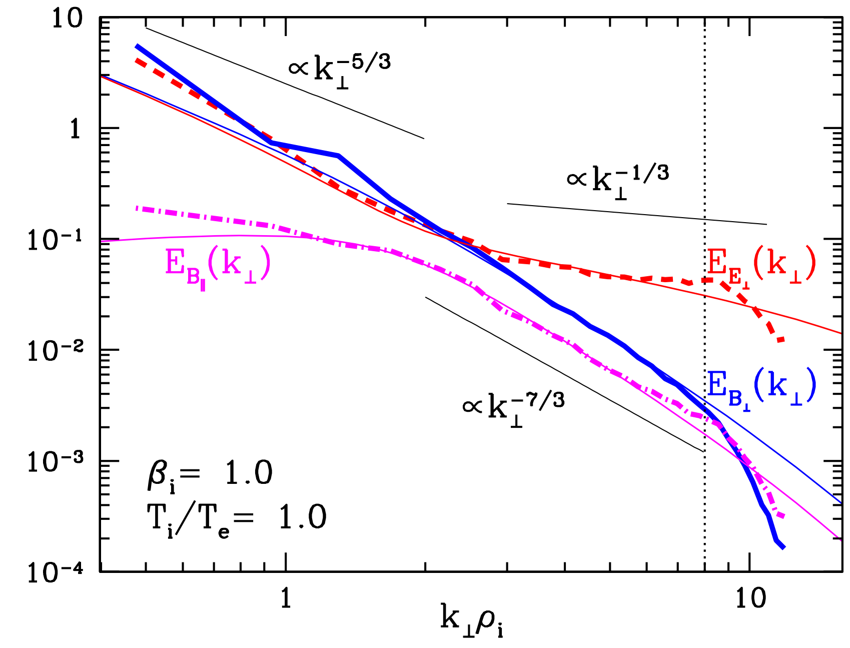

Howes 2008

✓ For $\beta_i = 0.1$ and 1

- A familiar AW/KAW transition at $k_\perp \rho_i = 1$

Result : k-spectrum (low-mid β_i)

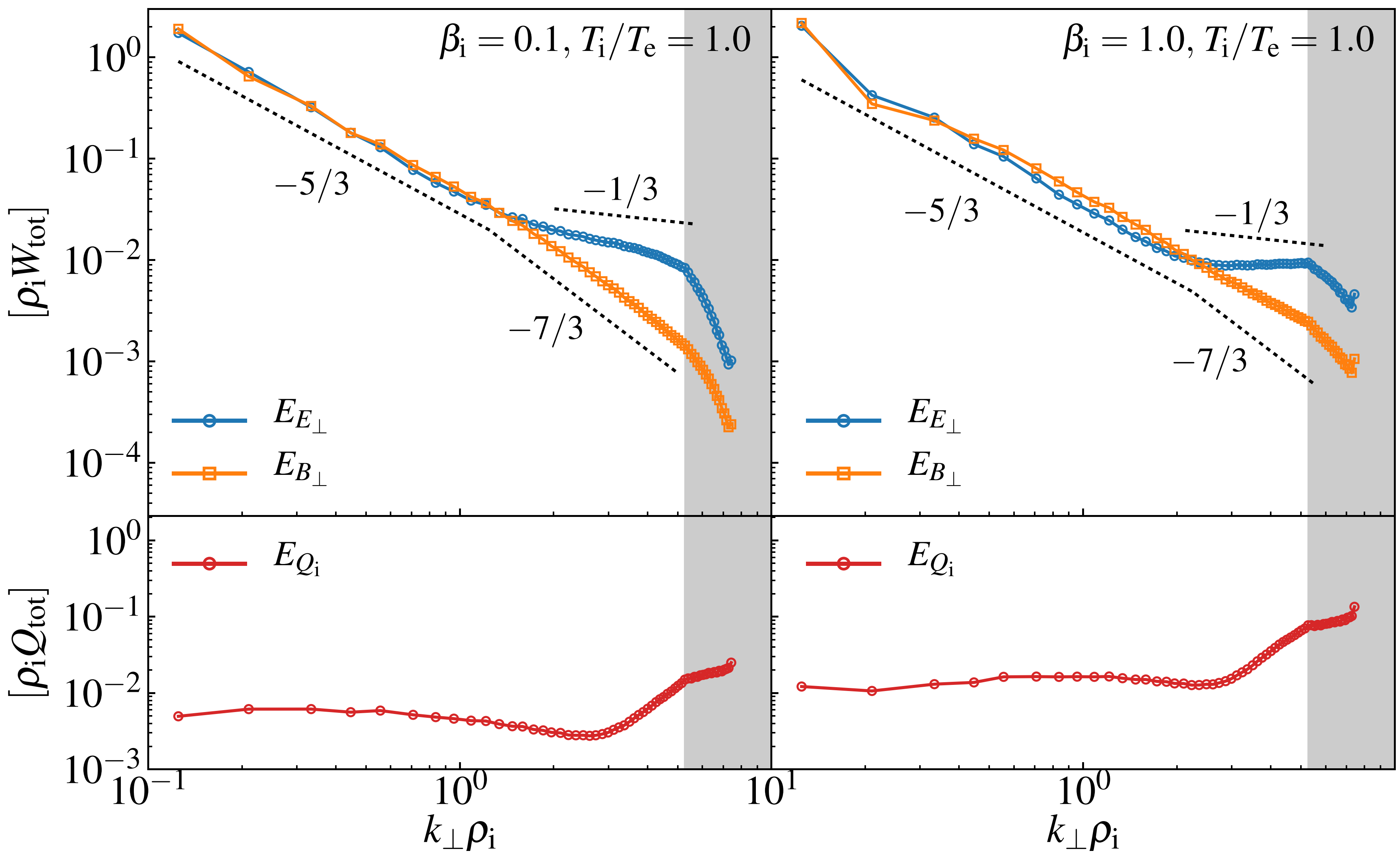

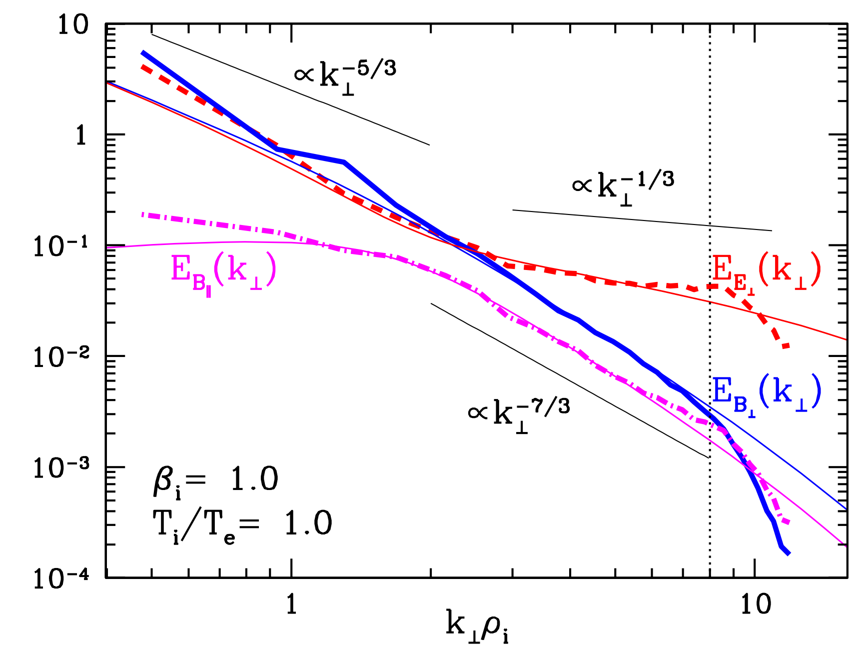

Howes 2008

✓ For $\beta_\mathrm{i} = 0.1$ and 1

- A familiar AW/KAW transition at $k_\perp \rho_\mathrm{i} = 1$
- Heating mainly at a grid scale (electron scale)

⬆ consistent with Howes, Told, …

Result : k-spectrum (high β_i)

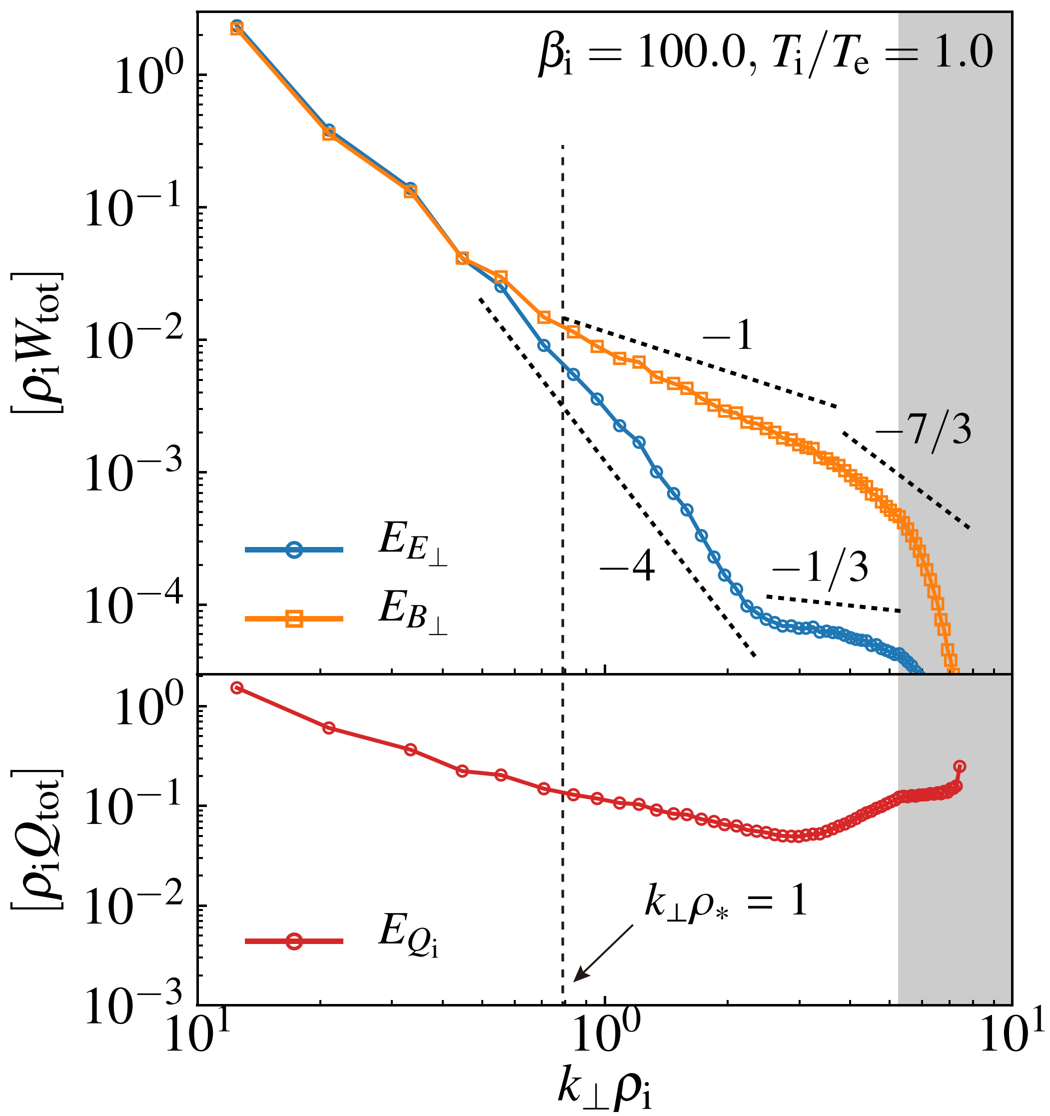

✓ For $\beta_i = 100$

- Huge drop of electric field $\leftarrow$ $\Phi_{\mathbf{k}} = \pm \dfrac{k_\perp \rho_i}{\sqrt{(1 + ZT_e/T_i)\left[2 + \beta_i(1 + ZT_e/T_i)\right]}} \Psi_{\mathbf{k}}$

(Schekochihin+ 2009)

Result : k-spectrum (high β_i)

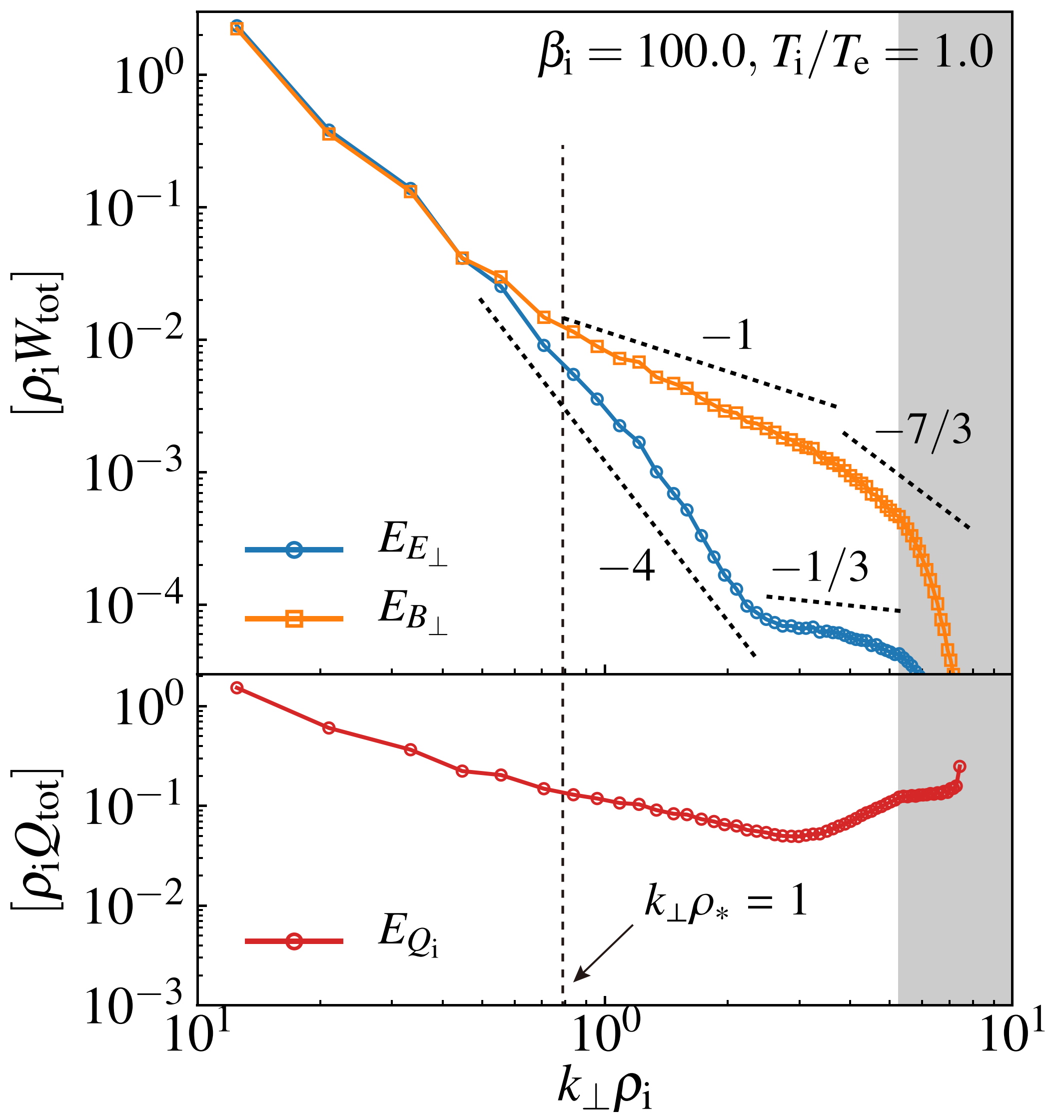

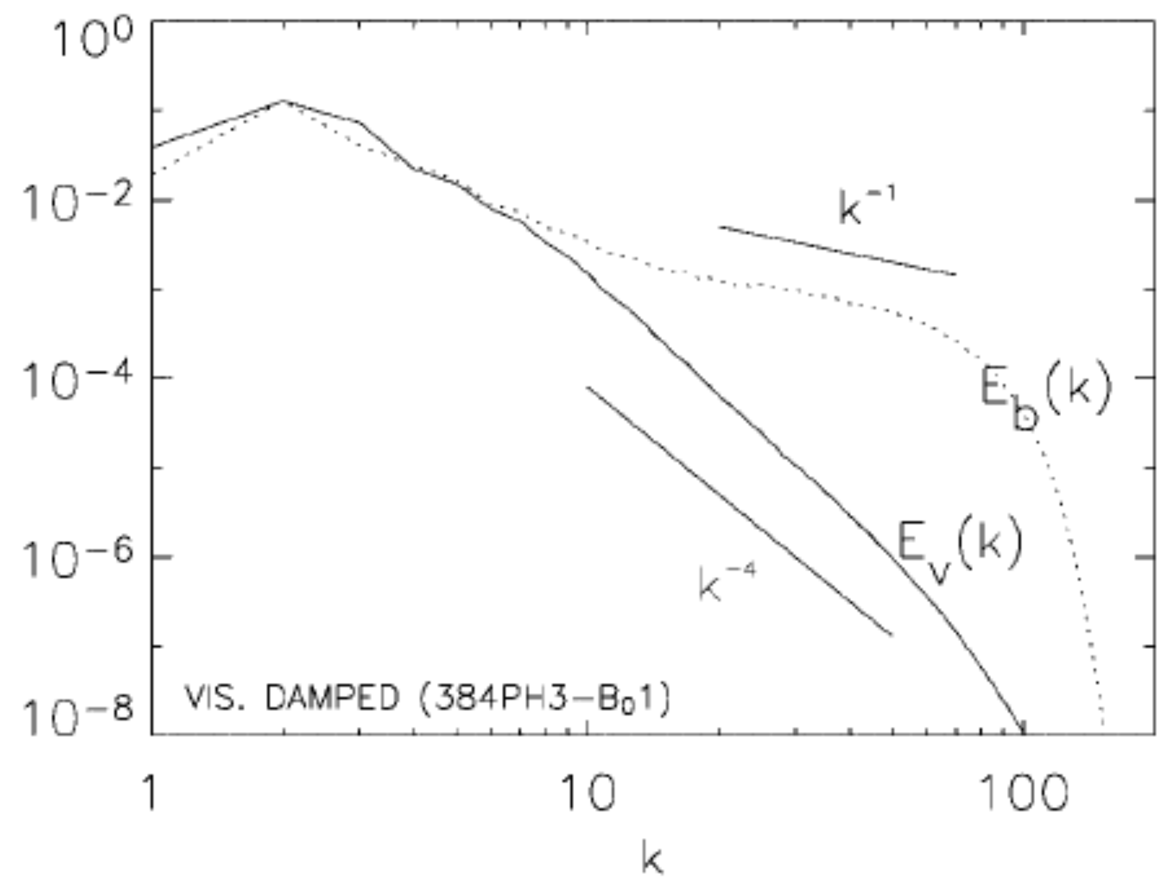

High Pm MHD turbulence, Cho+ 2002

✓ For $\beta_i = 100$

- Huge drop of electric field $\leftarrow$ $\Phi_{\mathbf{k}} = \pm \dfrac{k_\perp \rho_i}{\sqrt{(1 + ZT_e/T_i)\left[2 + \beta_i(1 + ZT_e/T_i)\right]}} \Psi_{\mathbf{k}}$

(Schekochihin+ 2009)

Result : k-spectrum (high β_{i})

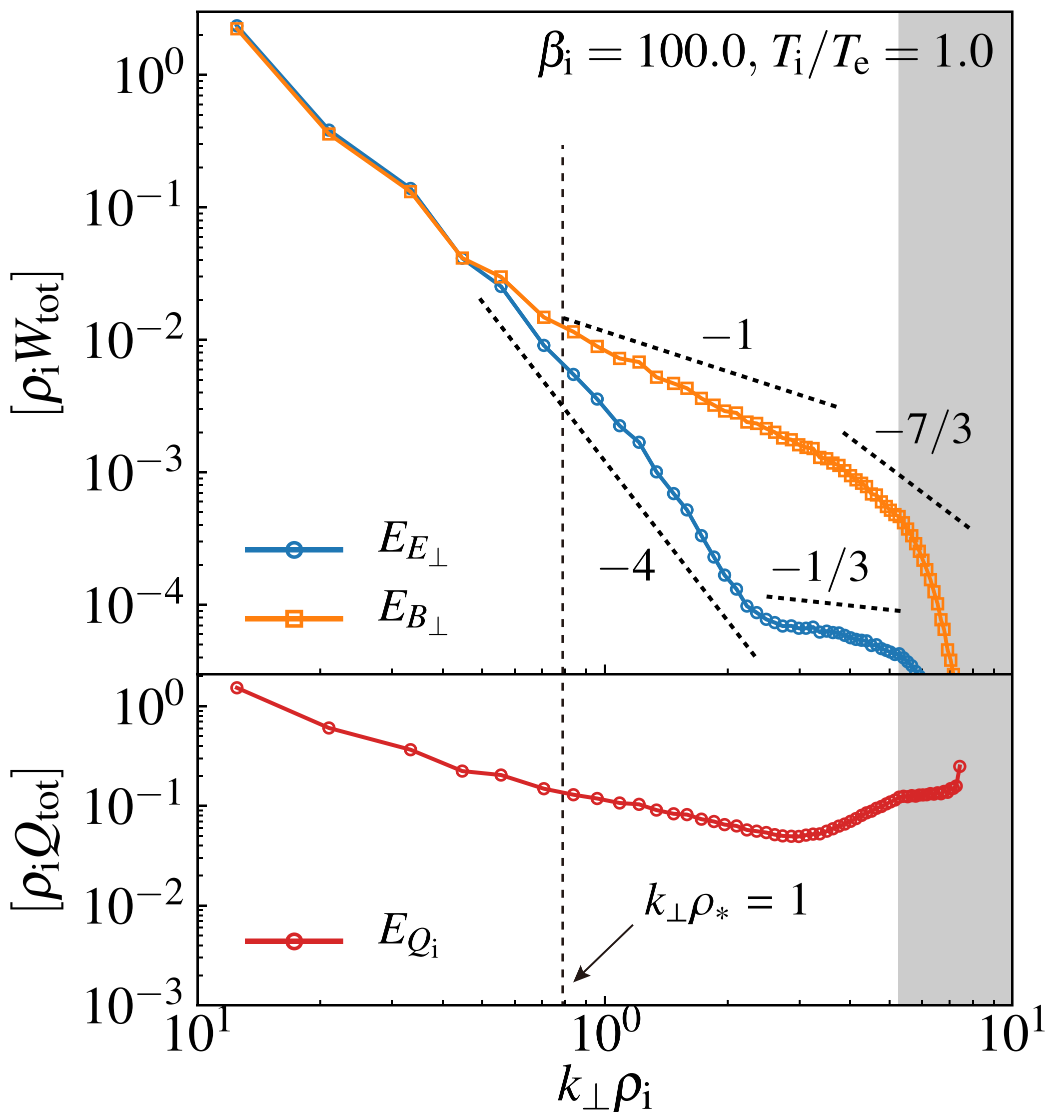

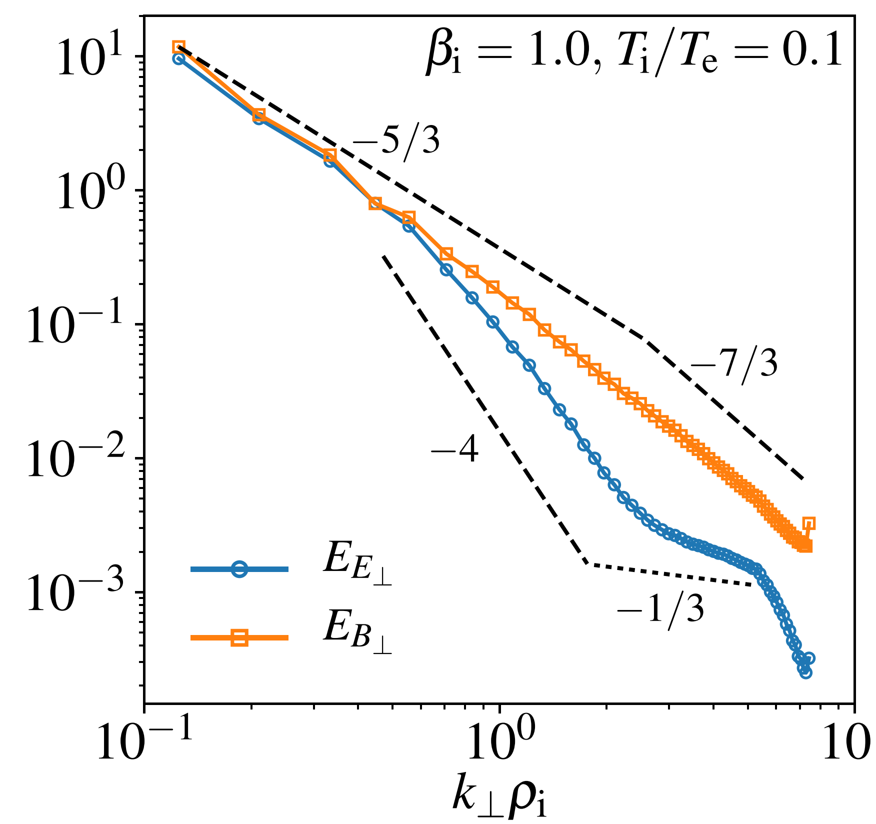

Similar drop for low $T_{\mathrm{i}}/T_{\mathrm{e}}$
but $E_{\mathrm{B}\perp}$ is as usual

✓ For $\beta_{\mathrm{i}} = 100$

- Huge drop of electric field $\leftarrow$ $\Phi_{\mathbf{k}} = \pm \dfrac{k_\perp \rho_{\mathrm{i}}}{\sqrt{(1 + ZT_{\mathrm{e}}/T_{\mathrm{i}})\left[2 + \beta_{\mathrm{i}}(1 + ZT_{\mathrm{e}}/T_{\mathrm{i}})\right]}} \Psi_{\mathbf{k}}$

(Schekochihin+ 2009)

Result : k-spectrum (high β_i)

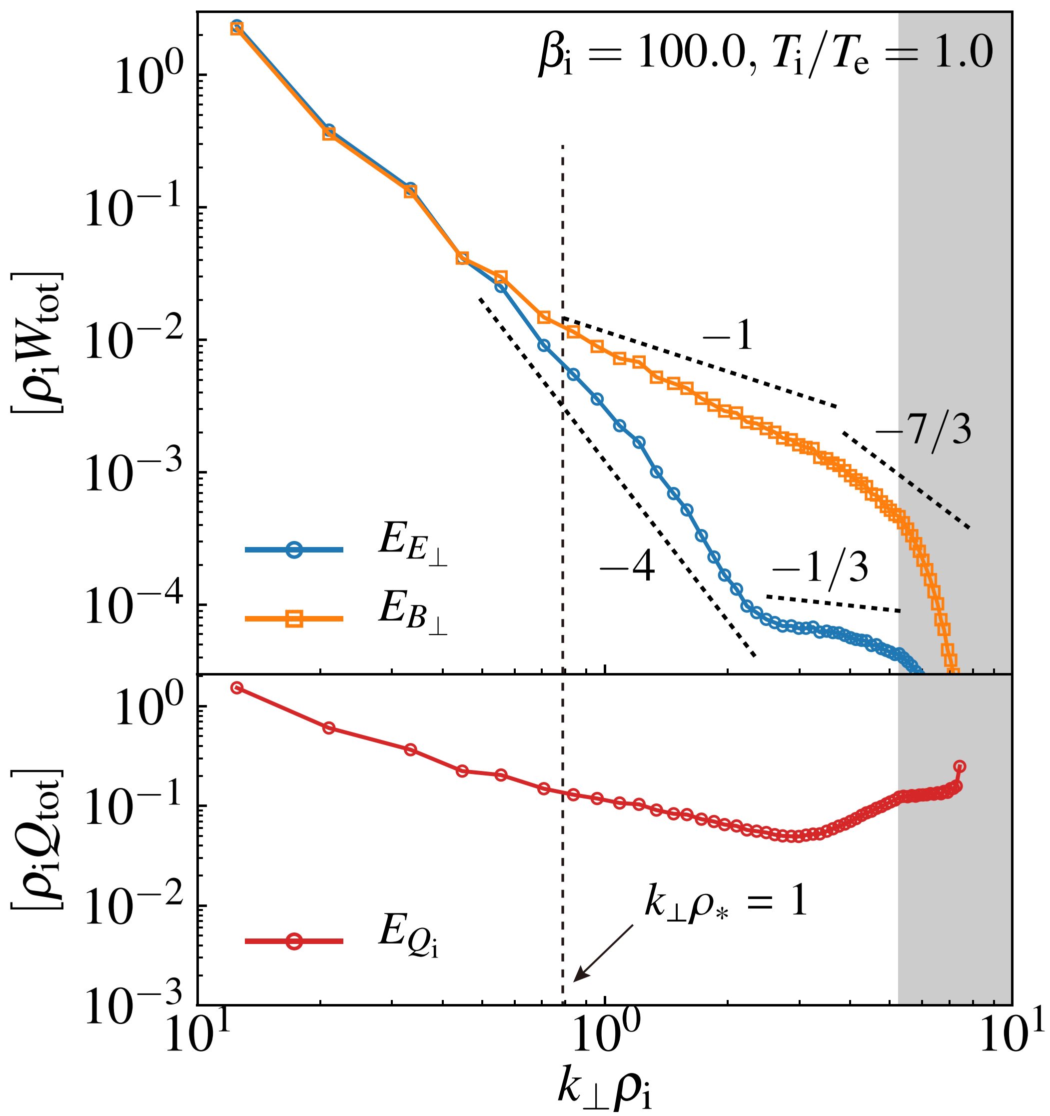

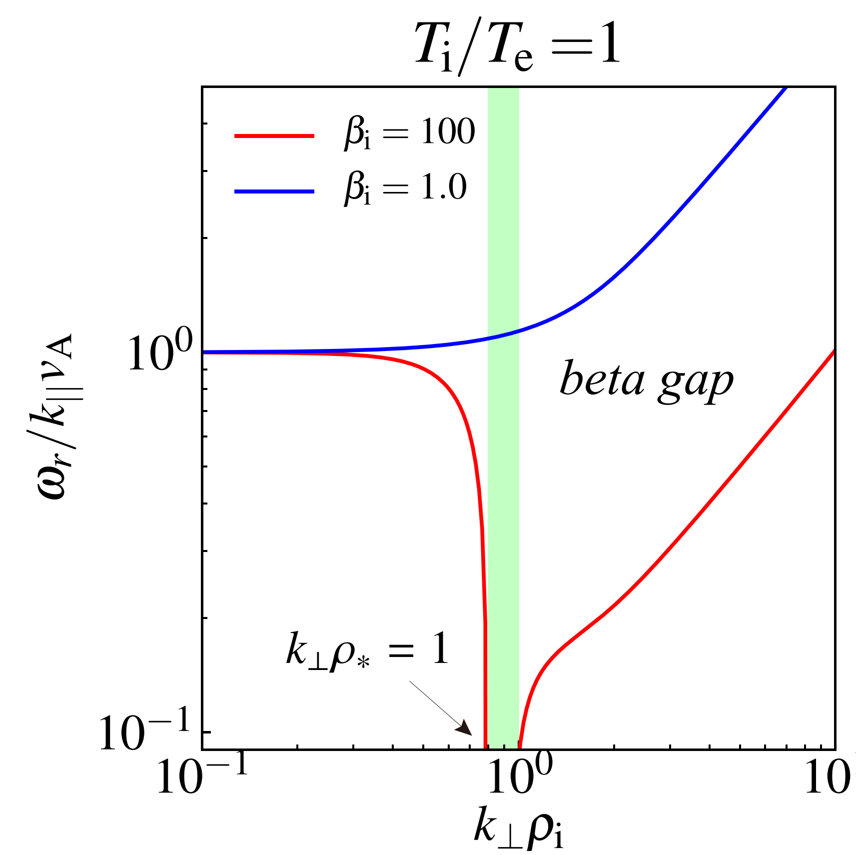

Zero Alfvén frequency region = beta gap

currently working on $\beta_\mathrm{i} = 10000$ (in backup slides)

✓ For $\beta_\mathrm{i} = 100$

- Huge drop of electric field $\leftarrow$ $\Phi_\mathbf{k} = \pm \dfrac{k_\perp \rho_\mathrm{i}}{\sqrt{(1 + ZT_\mathrm{e}/T_\mathrm{i})\left[2 + \beta_\mathrm{i}(1 + ZT_\mathrm{e}/T_\mathrm{i})\right]}} \Psi_\mathbf{k}$

(Schekochihin+ 2009)

Result : k-spectrum (low-mid β_i)

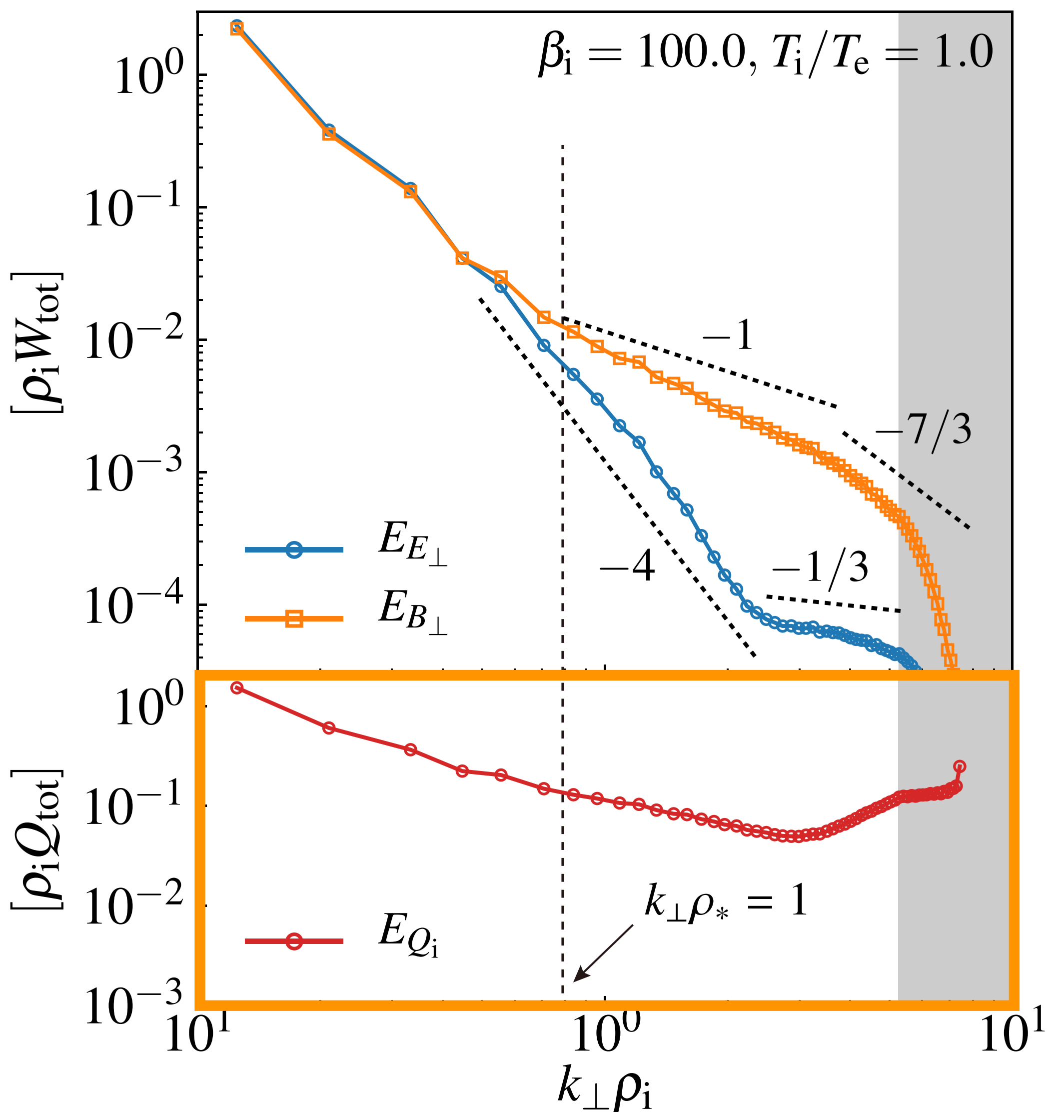

✓ For $\beta_i = 100$

- Huge drop of electric field $\leftarrow$ $\Phi_{\mathbf{k}} = \pm \dfrac{k_\perp \rho_i}{\sqrt{(1 + ZT_e/T_i)\left[2 + \beta_i(1 + ZT_e/T_i)\right]}} \Psi_{\mathbf{k}}$

(Schekochihin+ 2009)

- Heating occurs at $k_\perp \rho_i < 1$

Result : velocity spectrum

- ✓ Hermite-Laguerre spectrum $\hat{g}_{m,\ell} = \int_{-\infty}^{\infty} \mathrm{d}v_{\|} \frac{H_m(v_{\|}/v_{\mathrm{thi}})}{\sqrt{2^m m!}} \int_0^{\infty} \mathrm{d}(v_{\perp}^2)\, L_\ell(v_{\perp}^2) g(v_{\|}, v_{\perp}^2)$

$$g = h - \frac{Ze}{T_{\mathrm{i}}} \langle \phi \rangle_{\mathbf{R}_{\mathrm{i}}} F_{\mathrm{i}}$$

- ✓ Large m : small scale in $v_{\|}$, Large ℓ : small scale in $v_{\perp}$

Result : velocity spectrum

- ✓ Hermite-Laguerre spectrum $\hat{g}_{m,\ell} = \int_{-\infty}^{\infty} \mathrm{d}v_\parallel \frac{H_m(v_\parallel / v_{\mathrm{thi}})}{\sqrt{2^m m!}} \int_0^\infty \mathrm{d}(v_\perp^2)\, L_\ell(v_\perp^2) g(v_\parallel, v_\perp^2)$

$$g = h - \frac{Ze}{T_{\mathrm{i}}} \langle \phi \rangle_{\mathbf{R}_{\mathrm{i}}} F_{\mathrm{i}}$$

- ✓ Large m : small scale in $v_\parallel$, Large ℓ : small scale in $v_\perp$

$k_\perp$ vs m

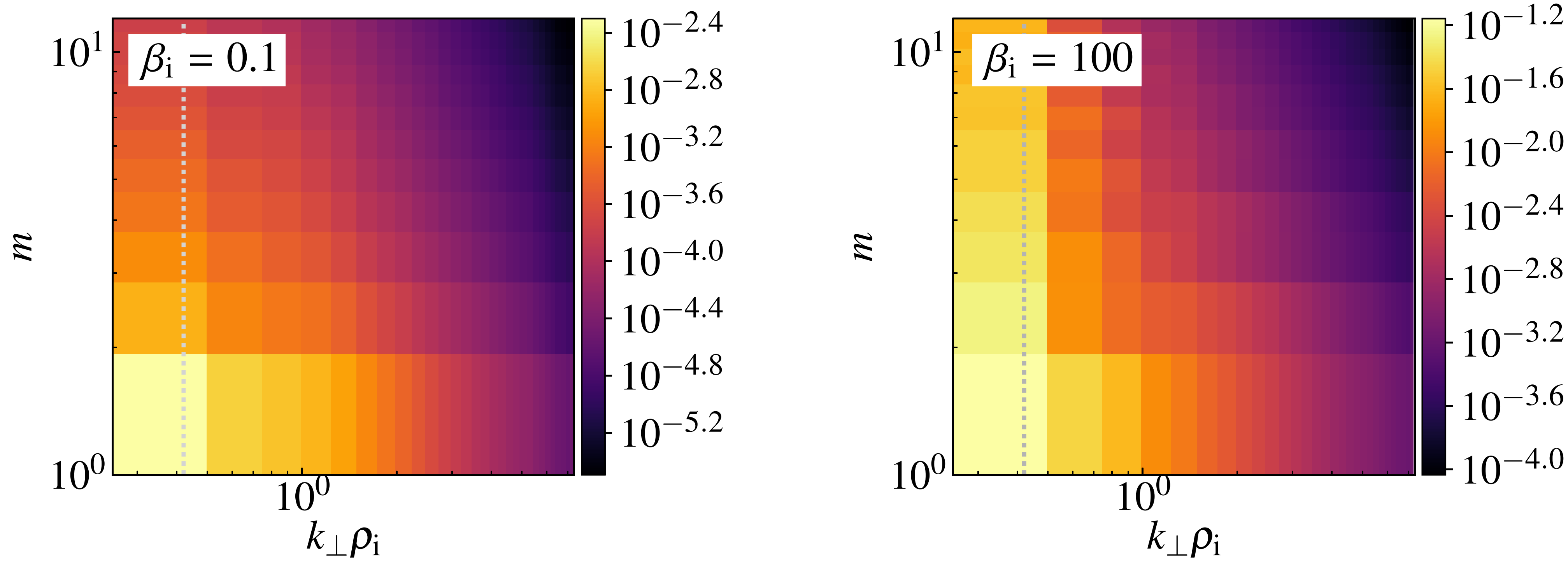

Result : velocity spectrum

✓ Hermite-Laguerre spectrum $\hat{g}_{m,\ell} = \int_{-\infty}^{\infty} \mathrm{d}v_\parallel \frac{H_m(v_\parallel/v_{\mathrm{thi}})}{\sqrt{2^m m!}} \int_0^\infty \mathrm{d}(v_\perp^2)\, L_\ell(v_\perp^2) g(v_\parallel, v_\perp^2)$

$$g = h - \frac{Ze}{T_\mathrm{i}} \langle \phi \rangle_{\mathbf{R}_\mathrm{i}} F_\mathrm{i}$$

✓ Large m : small scale in $v_\parallel$, Large ℓ : small scale in $v_\perp$

$k_\perp$ vs m

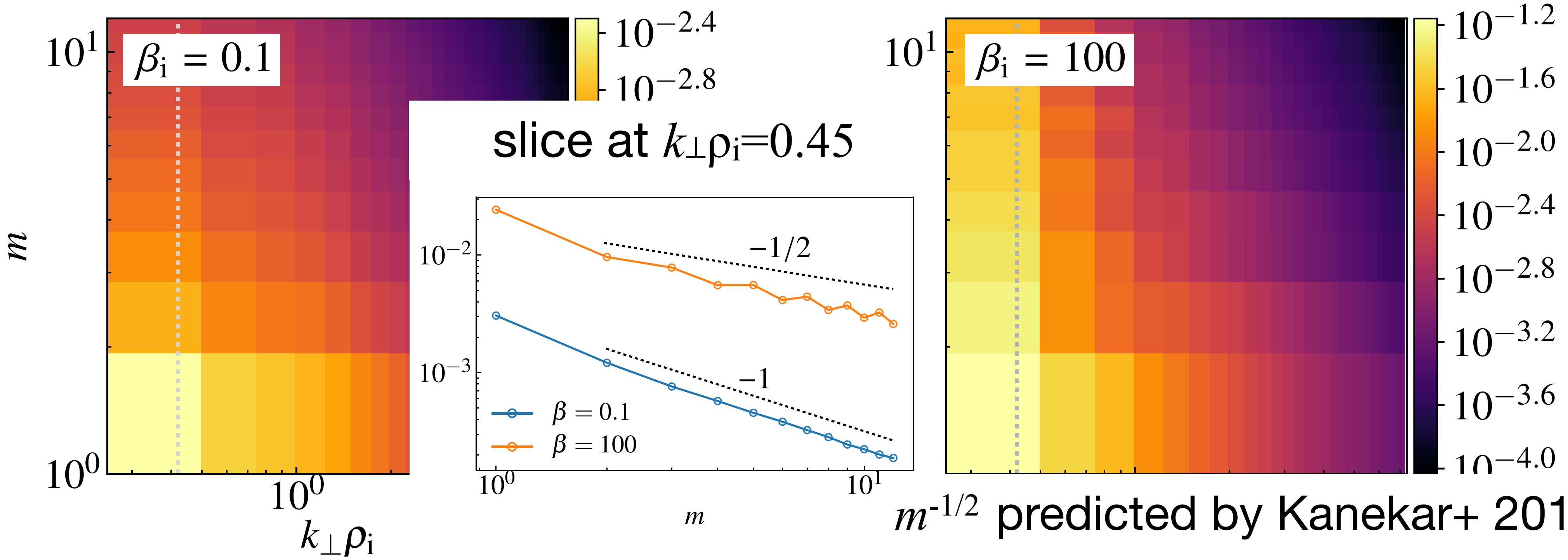

$m^{-1/2}$ predicted by Kanekar+ 2015

Result : velocity spectrum

- ✓ Hermite-Laguerre spectrum $\hat{g}_{m,\ell} = \int_{-\infty}^{\infty} \mathrm{d}v_{\parallel} \frac{H_m(v_{\parallel}/v_{\mathrm{thi}})}{\sqrt{2^m m!}} \int_0^{\infty} \mathrm{d}(v_{\perp}^2)\, L_{\ell}(v_{\perp}^2) g(v_{\parallel}, v_{\perp}^2)$

$$g = h - \frac{Ze}{T_{\mathrm{i}}} \langle \phi \rangle_{\mathbf{R}_{\mathrm{i}}} F_{\mathrm{i}}$$

- ✓ Large m : small scale in $v_{\parallel}$, Large ℓ : small scale in $v_{\perp}$

- ✓ Ion heating at high β_{i} ← linear Landau damping

$k_{\perp}$ vs m

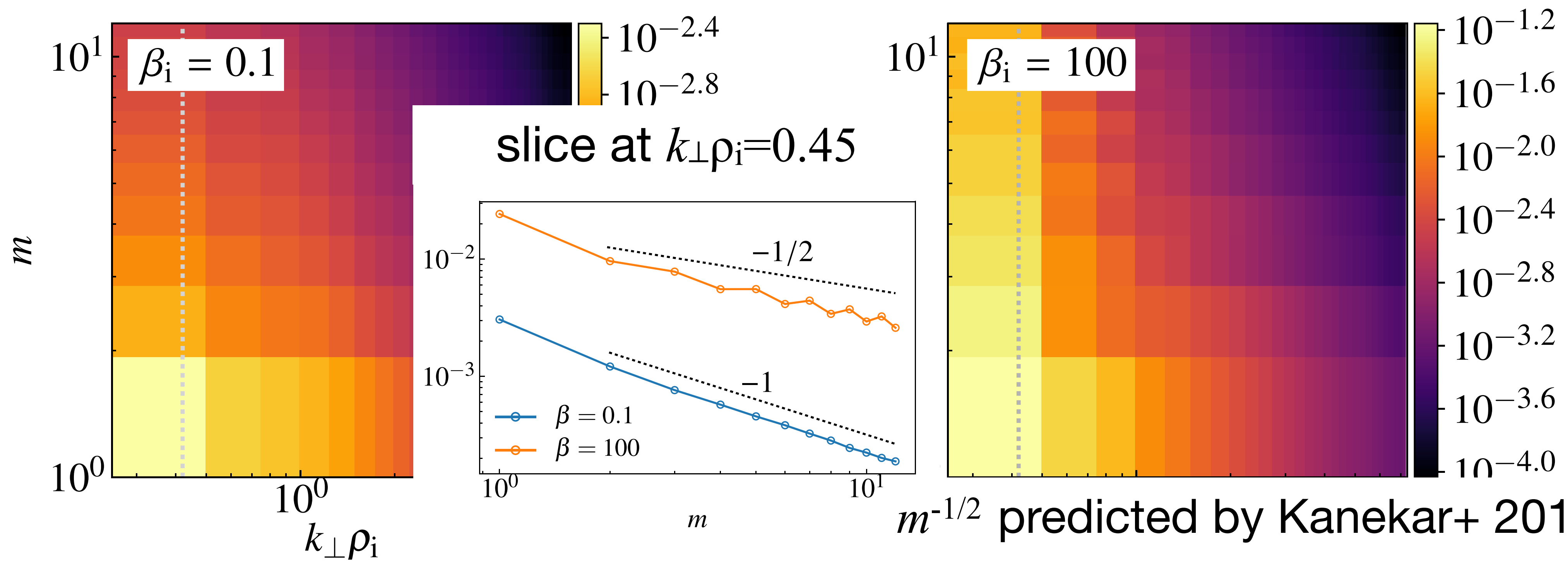

$m^{-1/2}$ predicted by Kanekar+ 2015

Result : velocity spectrum

- ✓ Hermite-Laguerre spectrum $\hat{g}_{m,\ell} = \int_{-\infty}^{\infty} \mathrm{d}v_\parallel \frac{H_m(v_\parallel/v_{\mathrm{thi}})}{\sqrt{2^m m!}} \int_0^{\infty} \mathrm{d}(v_\perp^2)\, L_\ell(v_\perp^2) g(v_\parallel, v_\perp^2)$

$$g = h - \frac{Ze}{T_\mathrm{i}} \langle \phi \rangle_{\mathbf{R}_\mathrm{i}} F_\mathrm{i}$$

- ✓ Large m : small scale in $v_\parallel$, Large ℓ: small scale in $v_\perp$

- ✓ Ion heating at high β_i ← linear Landau damping

$k_\perp$ vs m

6D EM by Cerri+ 2018

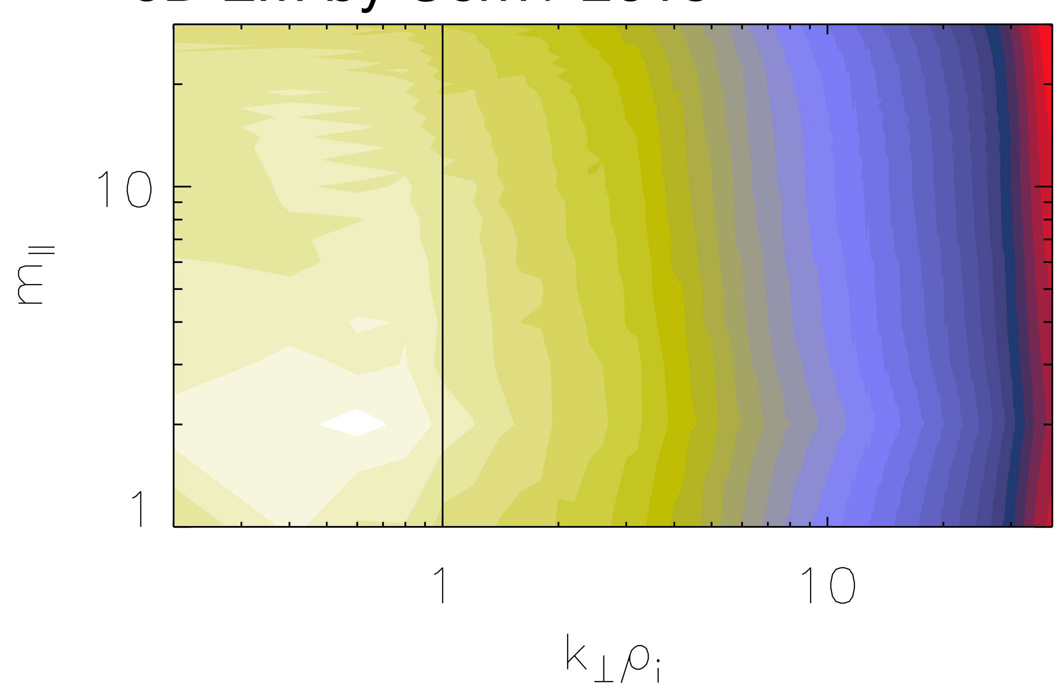

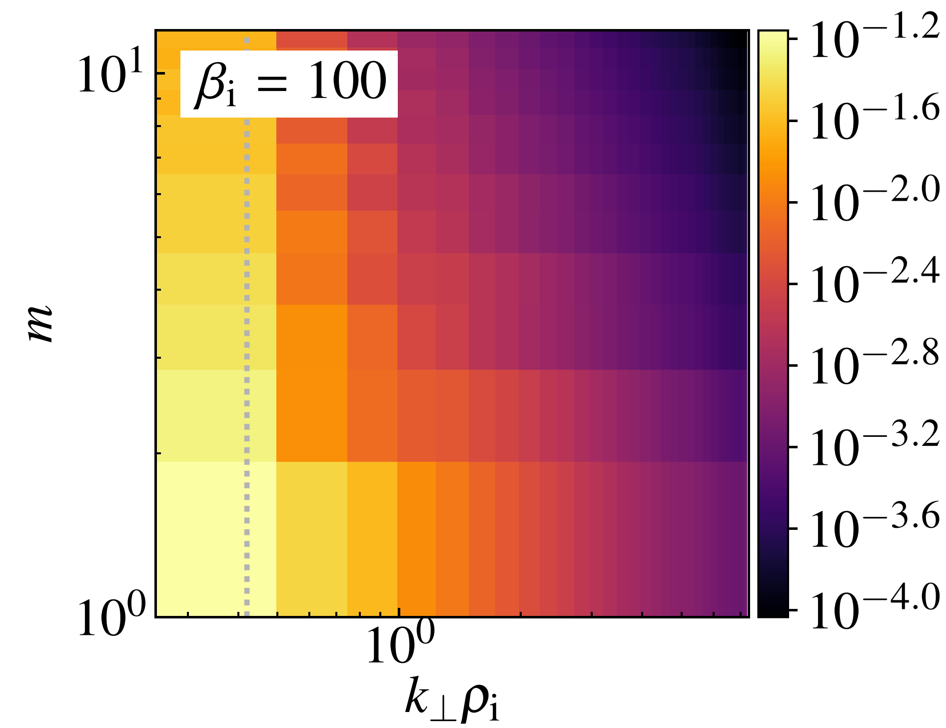

Result : velocity spectrum

- ✓ Hermite-Laguerre spectrum $\hat{g}_{m,\ell} = \int_{-\infty}^{\infty} dv_\parallel \frac{H_m(v_\parallel/v_{\rm thi})}{\sqrt{2^m m!}} \int_0^\infty d(v_\perp^2)\, L_\ell(v_\perp^2) g(v_\parallel, v_\perp^2)$

$$g = h - \frac{Ze}{T_{\rm i}} \langle \phi \rangle_{\mathbf{R}_{\rm i}} F_{\rm i}$$

- ✓ Large m : small scale in $v_\parallel$, Large ℓ : small scale in $v_\perp$

- ✓ Ion heating at high $\beta_{\rm i}$ ← linear Landau damping

$k_\perp$ vs ℓ

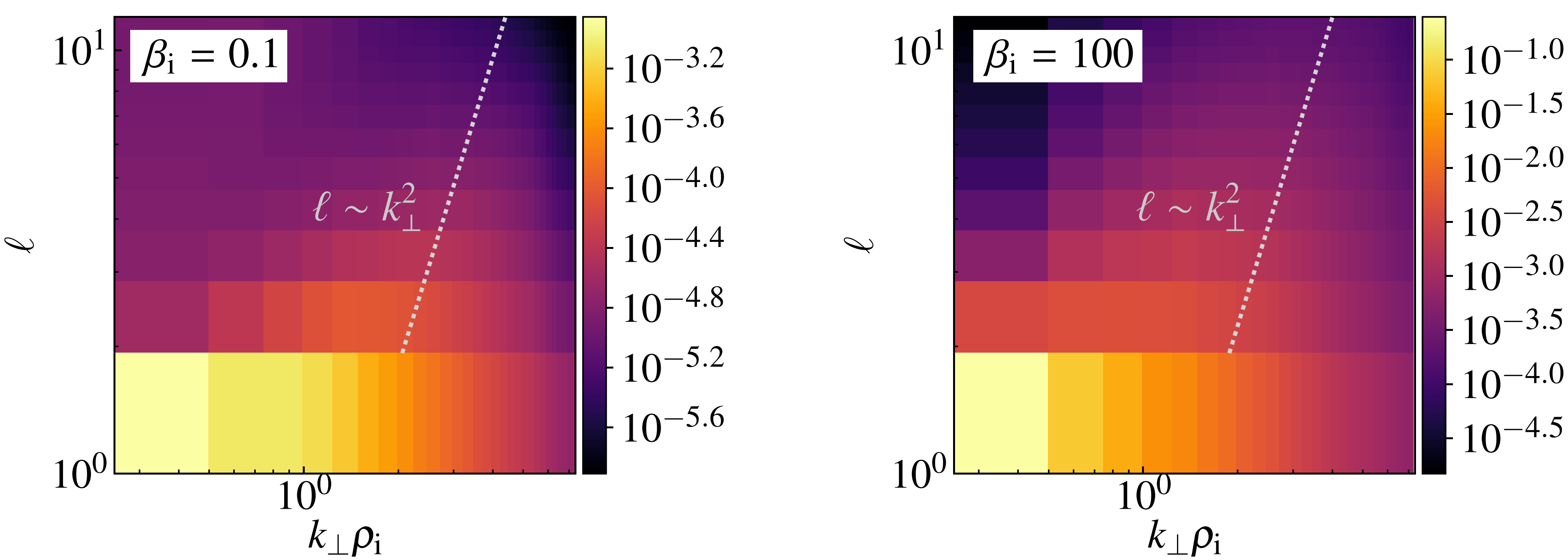

Result : velocity spectrum

- ✓ Hermite-Laguerre spectrum $\hat{g}_{m,\ell} = \int_{-\infty}^{\infty} dv_\parallel \frac{H_m(v_\parallel/v_{\rm thi})}{\sqrt{2^m m!}} \int_0^\infty d(v_\perp^2)\, L_\ell(v_\perp^2) g(v_\parallel, v_\perp^2)$

$$g = h - \frac{Ze}{T_{\rm i}} \langle \phi \rangle_{\mathbf{R}_{\rm i}} F_{\rm i}$$

- ✓ Large m : small scale in $v_\parallel$, Large ℓ : small scale in $v_\perp$
- ✓ Ion heating at high $\beta_{\rm i}$ ← linear Landau damping
- ✓ Diagonal structure in $(k_\perp, \ell)$ plane → nonlinear phase mixing

(Tatsuno+ 2009)

$k_\perp$ vs ℓ

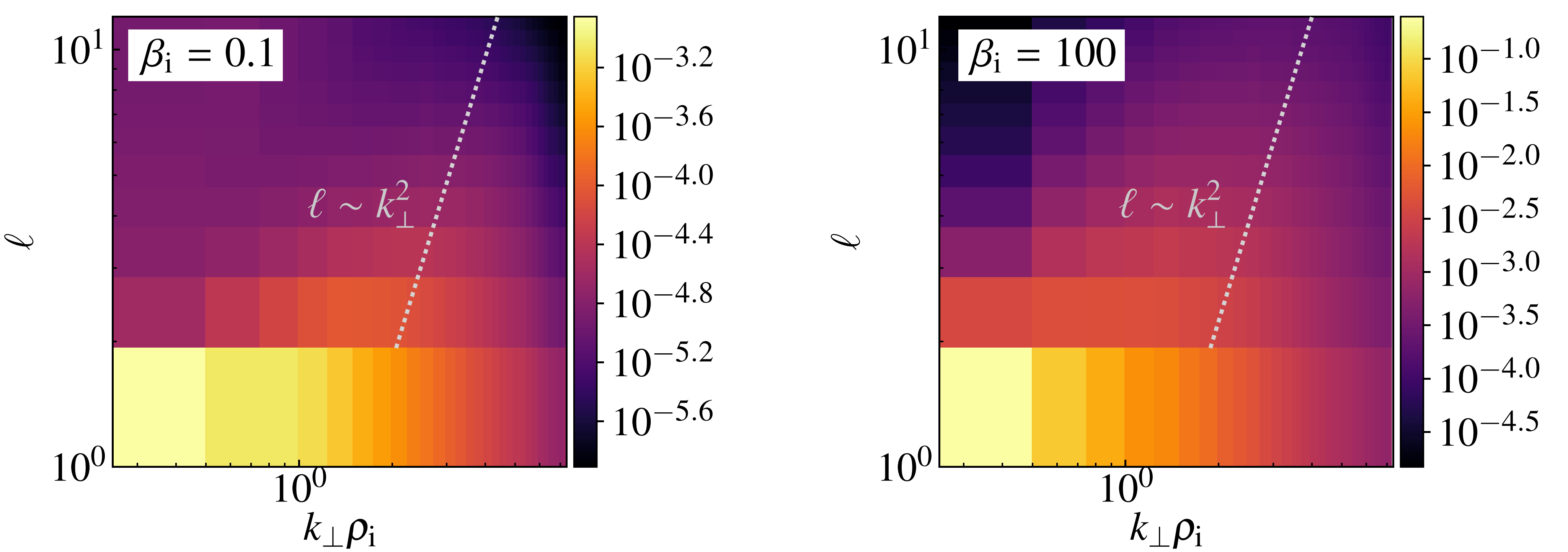

Result : velocity spectrum

- ✓ Hermite-Laguerre spectrum $\hat{g}_{m,\ell} = \int_{-\infty}^{\infty} \mathrm{d}v_{\parallel} \frac{H_m(v_{\parallel}/v_{\mathrm{thi}})}{\sqrt{2^m m!}} \int_0^{\infty} \mathrm{d}(v_{\perp}^2)\, L_{\ell}(v_{\perp}^2) g(v_{\parallel}, v_{\perp}^2)$

$$g = h - \frac{Ze}{T_{\mathrm{i}}} \langle \phi \rangle_{\mathbf{R}_{\mathrm{i}}} F_{\mathrm{i}}$$

- ✓ Large m : small scale in $v_{\parallel}$, Large ℓ : small scale in $v_{\perp}$
- ✓ Ion heating at high β_{i} ← linear Landau damping
- ✓ Diagonal structure in $(k_{\perp}, \ell)$ plane → nonlinear phase mixing

(Tatsuno+ 2009)

$k_{\perp}$ vs ℓ

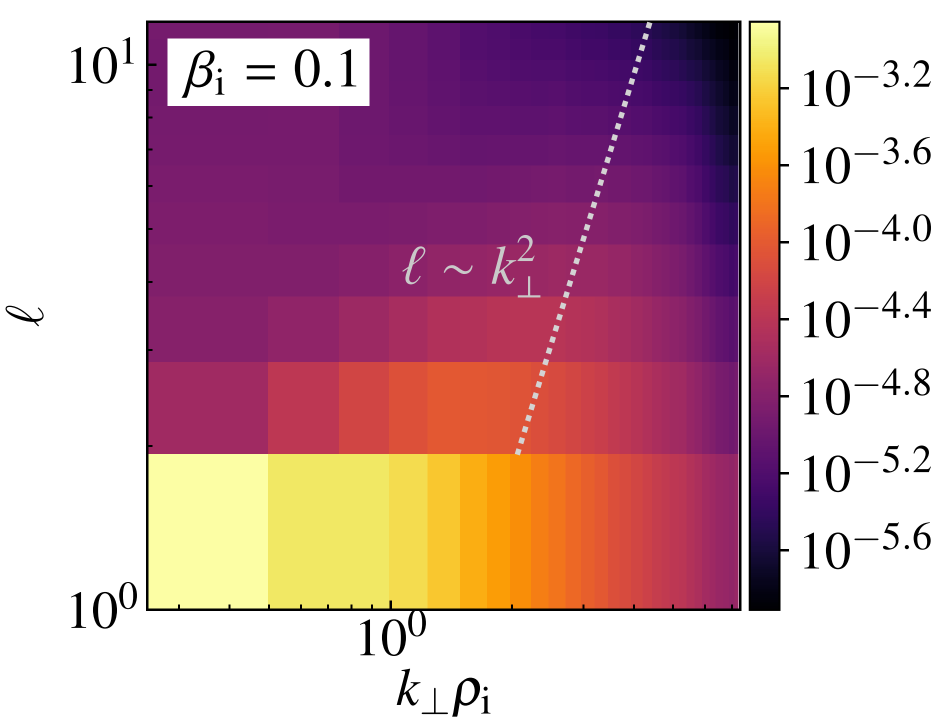

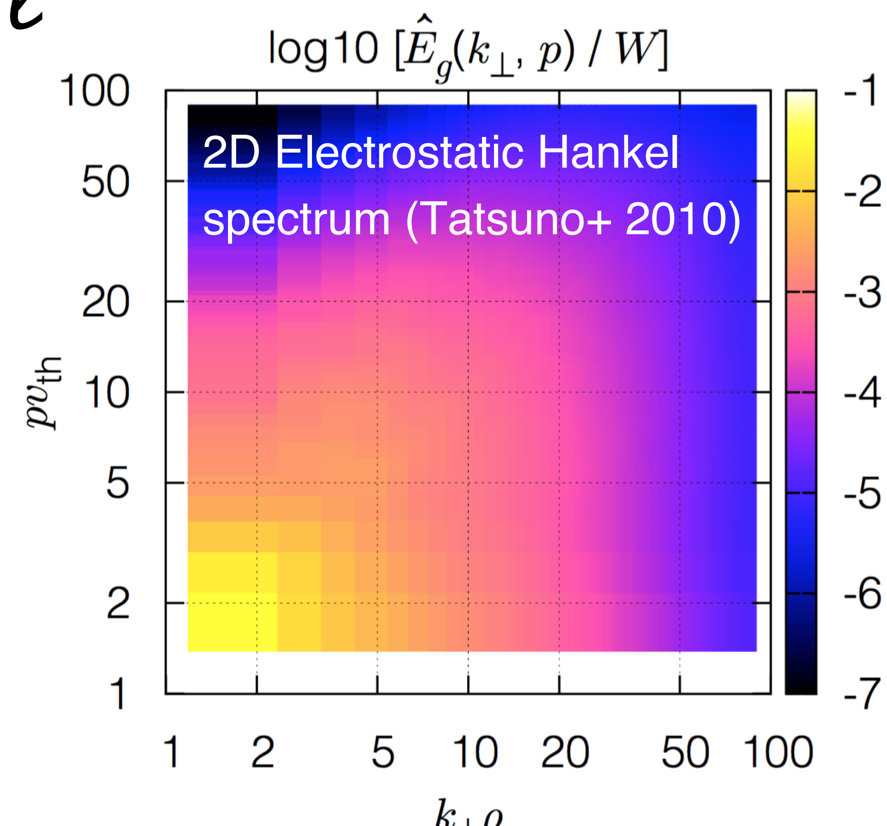

Result : velocity spectrum

- ✓ Hermite-Laguerre spectrum $\hat{g}_{m,\ell} = \int_{-\infty}^{\infty} \mathrm{d}v_\parallel \frac{H_m(v_\parallel / v_{\mathrm{thi}})}{\sqrt{2^m m!}} \int_0^\infty \mathrm{d}(v_\perp^2)\, L_\ell(v_\perp^2) g(v_\parallel, v_\perp^2)$

$$g = h - \frac{Ze}{T_\mathrm{i}} \langle \phi \rangle_{\mathbf{R}_\mathrm{i}} F_\mathrm{i}$$

- ✓ Large m : small scale in $v_\parallel$, Large ℓ : small scale in $v_\perp$
- ✓ Ion heating at high β_i ← linear Landau damping
- ✓ Diagonal structure in $(k_\perp, \ell)$ plane → nonlinear phase mixing

(Tatsuno+ 2009)

$k_\perp$ vs ℓ

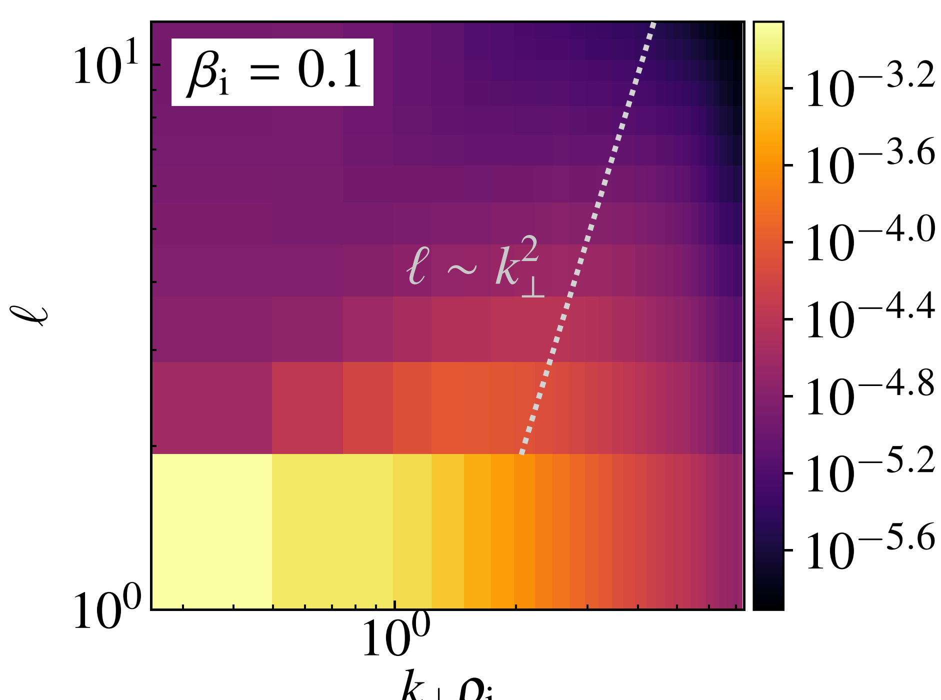

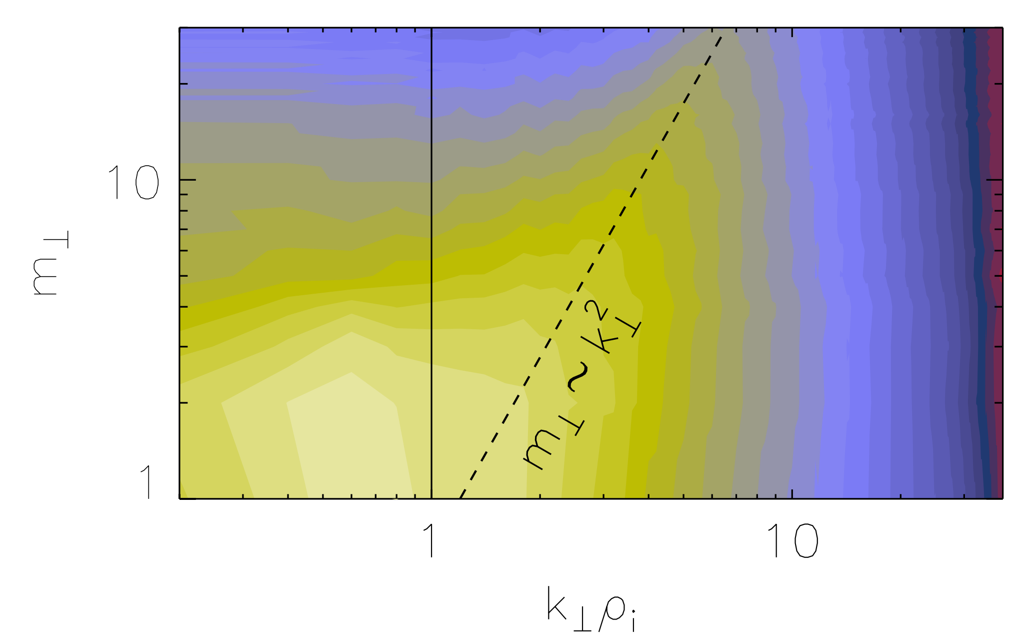

6D EM by Cerri+ 2018

Summary

- ✓ A new heating prescription
- ✓ The same trend as Howes' prescription, but appreciably different at high β_i and low β_i
- ✓ Q_i/Q_e is insensitive to T_i/T_e → Collisionless plasma prefers enhanced temperature inequality (except β_i=1)

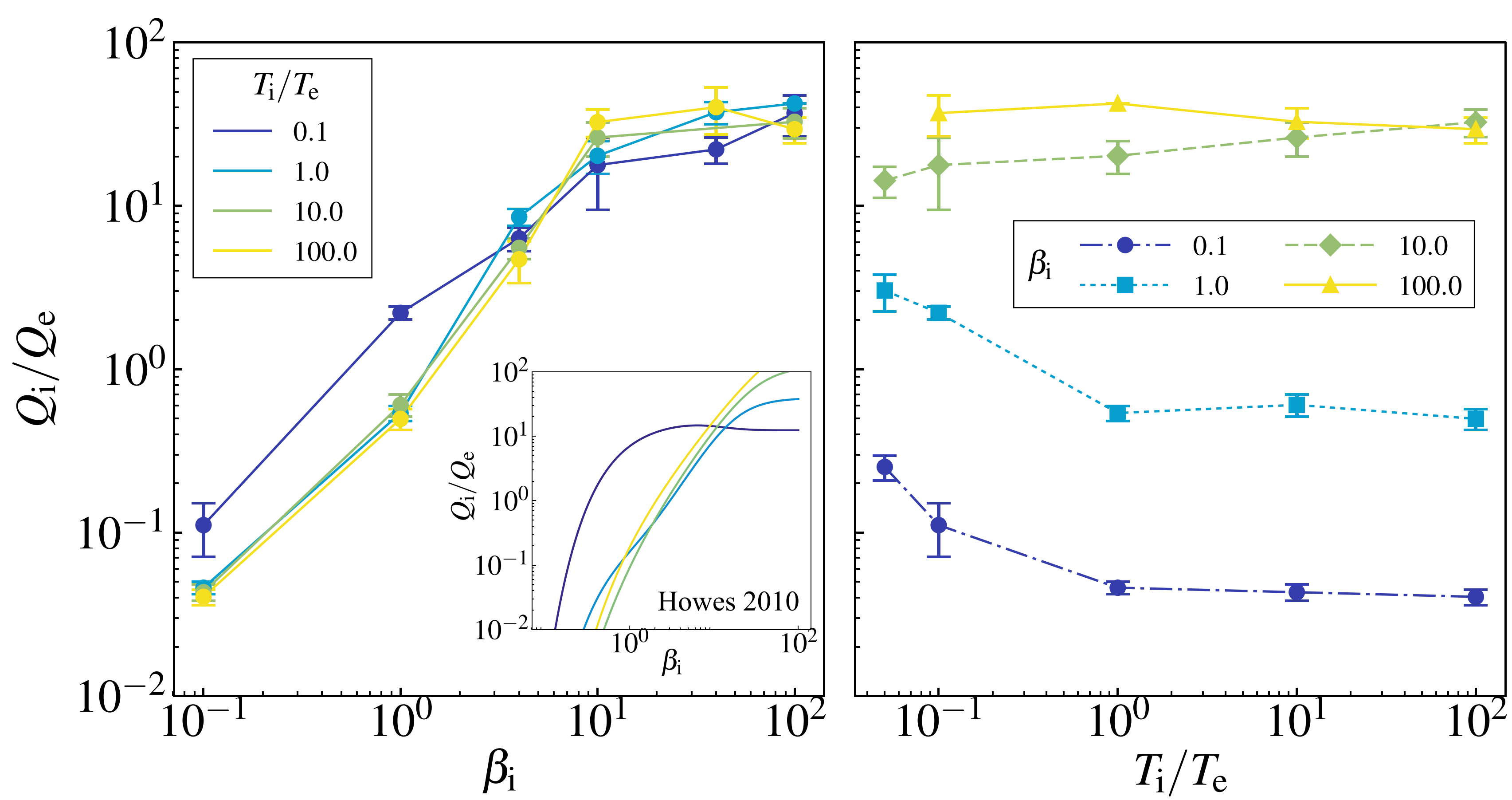

Summary

- ✓ A new heating prescription
- ✓ The same trend as Howes' prescription, but appreciably different at high β_i and low β_i
- ✓ $Q_\mathrm{i}/Q_\mathrm{e}$ is insensitive to $T_\mathrm{i}/T_\mathrm{e}$ → Collisionless plasma prefers enhanced temperature inequality (except β_i=1)
- ✓ Strong ion heating at high β_i via linear Landau damping

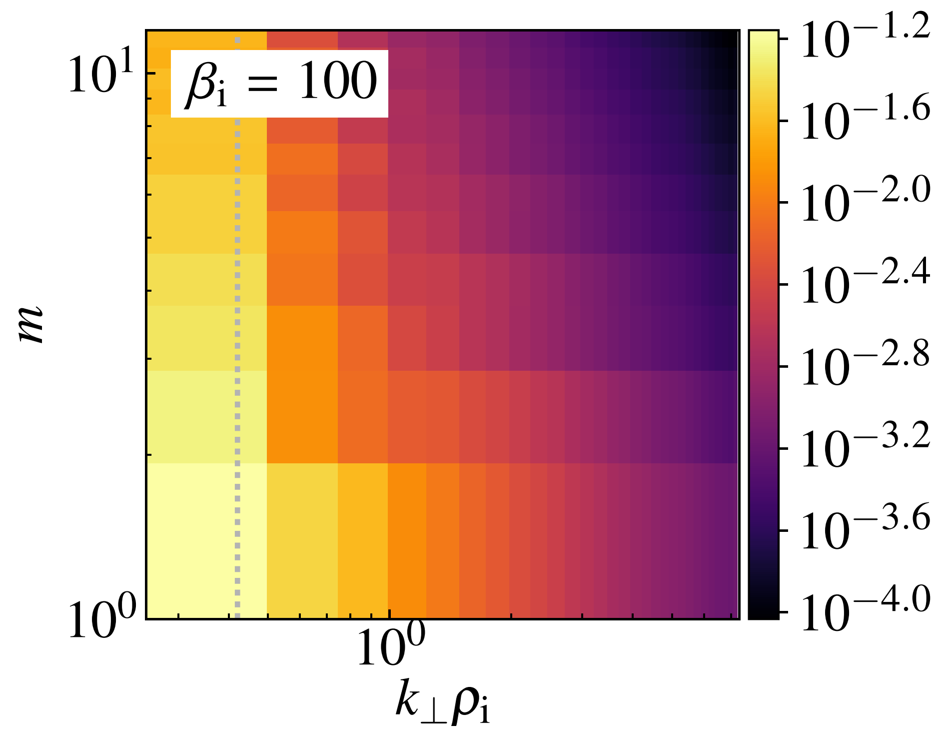

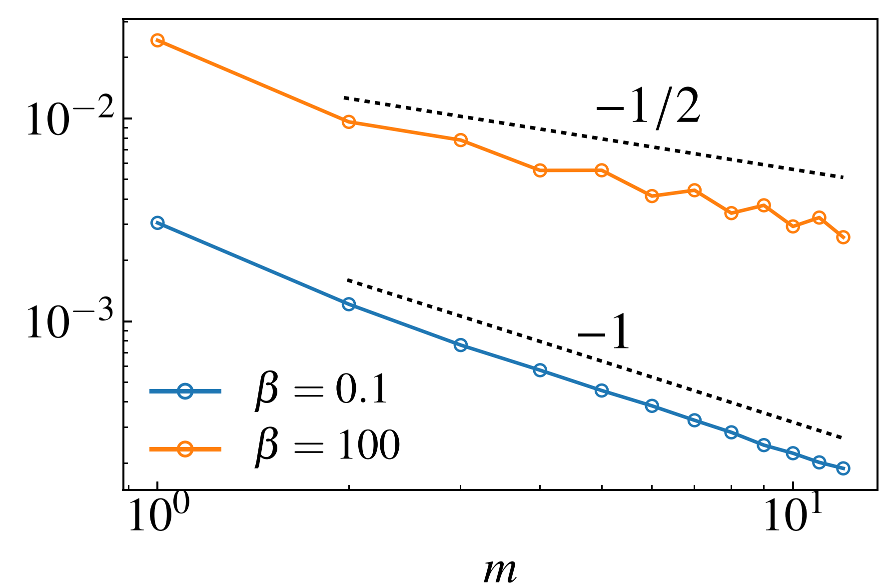

Summary

✓ A new heating prescription

✓ The same trend as Howes' prescription, but appreciably different at high β_i and low β_i

✓ Q_i/Q_e is insensitive to T_i/T_e → Collisionless plasma prefers enhanced temperature inequality (except β_i=1)

✓ Strong ion heating at high β_i via linear Landau damping

✓ Magnetically dominated spectra at high β_i

➡ investigation of nonlocal transfer in progress

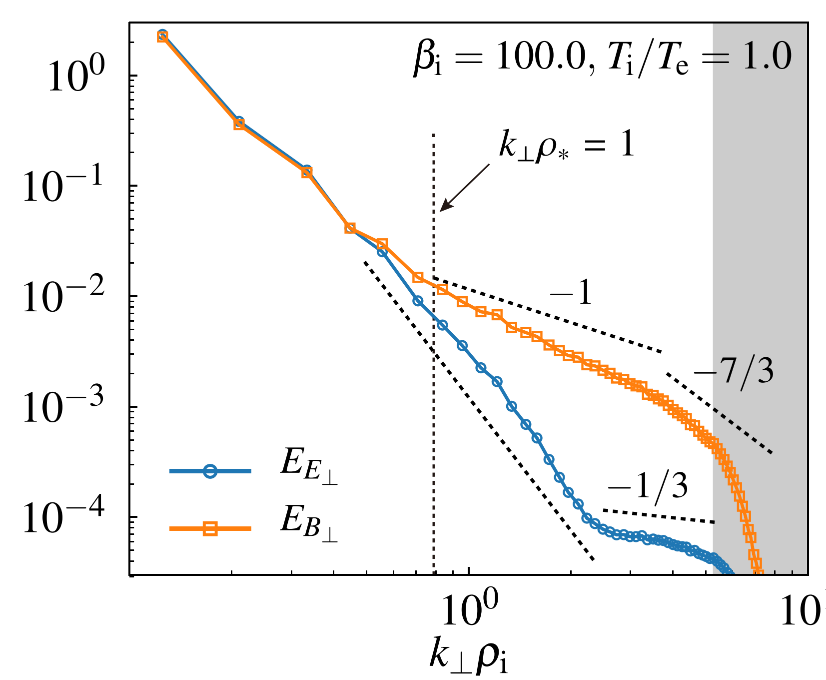

Summary

- ✓ A new heating prescription
- ✓ The same trend as Howes' prescription, but appreciably different at high β_i and low β_i
- ✓ $Q_\mathrm{i}/Q_\mathrm{e}$ is insensitive to $T_\mathrm{i}/T_\mathrm{e}$ → Collisionless plasma prefers enhanced temperature inequality (except $\beta_\mathrm{i}=1$)
- ✓ Strong ion heating at high β_i via linear Landau damping
- ✓ Magnetically dominated spectra at high β_i
  - ➡ investigation of nonlocal transfer in progress

Y. Kawazura, M. Barnes, and A. A. Schekochihin, arXiv: 1807.07702

Summary

- ✓ A new heating prescription
- ✓ The same trend as Howes' prescription, but appreciably different at high β_i and low β_i
- ✓ $Q_\mathrm{i}/Q_\mathrm{e}$ is insensitive to $T_\mathrm{i}/T_\mathrm{e}$ → Collisionless plasma prefers enhanced temperature inequality (except $\beta_\mathrm{i}=1$)
- ✓ Strong ion heating at high β_i via linear Landau damping
- ✓ Magnetically dominated spectra at high β_i
  - ➡ investigation of nonlocal transfer in progress

Future work

- ✓ Compressive mode driving
- ✓ Beta gap investigation

Application to accretion disks

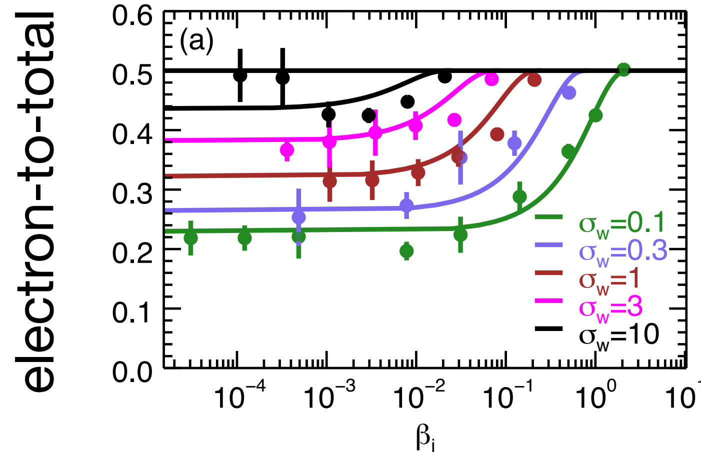

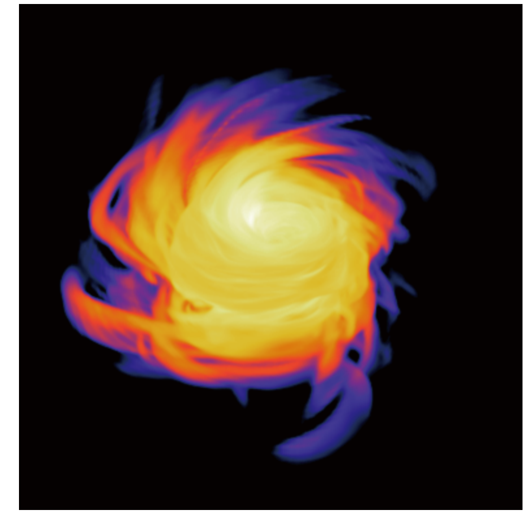

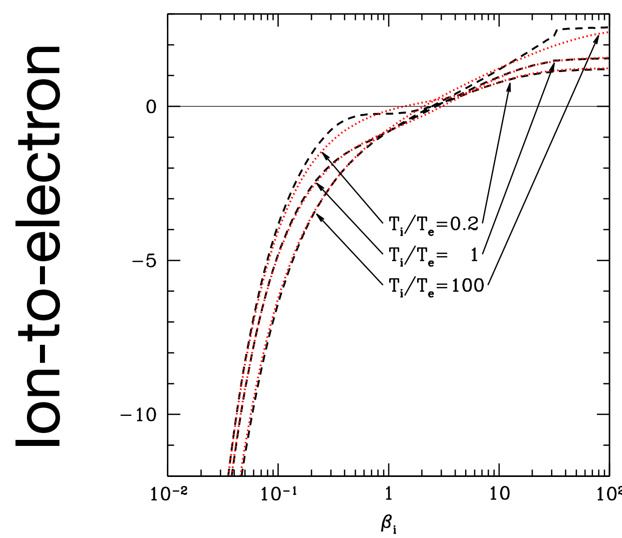

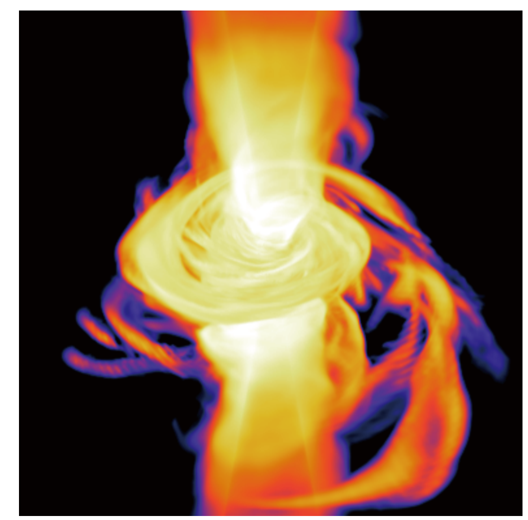

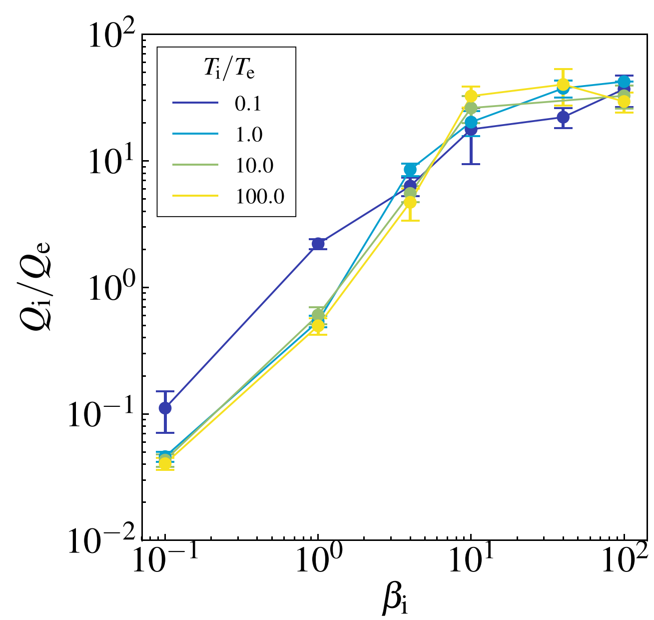

?

Beta gap

- ✓ High β_i ➞ A region with zero Alfvén wave frequency := beta gap
- ✓ The gap starts at $k_\perp \rho_* = 1, \ \rho_* \sim \rho_i \beta_i^{1/4}$ (Schekochihin+ in preparation)

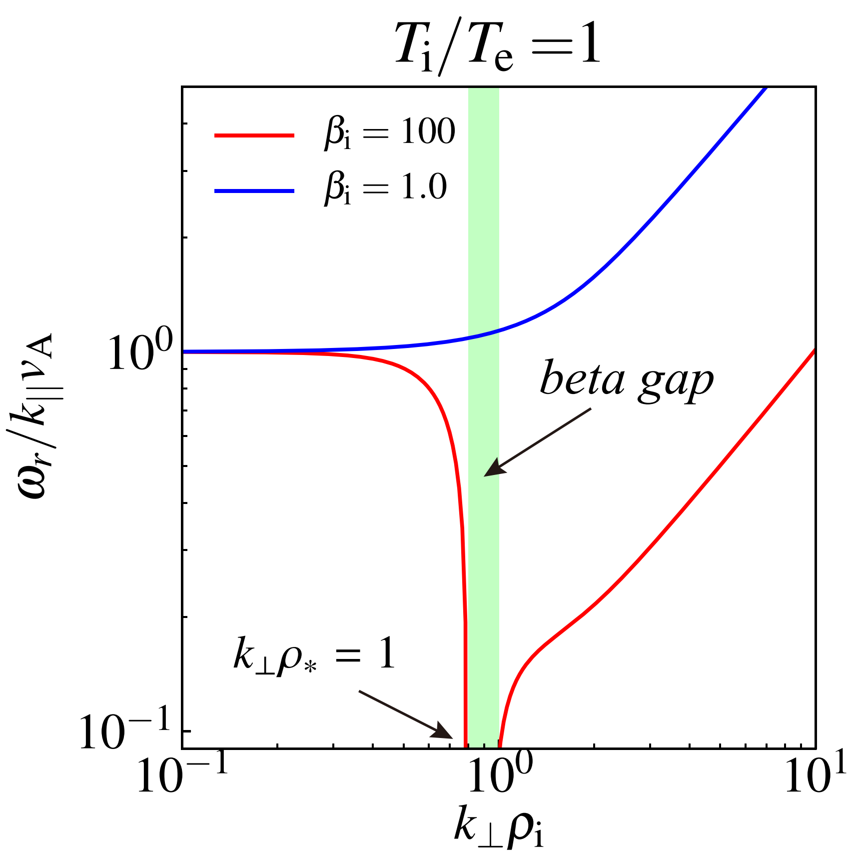

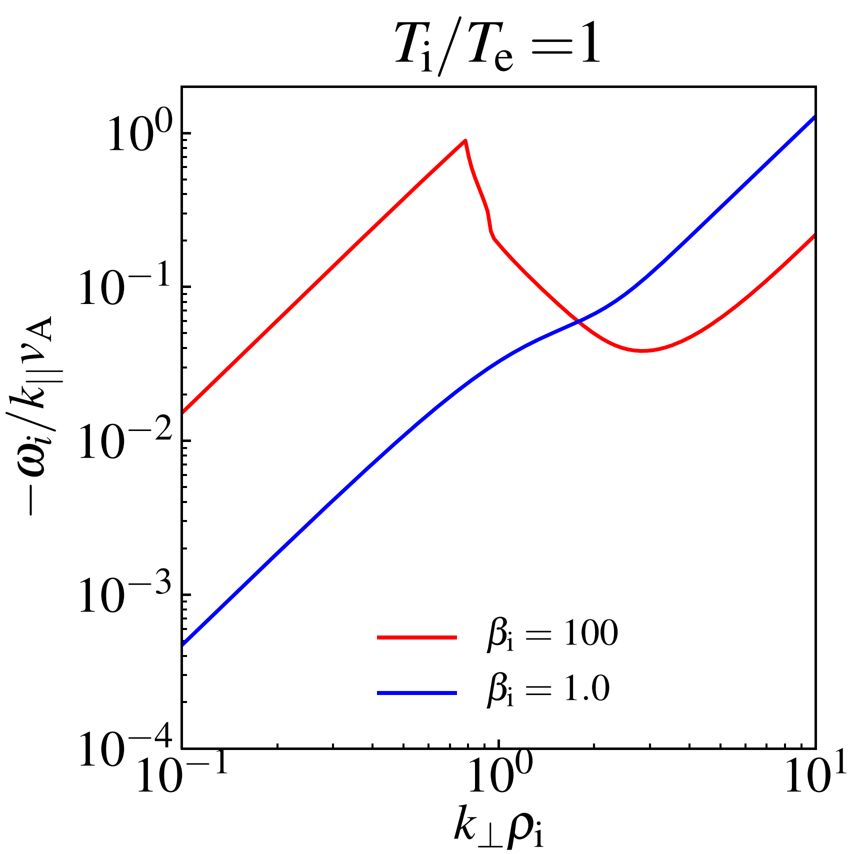

Beta gap

- ✓ High $\beta_{\rm i}$ → A region with zero Alfvén wave frequency := beta gap
- ✓ The gap starts at $k_\perp \rho_* = 1,\ \rho_* \sim \rho_{\rm i} \beta_{\rm i}^{1/4}$ (Schekochihin+ in preparation)
- ✓ The anomaly of spectrum emerges around $k_\perp \rho_* \sim 1$

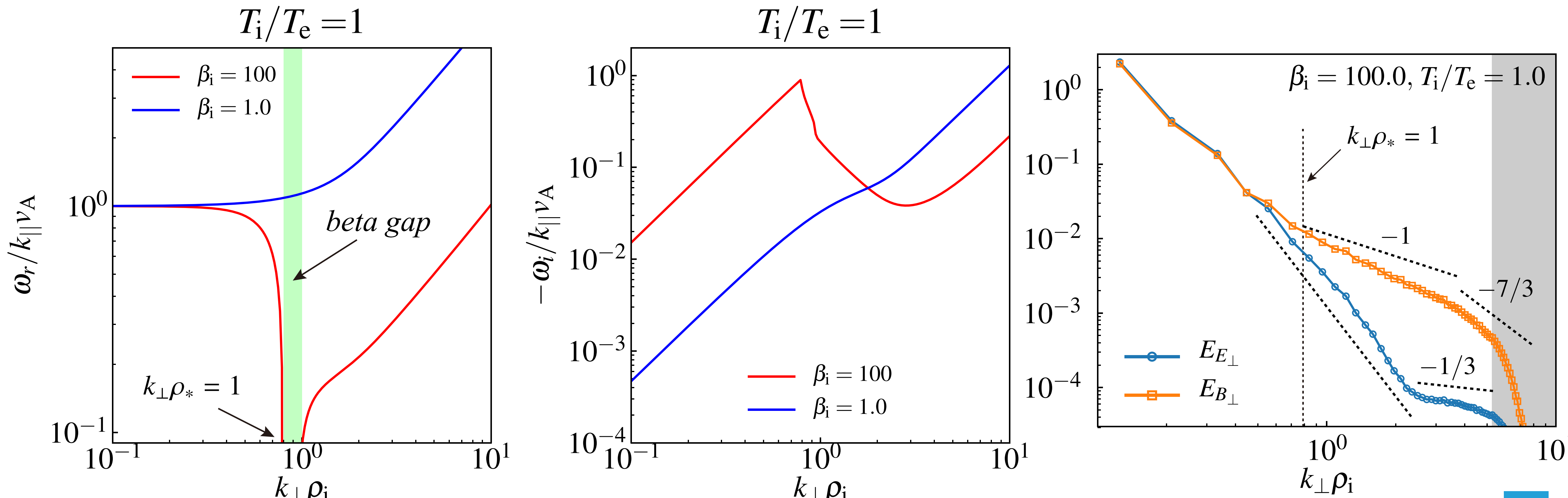

Beta gap

- ✓ High β_i → A region with zero Alfvén wave frequency := beta gap
- ✓ The gap starts at $k_\perp\rho_* = 1,\ \rho_* \sim \rho_i \beta_i^{1/4}$ (Schekochihin+ in preparation)
- ✓ The anomaly of spectrum emerges around $k_\perp\rho_* \sim 1$
- ✓ The ceiling of Q_i/Q_e starts at β_i that has a finite gap
- ✓ Howes prescription is ill-posed when the gap is present

$$Q_s(k_\perp) \sim (\gamma_s/\omega)\epsilon(k_\perp)/k_\perp$$

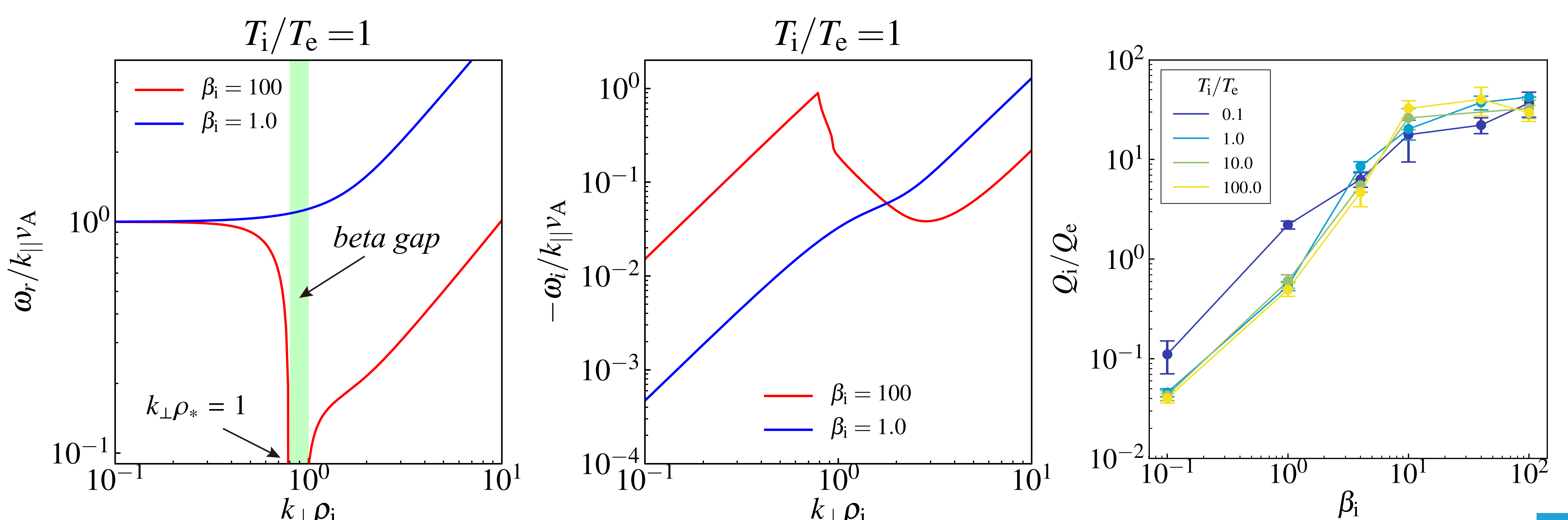

Beta gap

- ✓ High $\beta_{\rm i}$ → A region with zero Alfvén wave frequency := beta gap
- ✓ The gap starts at $k_\perp \rho_* = 1$, $\rho_* \sim \rho_{\rm i} \beta_{\rm i}^{1/4}$ (Schekochihin+ in preparation)
- ✓ The anomaly of spectrum emerges around $k_\perp \rho_* \sim 1$
- ✓ The ceiling of $Q_{\rm i}/Q_{\rm e}$ starts at $\beta_{\rm i}$ that has a finite gap
- ✓ Howes prescription is ill-posed when the gap is present

$$Q_s(k_\perp) \sim (\gamma_s/\omega)\epsilon(k_\perp)/k_\perp$$

- ✓ To understand the ceiling of $Q_{\rm i}/Q_{\rm e}$, we need to investigate the gap

Beta gap

- ✓ High β_i → A region with zero Alfvén wave frequency := beta gap
- ✓ The gap starts at $k_\perp \rho_* = 1, \;\; \rho_* \sim \rho_\mathrm{i} {\beta_\mathrm{i}}^{1/4}$ (Schekochihin+ in preparation)
- ✓ The anomaly of spectrum emerges around $k_\perp \rho_* \sim 1$
- ✓ The ceiling of $Q_\mathrm{i}/Q_\mathrm{e}$ starts at β_i that has a finite gap
- ✓ Howes prescription is ill-posed when the gap is present

$$Q_s(k_\perp) \sim (\gamma_s/\omega)\epsilon(k_\perp)/k_\perp$$

- ✓ To understand the ceiling of $Q_\mathrm{i}/Q_\mathrm{e}$, we need to investigate the gap
- ✓ Too narrow gap for $\beta_\mathrm{i} \sim 100$

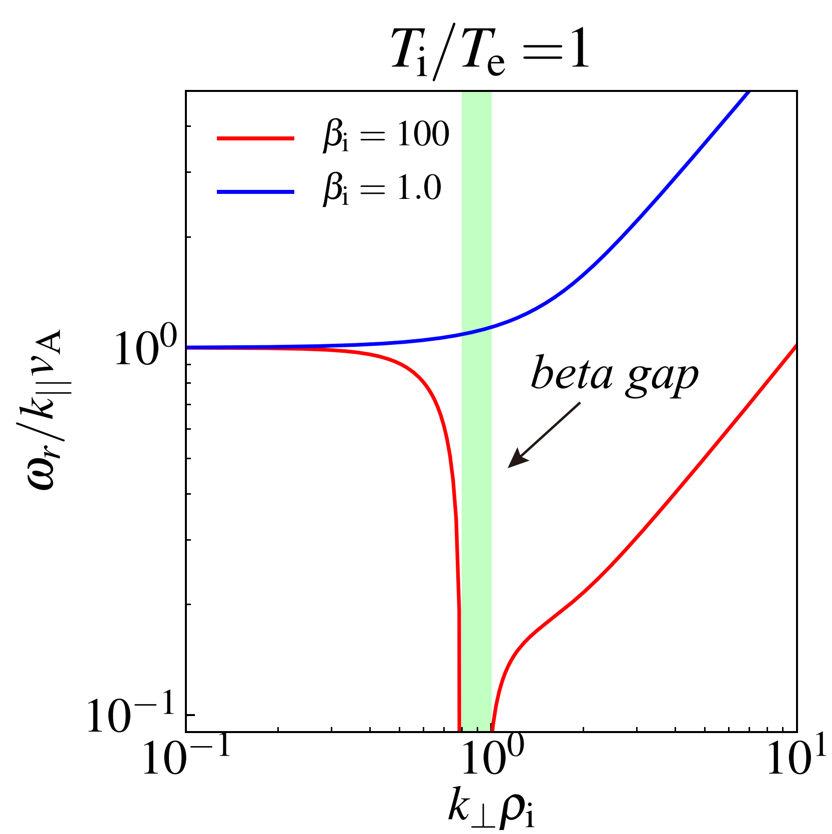

Beta gap

- ✓ High $\beta_{\rm i}$ → A region with zero Alfvén wave frequency := beta gap
- ✓ The gap starts at $k_\perp \rho_* = 1,\ \rho_* \sim \rho_{\rm i} {\beta_{\rm i}}^{1/4}$ (Schekochihin+ in preparation)
- ✓ The anomaly of spectrum emerges around $k_\perp \rho_* \sim 1$
- ✓ The ceiling of $Q_{\rm i}/Q_{\rm e}$ starts at $\beta_{\rm i}$ that has a finite gap
- ✓ Howes prescription is ill-posed when the gap is present

$$Q_s(k_\perp) \sim (\gamma_s/\omega)\epsilon(k_\perp)/k_\perp$$

- ✓ To understand the ceiling of $Q_{\rm i}/Q_{\rm e}$, we need to investigate the gap
- ✓ Too narrow gap for $\beta_{\rm i} \sim 100$
  - (1) Pressure anisotropy (Kunz+ 2018)

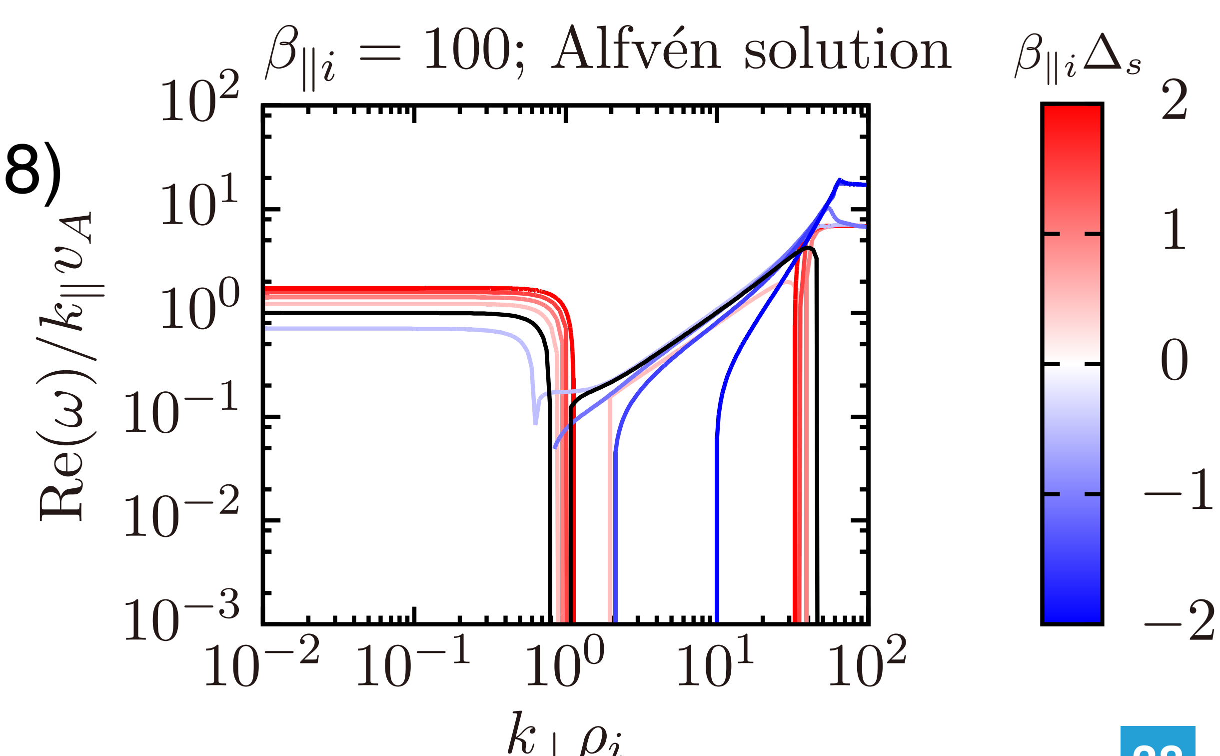

Beta gap

- ✓ High $\beta_{\rm i}$ ➞ A region with zero Alfvén wave frequency := beta gap
- ✓ The gap starts at $k_\perp \rho_* = 1, \ \rho_* \sim \rho_{\rm i} {\beta_{\rm i}}^{1/4}$ (Schekochihin+ in preparation)
- ✓ The anomaly of spectrum emerges around $k_\perp \rho_* \sim 1$
- ✓ The ceiling of $Q_{\rm i}/Q_{\rm e}$ starts at $\beta_{\rm i}$ that has a finite gap
- ✓ Howes prescription is ill-posed when the gap is present

$$Q_s(k_\perp) \sim (\gamma_s/\omega)\epsilon(k_\perp)/k_\perp$$

- ✓ To understand the ceiling of $Q_{\rm i}/Q_{\rm e}$, we need to investigate the gap
- ✓ Too narrow gap for $\beta_{\rm i} \sim 100$

  (1) Pressure anisotropy (Kunz+ 2018)

  $\boxed{\text{(2) Ultra-high } \beta_{\rm i}, \ \sim 10000}$

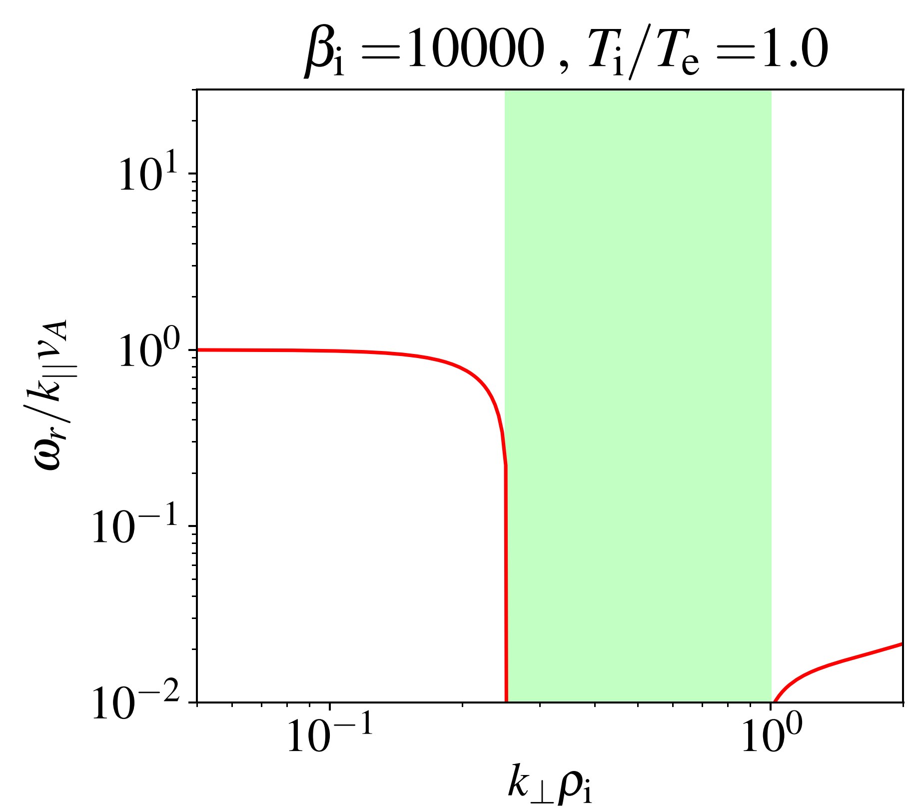

Beta gap

- ✓ High $\beta_{\rm i}$ → A region with zero Alfvén wave frequency := beta gap
- ✓ The gap starts at $k_\perp\rho_* = 1,\ \rho_* \sim \rho_{\rm i}\beta_{\rm i}^{1/4}$ (Schekochihin+ in preparation)
- ✓ The anomaly of spectrum emerges around $k_\perp\rho_* \sim 1$
- ✓ The ceiling of $Q_{\rm i}/Q_{\rm e}$ starts at $\beta_{\rm i}$ that has a finite gap
- ✓ Howes prescription is ill-posed when the gap is present

$$Q_s(k_\perp) \sim (\gamma_s/\omega)\epsilon(k_\perp)/k_\perp$$

- ✓ To understand the ceiling of $Q_{\rm i}/Q_{\rm e}$, we need to investigate the gap
- ✓ Too narrow gap for $\beta_{\rm i} \sim 100$

  (1) Pressure anisotropy (Kunz+ 2018)

  $\boxed{\text{(2) Ultra-high } \beta_{\rm i},\ \sim 10000}$

- ✓ Ultra-high $\beta_{\rm i}$ is numerically difficult

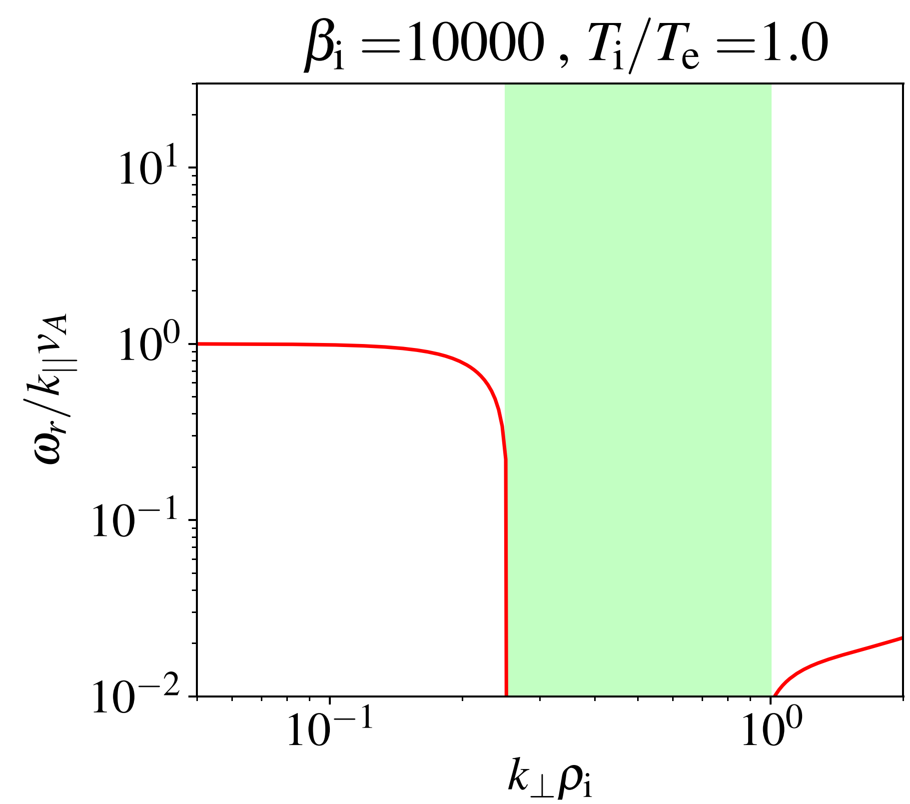

Beta gap

- ✓ High β_i → A region with zero Alfvén wave frequency := beta gap
- ✓ The gap starts at $k_\perp \rho_* = 1$, $\rho_* \sim \rho_\mathrm{i} {\beta_\mathrm{i}}^{1/4}$ (Schekochihin+ in preparation)
- ✓ The anomaly of spectrum emerges around $k_\perp \rho_* \sim 1$
- ✓ The ceiling of $Q_\mathrm{i}/Q_\mathrm{e}$ starts at β_i that has a finite gap
- ✓ Howes prescription is ill-posed when the gap is present

$$Q_s(k_\perp) \sim (\gamma_s/\omega)\epsilon(k_\perp)/k_\perp$$

- ✓ To understand the ceiling of $Q_\mathrm{i}/Q_\mathrm{e}$, we need to investigate the gap
- ✓ Too narrow gap for $\beta_\mathrm{i} \sim 100$
  - (1) Pressure anisotropy (Kunz+ 2018)
  - (2) Ultra-high β_i, ~ 10000
- ✓ Ultra-high β_i is numerically difficult
- ✓ ${\beta_\mathrm{i}}^{1/2}$ times more computational time

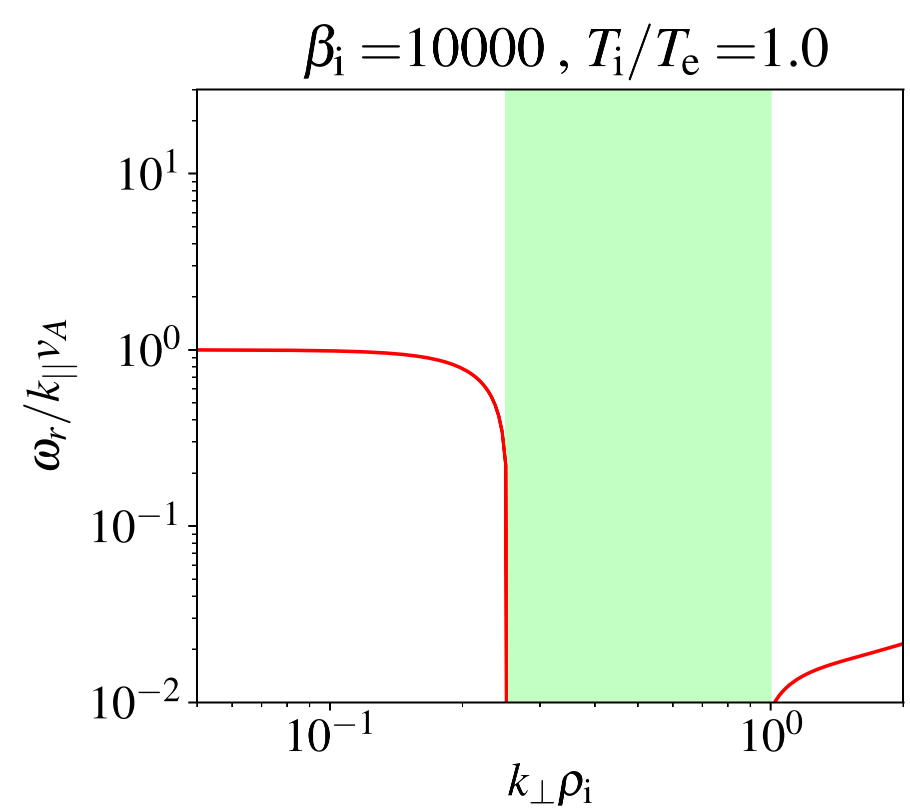

Beta gap

- ✓ High β_i ➞ A region with zero Alfvén wave frequency := beta gap
- ✓ The gap starts at $k_\perp \rho_* = 1, \ \rho_* \sim \rho_\mathrm{i} {\beta_\mathrm{i}}^{1/4}$ (Schekochihin+ in preparation)
- ✓ The anomaly of spectrum emerges around $k_\perp \rho_* \sim 1$
- ✓ The ceiling of $Q_\mathrm{i}/Q_\mathrm{e}$ starts at β_i that has a finite gap
- ✓ Howes prescription is ill-posed when the gap is present

$$Q_s(k_\perp) \sim (\gamma_s/\omega)\epsilon(k_\perp)/k_\perp$$

- ✓ To understand the ceiling of $Q_\mathrm{i}/Q_\mathrm{e}$, we need to investigate the gap
- ✓ Too narrow gap for $\beta_\mathrm{i} \sim 100$

  (1) Pressure anisotropy (Kunz+ 2018)

  (2) Ultra-high β_i, ~ 10000

- ✓ Ultra-high β_i is numerically difficult
- ✓ ${\beta_\mathrm{i}}^{1/2}$ times more computational time
- ✓ 4D model for the gap (Schekochihin+ in preparation)

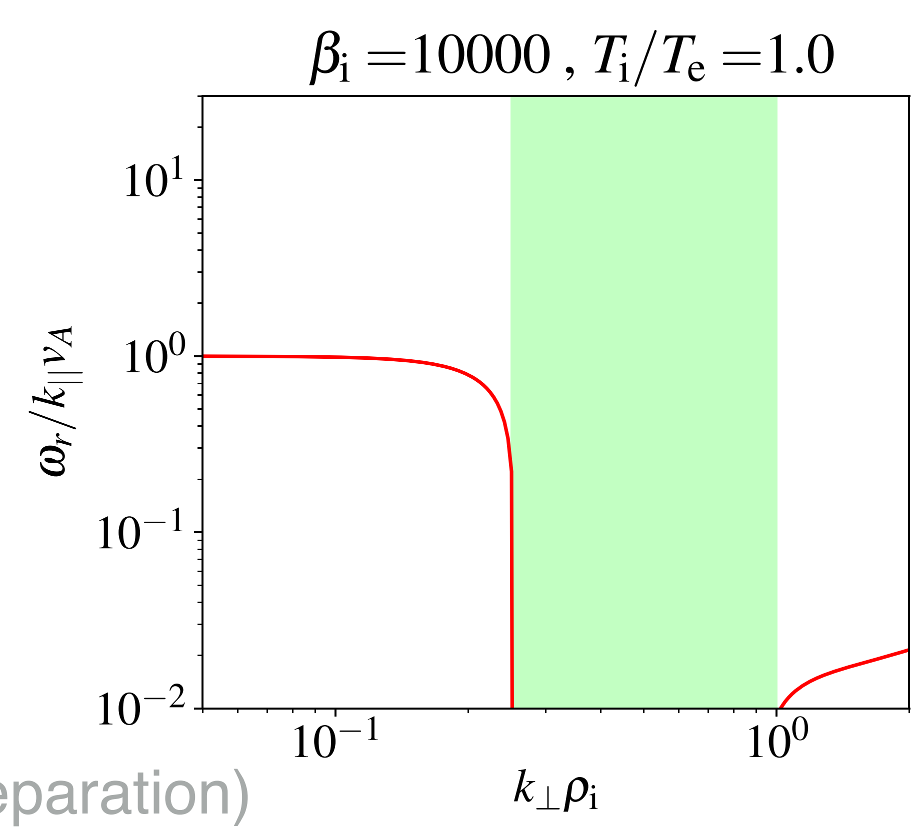

Result : k-spectrum

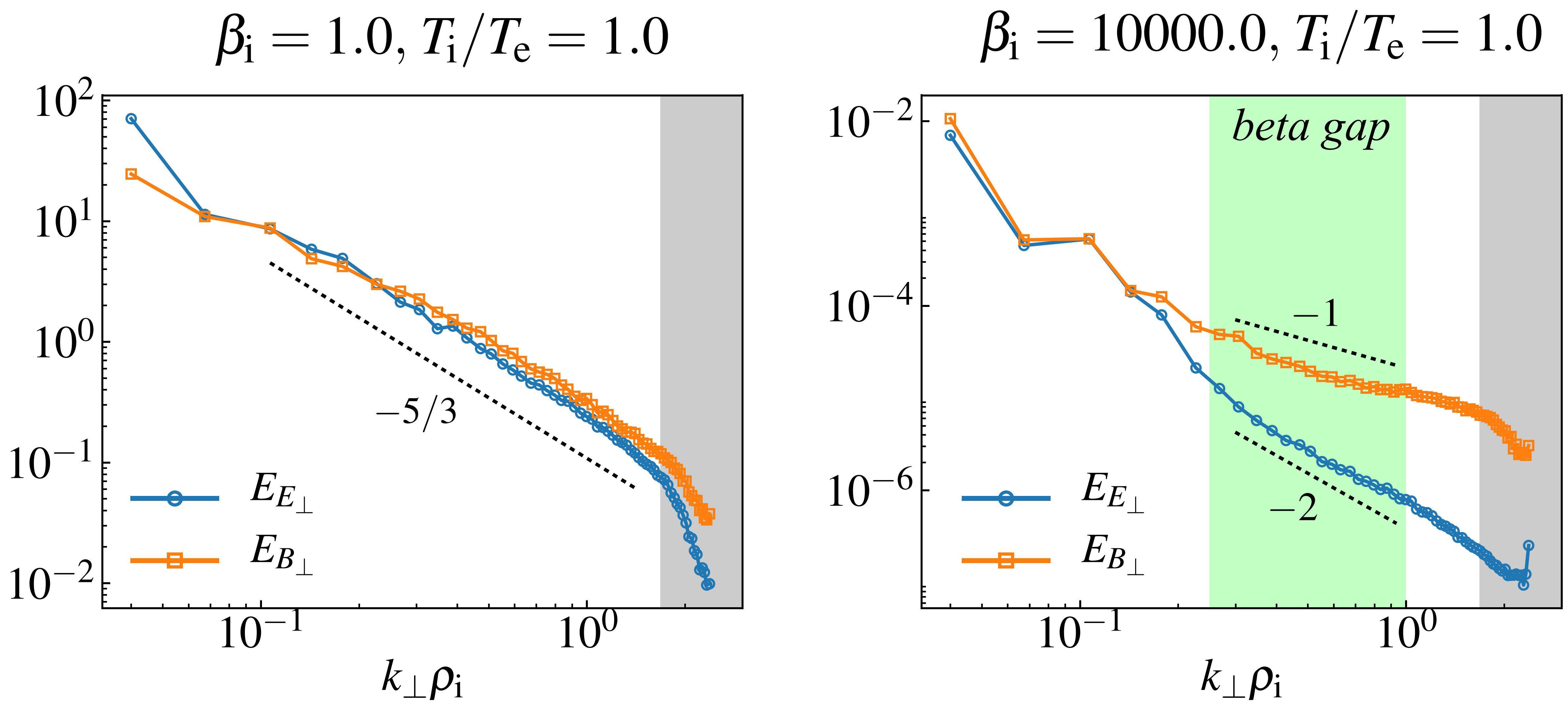

Result : k-spectrum

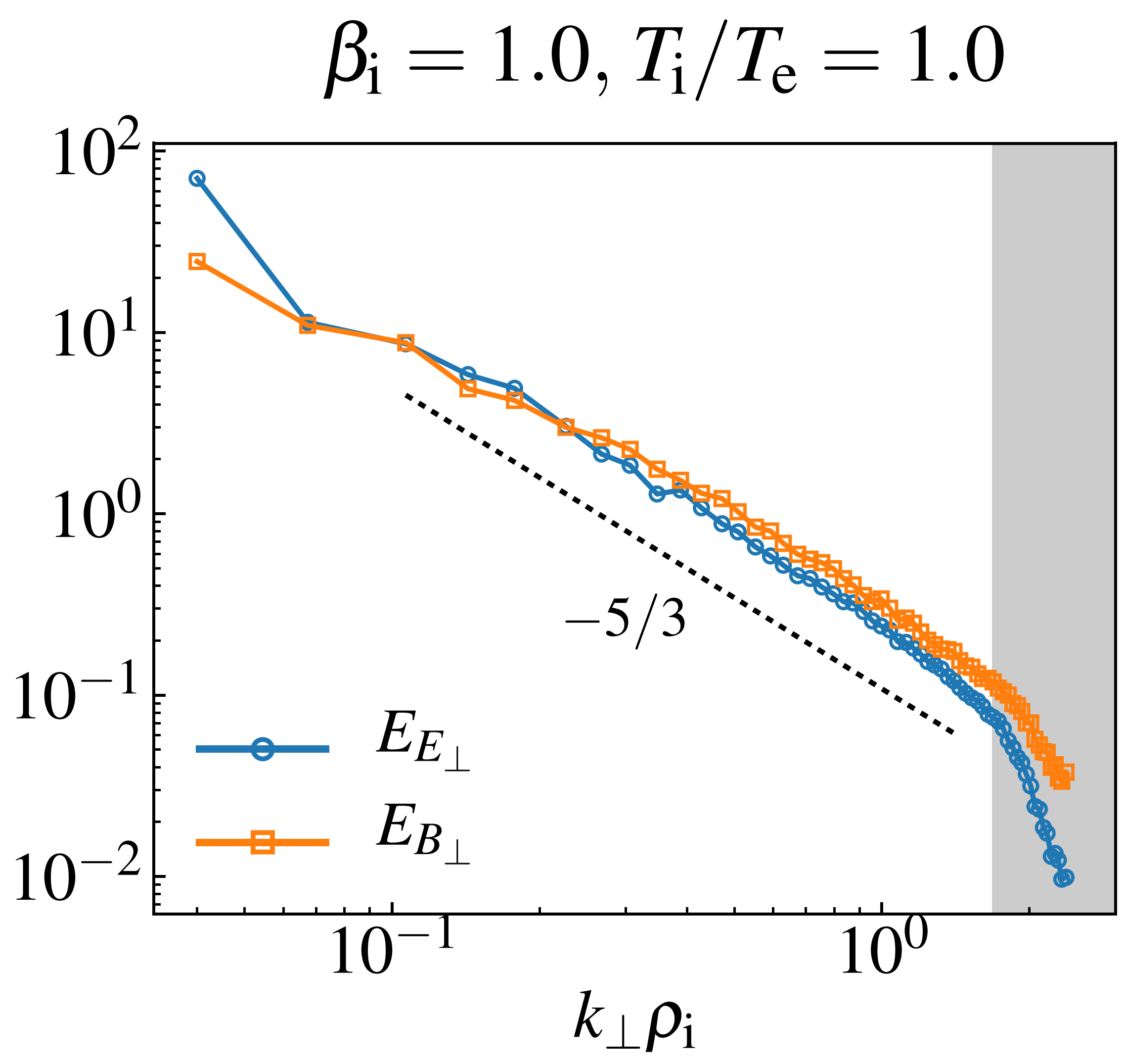

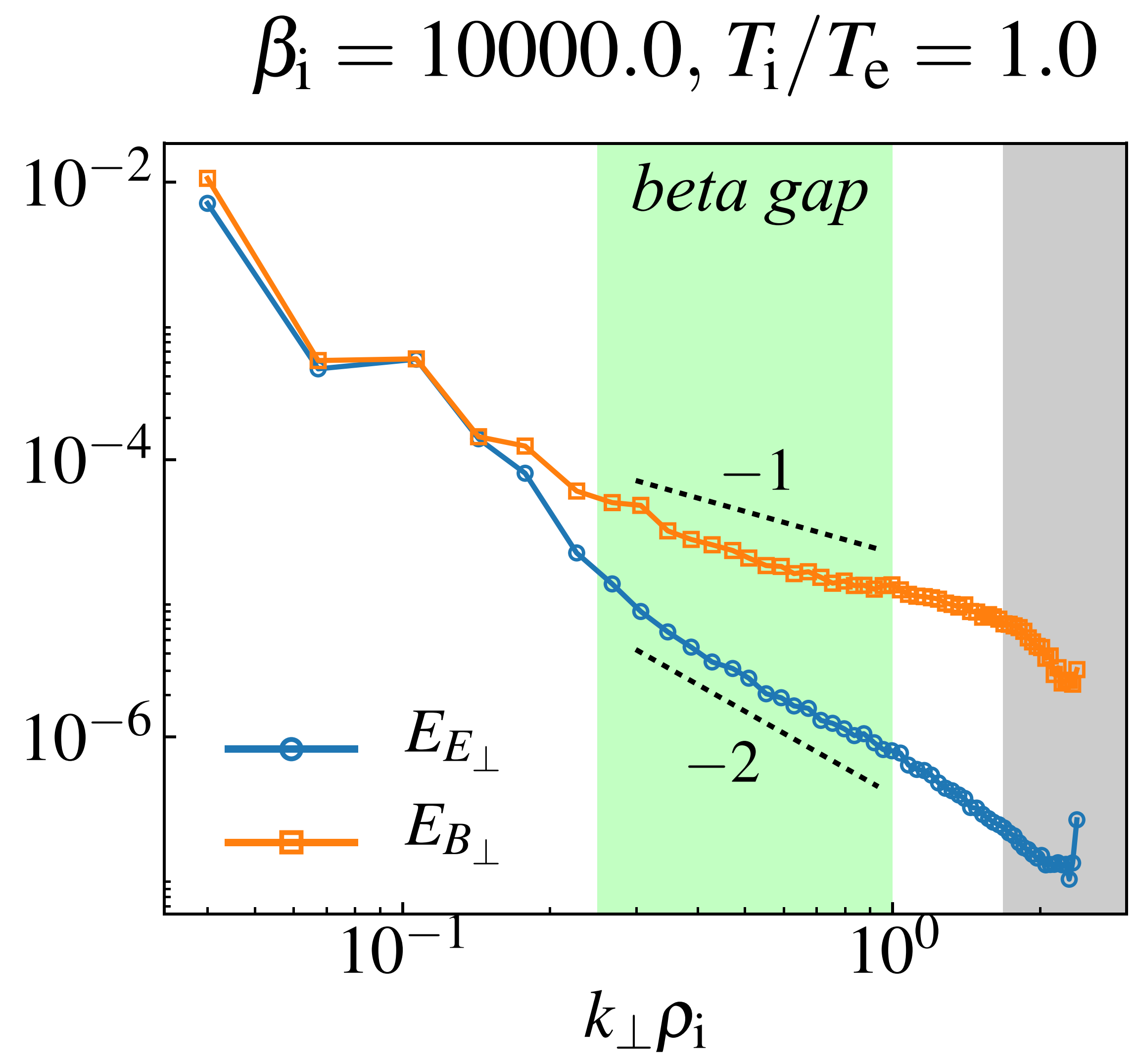

✓ The anomaly of spectrum emerges around $k_\perp \rho_* = 1$

Result : k-spectrum

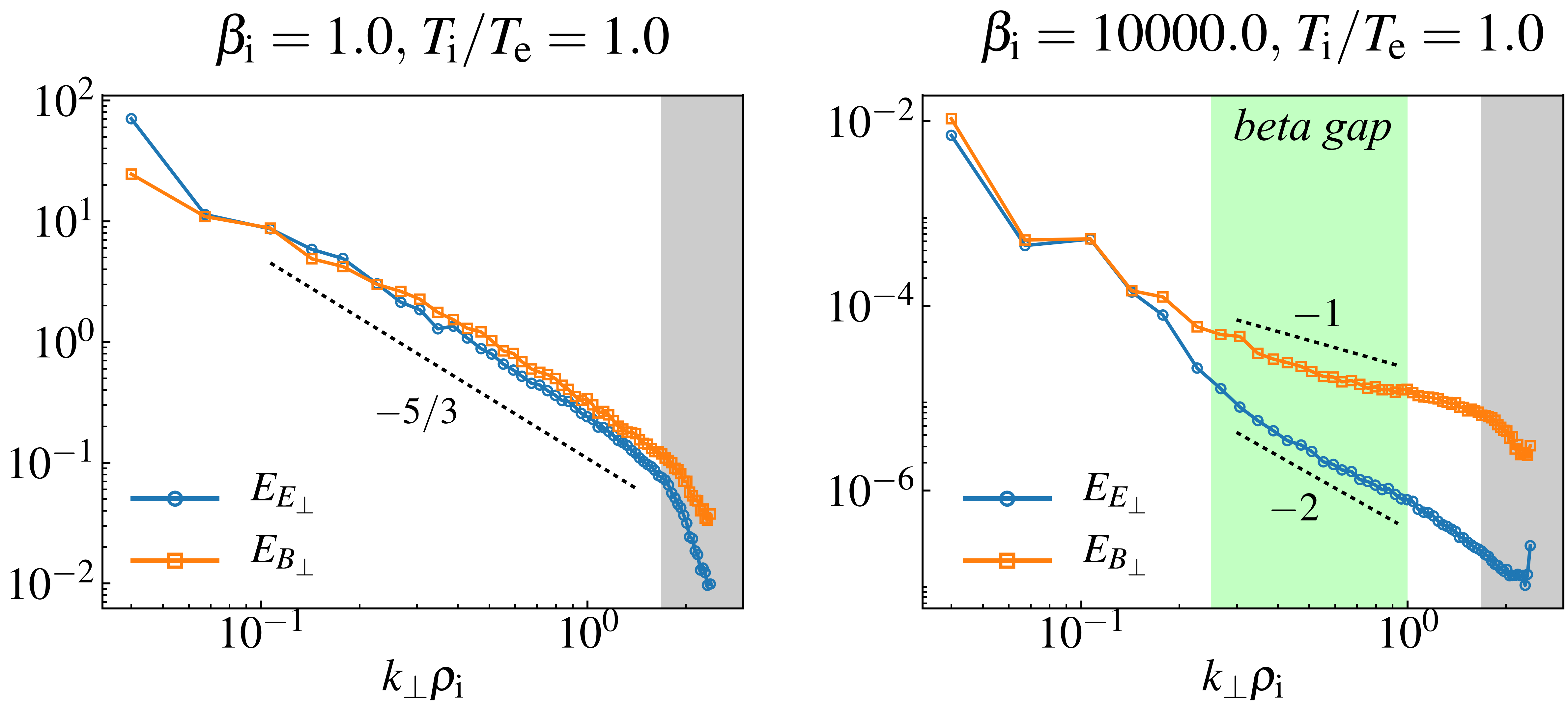

- ✓ The anomaly of spectrum emerges around $k_\perp \rho_* = 1$
- ✓ Magnetically dominated turbulence in the gap (and maybe further)

Critical balance

✓ Nonlinear decorrelation time ~ linear propagation time; $\omega_{\rm nl} \neq \omega_{\rm A}$

(Goldreich & Sridhar 1995)

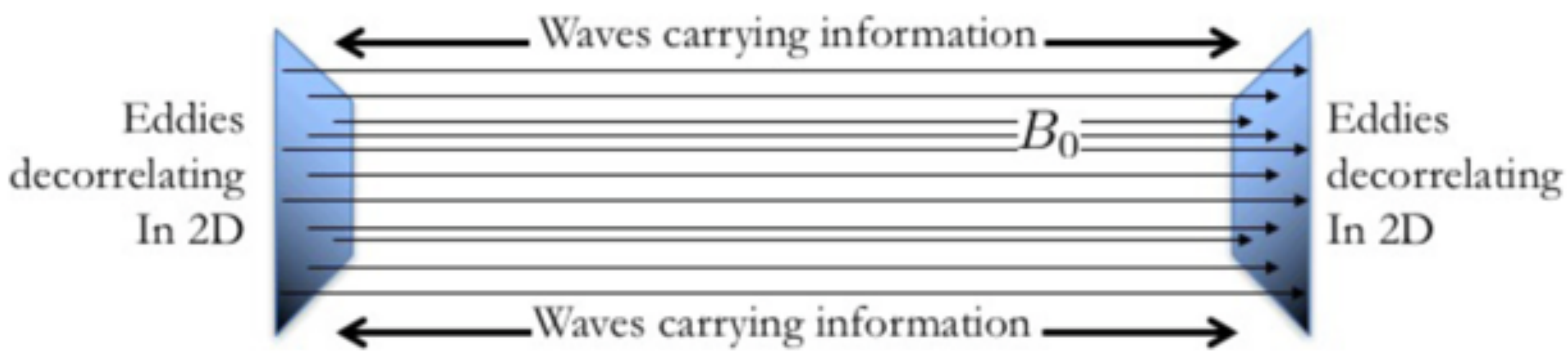

(Schekochihin in preparation)

✓ Confirmed numerically and experimentally

✓ What would happen to CB in the gap, $\omega_{\rm A} = 0$?

✓ CB is an essential assumption in Howes' heating prescription

Result : time-spectrum

✓ Spatio-temporal spectrum

$$E_{B_\perp}(k_\perp, \omega)/E_{B_\perp}(k_\perp, 0)$$

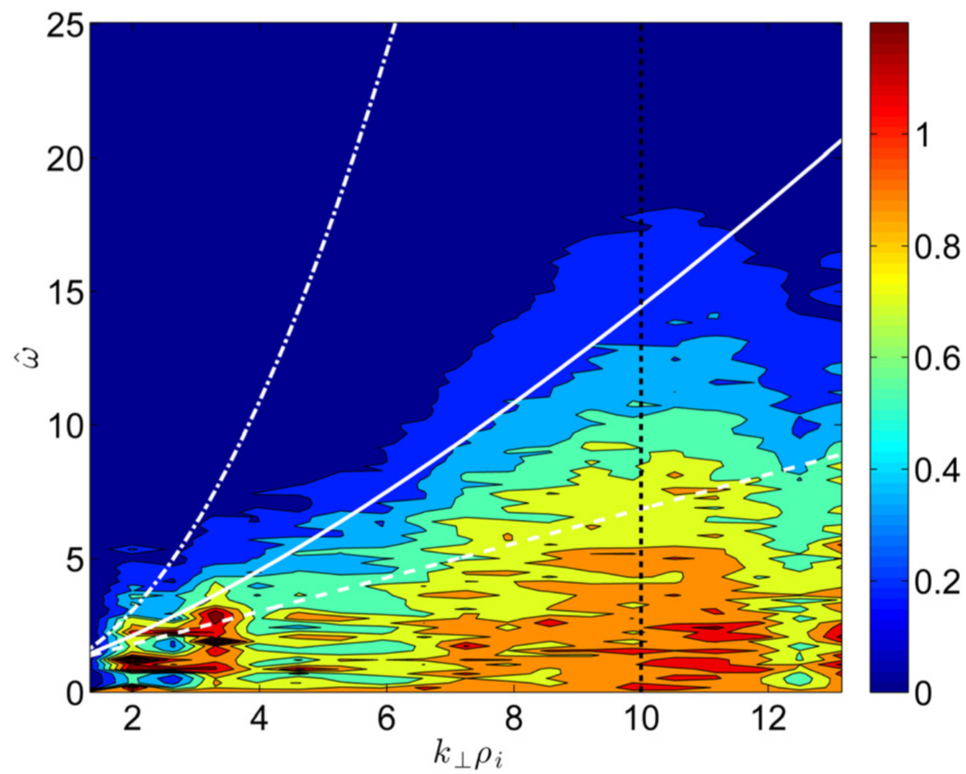

Sub Larmor spectrum for $\beta_\mathrm{i} = 1$ (TenBarge & Howes 2012)

Result : time-spectrum

✓ Spatio-temporal spectrum

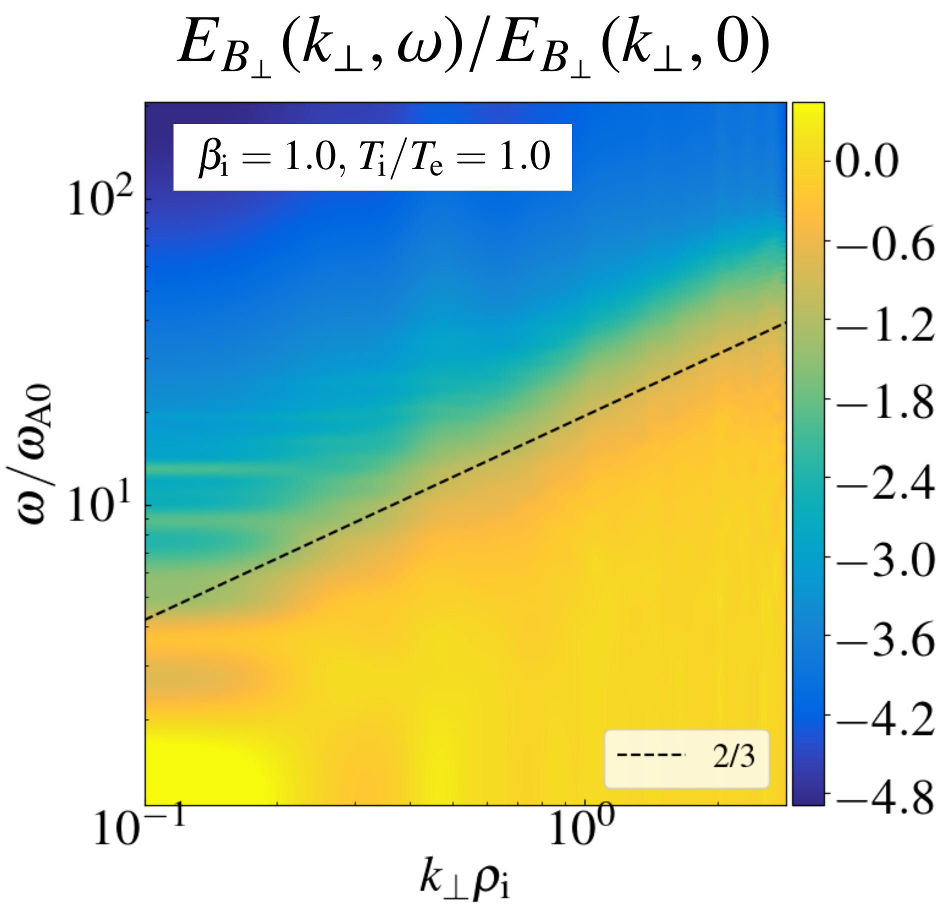

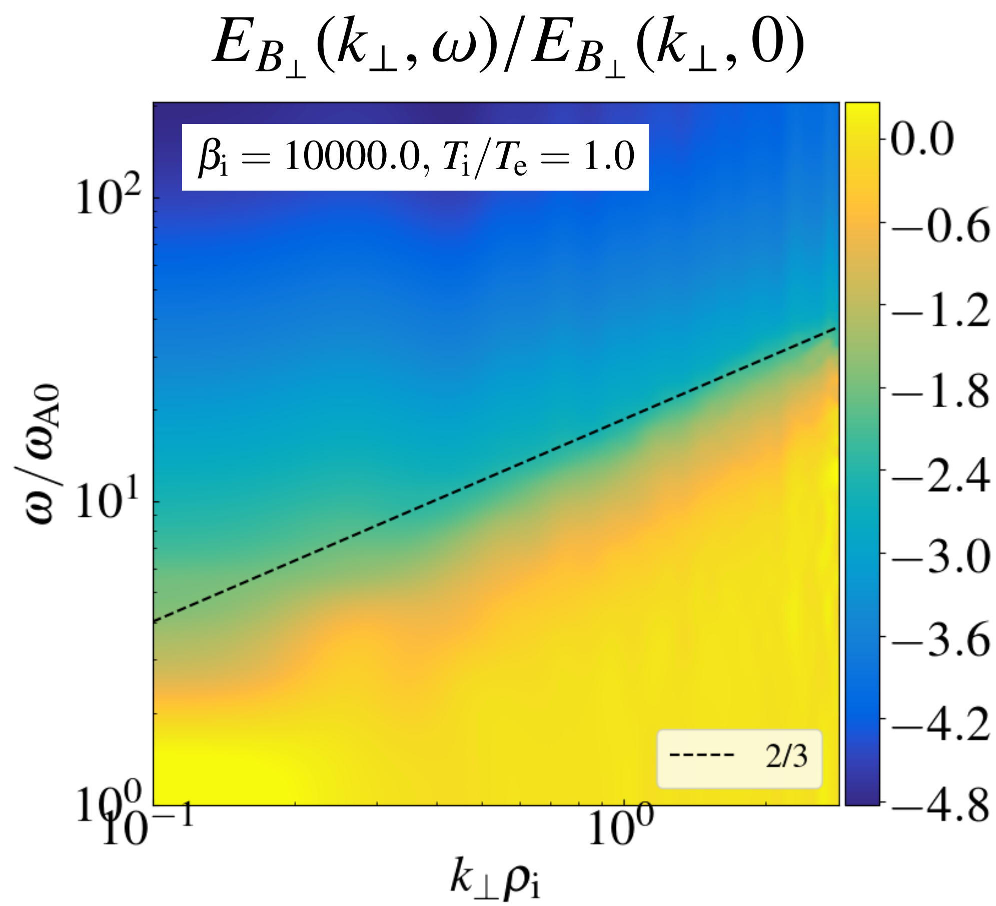

Result : time-spectrum

✓ Spatio-temporal spectrum

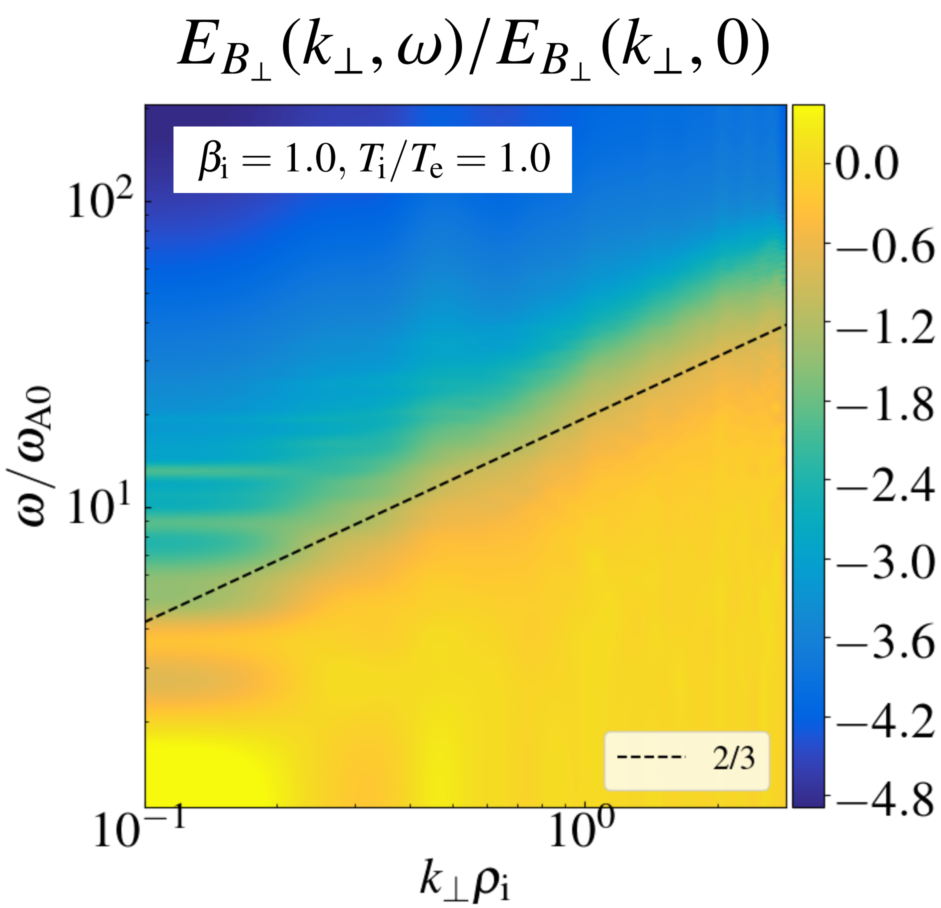

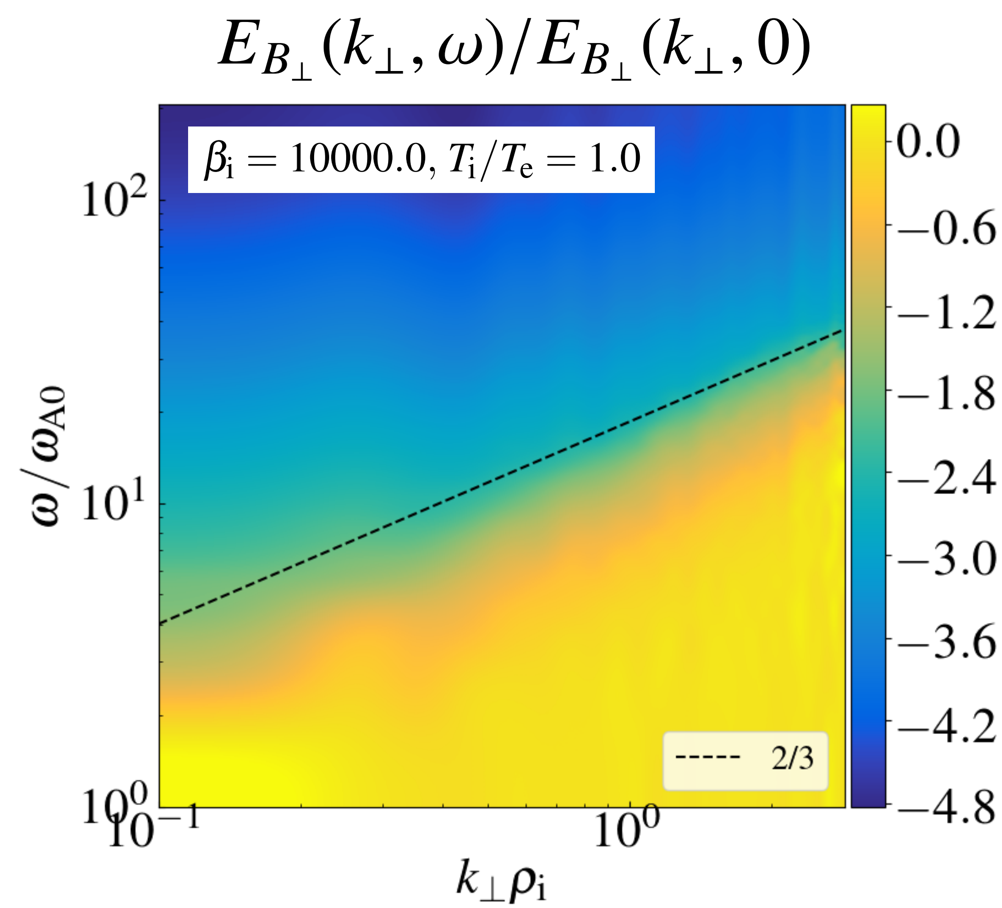

✓ For $\beta_i = 1$ (the same as MHD), $\omega_{nl} = \omega_{AW} = k_{\parallel} v_A \sim k_\perp{}^{2/3}$

Result : time-spectrum

- ✓ Spatio-temporal spectrum

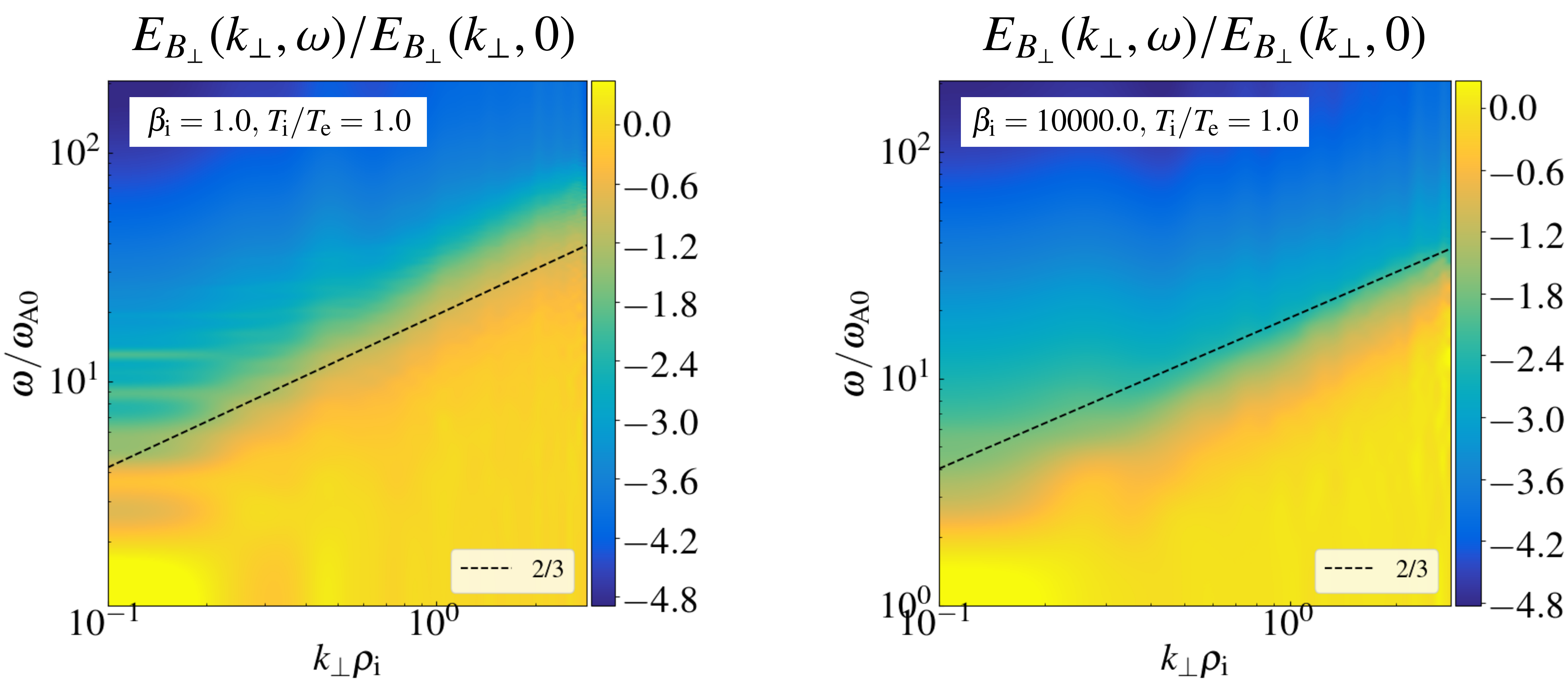

- ✓ For $\beta_i = 1$ (the same as MHD), $\omega_{nl} = \omega_{AW} = k_\parallel v_A \sim k_\perp{}^{2/3}$
- ✓ No difference between w/ gap and w/o gap

Result : time-spectrum

✓ Spatio-temporal spectrum

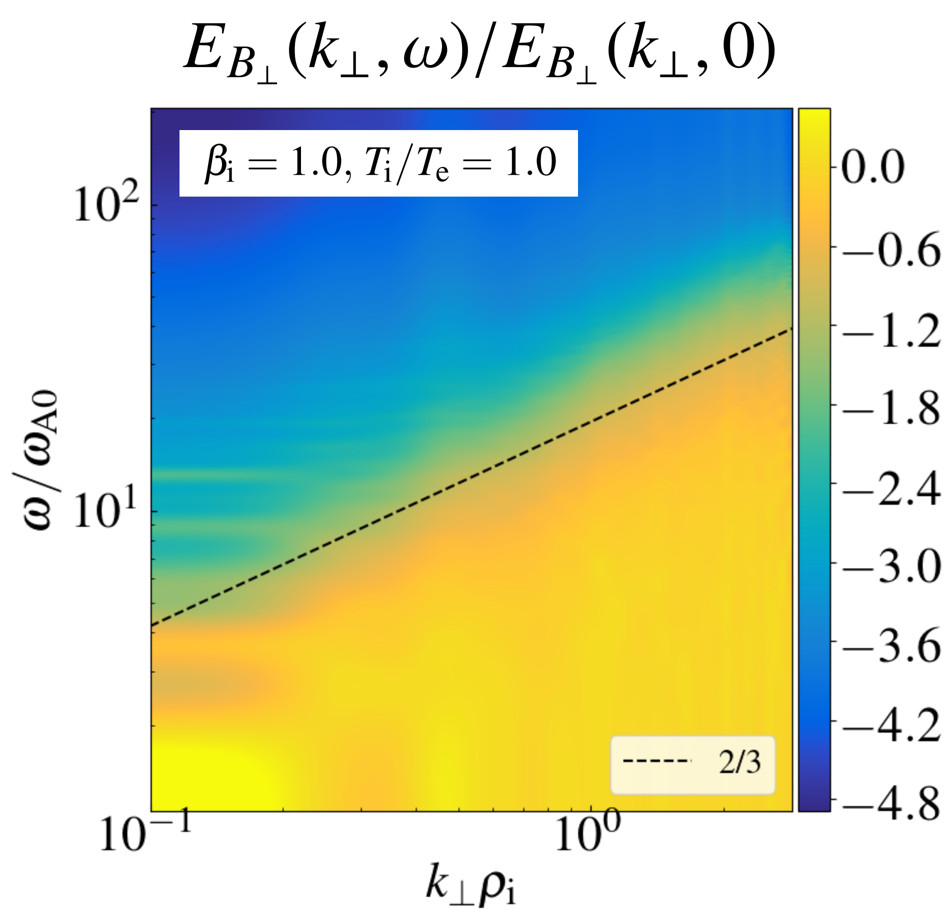

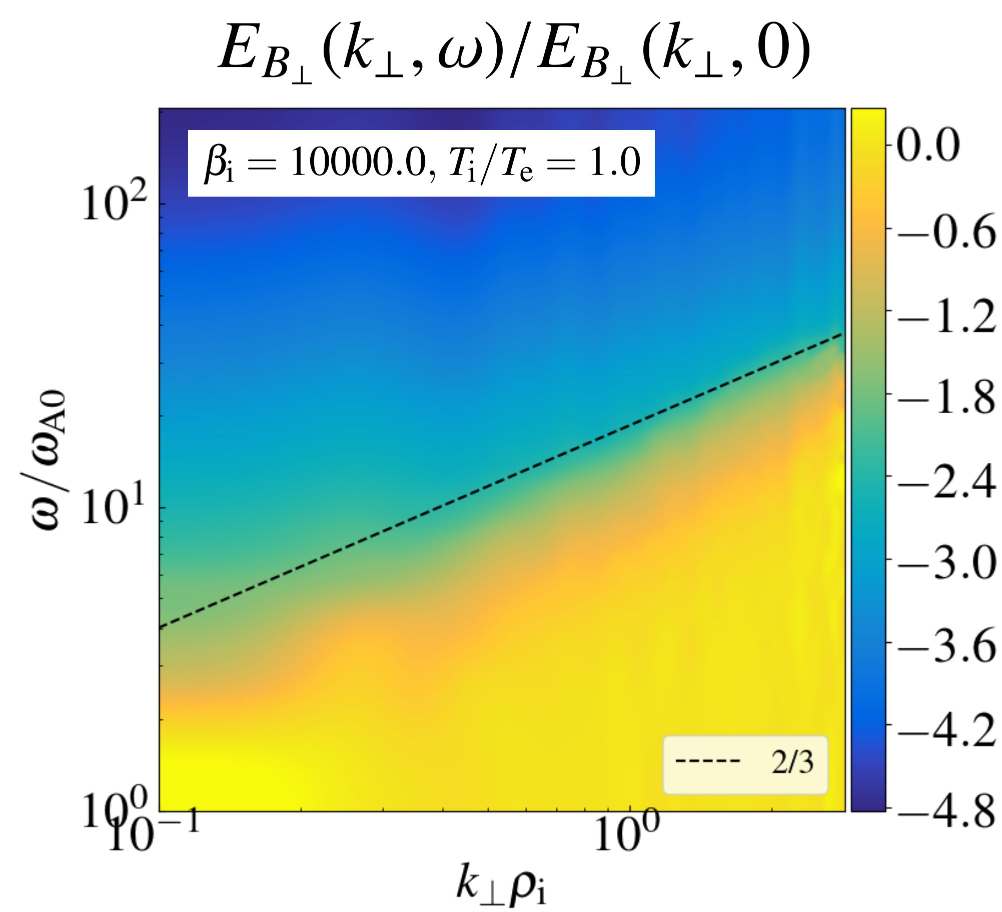

✓ For $\beta_i = 1$ (the same as MHD), $\omega_{nl} = \omega_{AW} = k_{\|} v_A \sim k_\perp{}^{2/3}$

✓ No difference between w/ gap and w/o gap

✓ For $\beta_i = 10000$, $\omega_{nl} \neq \omega_{AW}$

Result : time-spectrum

- ✓ Spatio-temporal spectrum

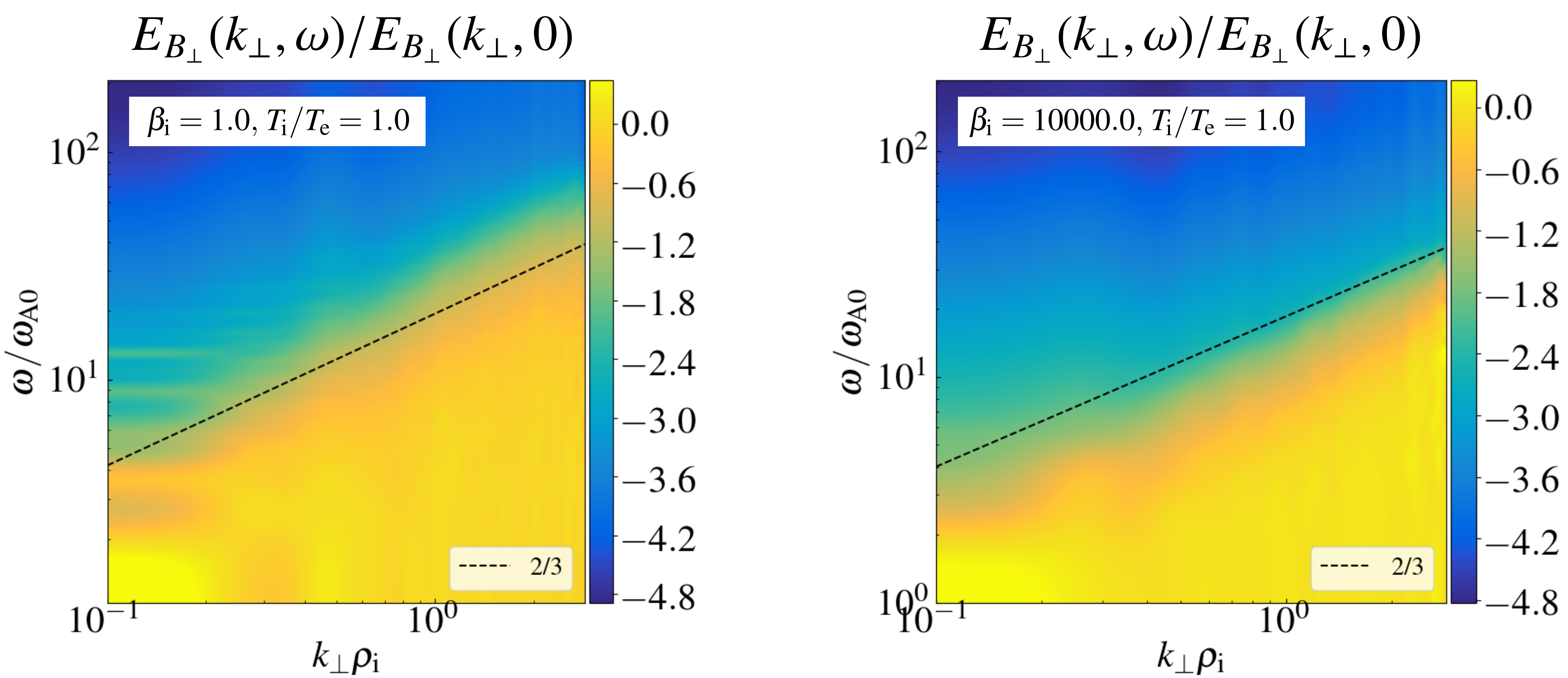

- ✓ For $\beta_i = 1$ (the same as MHD), $\omega_{nl} = \omega_{AW} = k_\| v_A \sim k_\perp{}^{2/3}$
- ✓ No difference between w/ gap and w/o gap
- ✓ For $\beta_i = 10000$, $\omega_{nl} \neq \omega_{AW}$
- ✓ How is this related to the ceiling? → future work

Phase space cascade

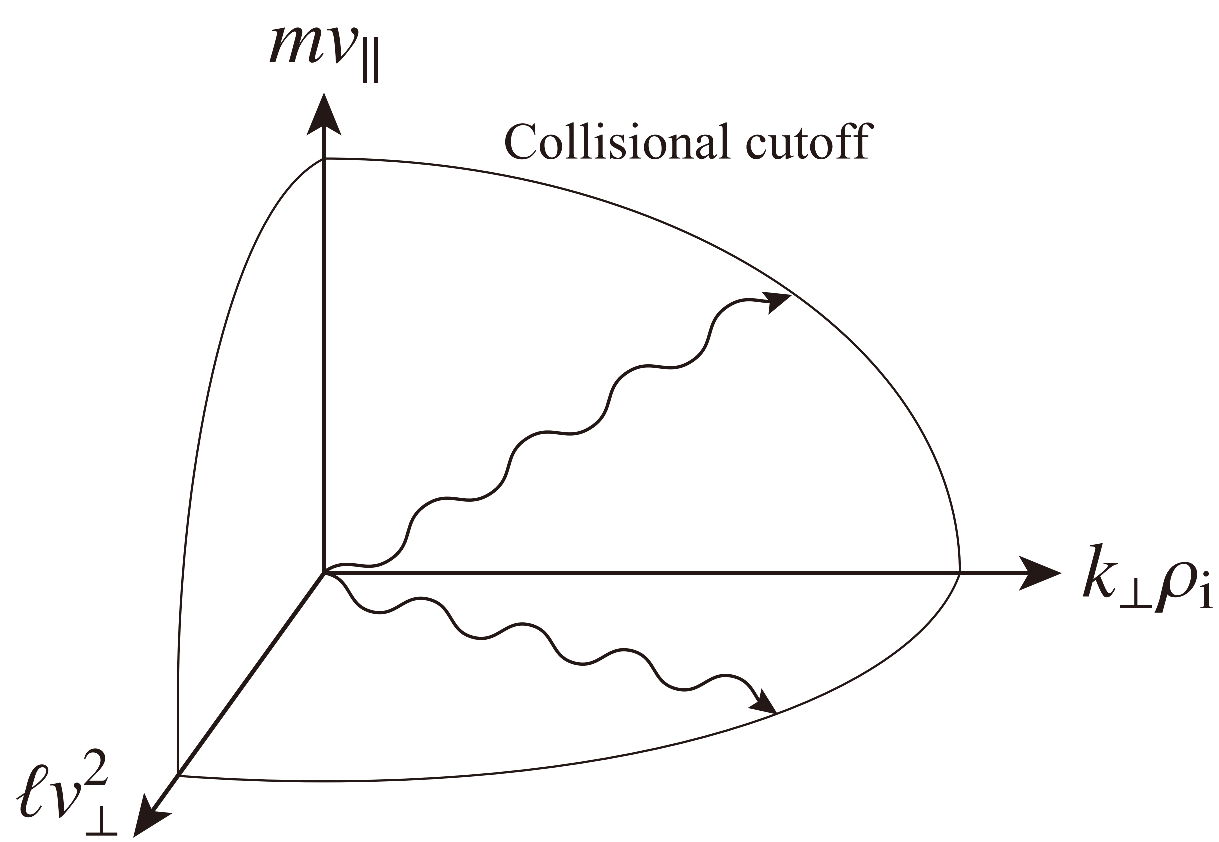

- ✓ The energy related to the ion distribution function, $\int d^3x \int d^3v\ \delta f^2/2$, cascades in 5D phase space
- ✓ Emergence of the small scale structure in the velocity space
- ✓ Eventually hits the collisional cutoff → heating
- ✓ Where this dissipation occurs is important
  - ➡ spectral analysis in the phase space